THESIS

SELECTION AND FLUORESCENCE BASED SCREENING OF ALGAL STRAINS FOR TEMPERATURE TOLERANCE AND INCREASED PRODUCTIVITY FOR INDUSTRIAL SCALE CULTIVATION

Submitted by

Conor Bertucci

Department of Biology

In partial fulfillment of the requirements

For the Degree of Master of Science

Colorado State University

Fort Collins, Colorado

Spring 2025

Master's Committee:

Advisor: Graham Peers

Arjun Khakar
Christie Peebles
Anireddy Reddy

ABSTRACT

SELECTION AND FLUORESCENCE-BASED SCREENING OF ALGAL STRAINS FOR TEMPERATURE TOLERANCE AND INCREASED PRODUCTIVITY FOR INDUSTRIAL SCALE CULTIVATION

Microalgae are emerging as a viable source of sustainable energy and bioproducts due to their rapid growth and capacity to produce valuable products. Their ability to grow in diverse, non-arable environments while minimizing resource use makes them a promising alternative to traditional crops for biofuel, feedstock, and other value-added products. Industrial-scale outdoor cultivation of microalgae subjects cells to dynamic environmental conditions such as fluctuating temperatures that can influence growth and biomass accumulation. This makes selecting a strain that can maintain high productivity crucial for industrial-scale cultivation.

The first aim of this thesis was to compare the growth and biomass accumulation of ten strains that were known for their high productivities in temperatures ranging from 18°C to 30°C. Of the ten selected strains, *Scenedesmus rubescens* NREL 46B-D3 and *Monoraphidium minutum* 26B-AM were determined to have the best overall growth performance in both temperatures and the highest biomass accumulation when grown at 30°C. *S. rubescens* and *M. minutum* exhibited an 88.5% and 22.6% higher average total organic carbon accumulation compared to the next highest performing strain tested.

The second aim of this thesis was to utilize gamma irradiation mutagenesis to generate mutants with improved biomass accumulation. Optimal LD90% dosages of 300 Gy and 75 Gy were determined for *S. rubescens* and *M. minutum* respectively. 3135 and 3356 putative mutants

were characterized for *S. rubescens* and *M. minutum,* respectively. A fluorescence-based screening approach was used to screen for putative mutants with altered photophysiology traits correlated with photosynthetic efficiency. A total of 37 *S. rubescens* putative mutants and 14 putative *M. minutum* mutants demonstrated repeated photophysiological alterations and were selected for growth comparisons between their wild type counterparts. Only one putative *M. minutum* mutant, *MRM J-325,* demonstrated improvements in specific growth rate compared to wild type. This assumed mutant will be scaled up for biomass accumulation experiments at large scale.

ACKNOWLEDGEMENTS

First and foremost, I would like to thank my parents, Gina and Greg, for their invaluable encouragement and support during my entire academic career. They've been incredible sources of guidance and moral support as I continue to navigate life's challenges and opportunities. I'll forever be thankful for what they have provided me. I'd also like to thank my brother, Christopher, who I could always call to shoot the breeze with, never failing to make me laugh. My grandparents, Louis and Simone, were always great sources of life advice and family stories. Calling Louis was always a surefire way to stay on the phone for over two hours, with more conversational tangents than most people could comprehend. He always had some form of advice to offer, and I was all ears for it. My grandparents, Joe and Valerie, while they did not get to see me finish my graduate degree, were always supportive of my academic pursuits and eager to hear more about my endeavors. Joe is to blame for my obsession with cars and I wish he could be here to see how I've continued his passion.

My girlfriend, Hannah Horowitz, has been an incredible partner and friend over the past three years. The unconditional support she provided me with during some of my most trying moments in life will never go unrecognized. On top of that, the home-cooked meals that she prepared for me did numbers for my emotional and physical health. I'm overwhelmingly excited to see what the future holds for us.

To all my close friends from Michigan and Louisiana, Casey, Hiroki, Patrick, Michael, Jericho, Mat, Quan, Brian, Ishan, Jack, Monti, Alex, Evan, Xavier, and Alassane, thank you for keeping in touch over the years. Talking and playing video games online together after work kept our bonds strong and provided a comfortable place to return, especially in times of stress.

Thank you to all of my Colorado friends, Kristian, Lizzy, Nicki, Ryleigh, Kalia, Kyle, and Tyler. I am extremely grateful to have found a close circle of friends so quickly. You all have been crucial in making my time here memorable. My roommates, Oliver and Max, have been like brothers to me over the past year and I've enjoyed every moment bonding with them.

I would like to thank my advisor, Dr. Graham Peers, and my committee members Dr. Arjun Khakar, Dr Christie Peebles, and Dr. Anireddy Reddy. Graham shaped me into a significantly better scientist and critical thinker than I was when I arrived in the lab. Notably, Graham tailored his suggestions for improvement towards the career path that I intend to pursue, which will undoubtedly benefit my future success. Graham would always treat everyone in the lab for coffee runs and was entertaining to talk to as he never failed to have an engaging story or a connection to any topic that came up in conversation. Arjun, Reddy, and Christie were very helpful during the development of my research approach. Shout out to Reddy's class, Molecular Aspects of Plant Development co-taught by Amanda Broz. This was one of the most challenging and insightful courses I took while at CSU. I apologize to both of you for nodding off every once and a while in class. I was adjusting to my first semester and had to start power-napping under my desk before class to avoid this.

My labmates, Andrew, Tessema, Brandon, and Kalia, contributed greatly to the success of my research. It was a pleasure coming into the lab every day and getting to work with you all. Andrew, Tessema, and Brandon were always there for me when I had general questions or needed assistance with experiments. My friendship with Andrew was solidified the moment I arrived at CSU, and I can't think of another person I'd rather grab beers, watch Family Guy compilations, and do character impressions with. You're a real one bud.

I want to thank DeeDee Wright for guiding me and helping me develop my teaching skills as well as allowing me to barge into her office to talk about whatever was on my mind at the time. Next, I'd like to thank Justin Bell for his help with my mutagenesis experiments. Even when I e-mailed him at the last minute, he still found time to process my samples. I'd like to thank Ken Reardon for allowing me to use his lab space and equipment.

Lastly, I'd like to give a shout out to Anthony Bourdain, Hideo Kojima, and James May in no particular order for being influential and entertaining figures in my life recently.

TABLE OF CONTENTS

GENERAL INTRODUCTION

1. Microalgae as an alternative crop for food, fuel, and other high value bioproducts

By 2050, the world's population is projected to reach nearly 10 billion people, driving a dramatic increase in demand for food, fuel, and other essential resources. As a result, there is growing interest in sustainable alternatives that can meet these needs without further depleting finite land and resources. Algae, with their ability to produce high-value products while thriving in non-arable environments, are gaining attention as a viable solution to address both food and fuel shortages in the future. In recent decades, microalgae have become a prospective alternative to terrestrial crops as a food and biodiesel source due to their fast growth rate and ability to produce high value products such as proteins, triacylglycerols (TAG), carbohydrates, and pigments (Demirbas, 2011; Veillette et al., 2018). In 2016, the global production of algae biomass was estimated at around 32.67 million tonnes (fresh weight) [Araújo, 2021]. Although exact figures on its distribution between food and fuel are limited, most of this biomass is believed to be used for food-related purposes, including human consumption, animal feed, and nutritional supplements. Additionally, microalgae can thrive in a wide range of culturing conditions such as water quality, pH, and temperature and have simple growth requirements such as light, carbon, nitrogen, phosphorus, and essential micro-nutrients (Gong & Jiang, 2011; Benedetti et al., 2018; Demirbas, 2011). This allows for algae to be cultivated in non-arable environments that terrestrial crops cannot tolerate. Increased government subsidization of biofuel production using crops such as corn, rapeseed, and soybeans has caused a "food vs. fuel" controversy to arise that challenges whether terrestrial crops should be grown on arable land for use as biofuels instead of food (Singh, et al., 2011; Amaro et al., 2011; USDA, 2022). These

combined factors help pave the way for algae to emerge as an alternative to terrestrial crops for biofuel production.

Microalgae have been shown to have high productivity and are able to double their biomass in under 24h when in exponential growth phase (Feng et al., 2014; Weissman et al., 2018; Mann and Myers, 1968). Mass-scale cultivation methods for algae such as open raceway ponds (ORP) and photobioreactors (PBR) have been established over the years, each with their own advantages and disadvantages. Open raceway ponds are the most common cultivation systems that prioritize low setup cost and energy usage with the trade-off of lower control of growth parameters (temperature and contamination) and a lower areal productivity, between 6-14 g m^{-2} day^{-1} as demonstrated by de Vree et al. (2015) and 20 g m^{-2} day^{-1} by Blanco et al. (2007). Photobioreactors are closed cultivation systems that come in different configurations such as flat panel and tubular PBRs that prioritize greater control over cultivation parameters and higher areal biomass with the trade-off of costing 4-9 times more to scale up than ORPs and have a higher energy requirement to operate (de Vree et al, 2015; Acién Fernández et al., 2013; Dogaris et al., 2015; Zhu, Y., et al., 2018). PBR systems tend to have higher areal productivity than ORPs due to their efficient layout, light absorption, gas transfer, and culture mixing (de Vree et al., 2015; Kumar, K. et al., 2015; Acién Fernández et al., 2013). In the study conducted by de Vree et al. (2015), an areal productivity of 24 g m^{-2} day^{-1} using a flat panel PBR was demonstrated. These findings highlight the importance of choosing the appropriate cultivation method based on the desired trade-off between cost, energy use, and productivity. These are crucial considerations when scaling up microalgae production for commercial applications. Both open raceway ponds and photobioreactors are capable of outperforming terrestrial crops in terms of their areal biomass productivity. Krisnawati & Adie, (2015) looked at biomass productivity of

several soybean genotypes and found an average biomass production of 5.2 g m^{-2} day^{-1}. Maize productivity in the corn belt of the United States was examined by Infante et al. (2018) and was determined that the mean areal productivity was 5.4 g m^{-2} day^{-1}.

Outdoor cultivation methods are all still subject to variations in environmental conditions such as temperature and light, where changes can occur on a minute, hour, and daily basis. Temperature fluctuations in open systems directly influence metabolic pathways such as lipid biosynthesis and enzymatic activity, creating a barrier to consistent biomass productivity (Barten et al., 2021; El-Sheekh et al., 2017). Strains like *Phaeodactylum tricornutum*, while cold-tolerant, fail to thrive at elevated temperatures (≥30°C), underscoring the need for thermally resilient candidates capable of maintaining growth across wide temperature variations (Pereira et al., 2021).

Among the numerous characterized algal strains, only a subset of them holds commercial relevance, cultivated primarily for their high-value compounds. *Chlorella vulgaris, Nannochloropsis spp*., *Scenedesmus obliquus, Dunaliella salina,* and *Haematococcus pluvialis* are a few of the strains utilized in commercial outdoor cultivation due to their unique physiological traits, adaptability to varying environmental conditions, and potential for high-value applications (Lee et al., 2018; Guccione et al., 2014; Chen et al., 2024; Chiu et al., 2009; Pereira et al., 2017; Hermawan et al., 2018; Teng et al., 2023). Specifically, they are ideal for applications such as biofuel production, pigment synthesis, wastewater treatment, and carbon sequestration. Selection of a strain for large scale can vary depending on the region where cultivation will take place. For example, in coastal regions or in areas with limited potable water, it can be advantageous to cultivate algal species adapted to high salinity marine environments which tend to have better contamination resistances and high lipid and pigment accumulation in

these conditions (Narala et al., 2016; Dogaris et al., 2015; Costa et al., 2019; Kumar, K. et al., 2015). Utilization of wastewater to cultivate algae has also been shown to be successful (Loftus & Johnson, 2019). Cheng et al. (2017) reported that unpasteurized swine wastewater was used to cultivate *Chlorella pyrenoidosa* with a higher biomass productivity than when grown using BG11 medium.

In addition to cultivating algae using saline or wastewater, the use of industrial flue gases as a carbon source has been shown to be a viable and sustainable alternative to using pure CO_2 as it has been shown to account for 20-25% of algal production operating costs (Molitor & Schnoor et al., 2020; He, L. et al., 2012; Vorisek et al., 2023). However, concentrated levels of CO_2 and other flue gas components such as SO_x and NO_x have been shown to hinder growth or be toxic to certain species of algae (Wang, X. et al., 2014; Cheng, J. et al., 2019; Chiu et al., 2008; Huang et al., 2016; Negoro et al., 1991). Wang, X. et al. (2014) examined how varying concentrations of CO_2 impacted biomass concentrations in the marine diatom *Chaetoceros muelleri* and found that the highest biomass content was seen at 10% CO_2 and began to decrease when CO_2 concentration was increased. Additionally, algal strains have been shown to tolerate up to 60ppm SO_x before growth inhibition begins and NO_x concentrations below 300ppm being tolerated (Huang et al., 2016; Negoro et al., 1991). The simulated flue gas used for this experiment will contain an average of 13% CO_2 as well as 23ppm SO_2 and 28ppm NO_x based on the flue gas produced by the Wyoming Integrated Test Center (WITC) in Gillette, WY, where algal strains will eventually be grown in outdoor raceway ponds.

This experiment initially focuses on screening and selecting microalgal strains that tolerate a wide temperature range and demonstrate high biomass productivity when grown with and without the presence of industrial flue gas. During this process, photophysiology and carbon

dynamics were monitored to further gauge any stresses or limitations that arose from the growth conditions. The two highest performing strains were then mutagenized to develop resilience to flue gas in order to increase biomass productivity over its non-mutagenized variants. These strains will be sent to the WITC where cultivation will be scaled up to 1000L raceway ponds using flue gas produced on-site to demonstrate the feasibility and potential for large-scale, sustainable production of algal biomass for various applications. Specifically, the biomass generated from this study will be used for the production of carbon nanofiber supercapacitor electrodes and ethylene glycol (Wang, T. et al., 2022; Jin et al., 2014).

2. Algal strain selection for temperature-based growth analysis

Ten algal species have been chosen for this experiment based on their documented rapid growth capabilities in optimal conditions. These include species from the genera *Nannochloropsis, Picochlorum, Scenedesmus, Monoraphidium, Phaeodactylum*, and two uncharacterized strains obtained from Arizona State University. Six of these strains were characterized by Huesemann et al. in a previous study to identify high productivity strains for industrial scale biofuel generation (Huesemann et al., 2023).

Nannochloropsis is a well characterized genus that has shown to have high productivity, high production of fatty acids when exposed to nitrogen depleted conditions, and contamination resistance (Ma, X. et al., 2016). Fakhry and El Maghraby, (2015) reported a 59% lipid content in *N. salina* when grown in medium containing 75% less nitrogen compared to 35% lipid content in standard medium. Contamination of cell cultures is a serious factor to consider in commercial algae cultivation as it can lead to cell populations crashing (Lam et al., 2018). *Nannochloropsis oceanica's* ability to resist contamination can be attributed to an extracellular secretion that

inhibits growth of protozoa which commonly graze on microalgae (Zhao, L. et al., 2021). Wild type *Nannochloropsis oceanica* has been selected for this experiment.

Picochlorum has been shown to tolerate high temperatures, salinity, and light intensity while maintaining a fast-doubling time in its optimal culturing conditions (Weissman et al., 2018; Dahlin et al., 2019). *Picochlorum renovo's* halophilic and thermophilic traits allow it to grow in ~3x sea water salinity and up to 45°C, making it an excellent prospective spring, summer, and fall strain for outdoor cultivation (Dahlin et al., 2019; Huesemann et al., 2023). *Picochlorum celeri* TG2 and *Picochlorum renovo* NREL 39-A8 have been selected for this study.

Species in the genus *Scenedesmus* are attractive for biodiesel production due to their high biomass productivities and lipid content (Vorisek et al., 2023; Shao et al., 2020; Feng et al., 2014; Huesemann et al., 2023; He, Q. et al., 2018). Li, F. et al. (2011) developed a mutant *Scenedesmus obliquus* that showed higher tolerance to CO_2 for flue gas CO_2 removal. De Jaeger et al. (2014) developed starchless mutants of *Scenedesmus obliquus* that produced an enhanced triacylglycerol content under photoautotrophic conditions. *S. obliquus* UTEX393, *S. acutus* LRB-AZ-0401, and *S. rubescens* NREL 46B-D3 have been selected due to their high specific growth rates and productivity (Huesemann et al., 2023).

Species in the genus *Monoraphidium* are freshwater dwelling algae that have been reported to tolerate a wide variety of temperatures (~14.5-35°C) while maintaining high biomass productivities (Ogden et al., 2019; He, L. et al., 2012). For this reason, they have been suggested to function well for winter cultivation. *Monoraphidium minutum* 26B-AM, the strain that was selected for this experiment, demonstrated stable growth in outdoor open raceway ponds with high productivity (Huesemann et al., 2023).

Phaeodactylum, a genus of marine diatoms, has gained commercial significance over the years due to its production of high-value products such as triacylglycerols, as well as various pigments including xanthophylls and carotenes. (Celi et al., 2022; Mann and Myers, 1968). *Phaeodactylum tricornutum,* a widely studied model strain, exhibits optimal growth at 18°C, rendering it more suitable for cultivation during the winter season. Gao et al. (2022) explored overexpression of a novel gene in *Phaeodactylum tricornutum* that affects cell morphology and reported higher lipid content and grazing resistance over wildtype. Wild type *Phaeodactylum tricornutum* was selected for this experiment.

Two uncharacterized strains, SAmud7, and SRTC14 were received from Arizona State University and were included because of their favorable growth rates that were previously tested in the Peers lab.

3. Biomass quantification and carbon dynamics of selected strains

An algal strain's efficiency at nutrient utilization into organic matter is directly tied to their productivity. Strains with higher productivity are therefore able to yield an increased quantity of high value products such as lipids, proteins, and carbohydrates (Assunção et al., 2017). Commercially desirable strains tend to be fast growing and capable of yielding high biomass quantities. Additionally, these strains often possess a resilience to environmental fluctuations, ensuring consistent productivity under dynamic growth conditions, making them ideal candidates for large-scale cultivation and bioproduct applications.

Quantifying algal biomass has traditionally been done by using dry ashing methods such as measuring ash free dry weight (AFDW) which involves filtering, washing, drying, ashing, and desiccating algal cultures (Hess et al., 2019; Nelson & Sommers, 2015). Organic matter in a sample is removed via combustion leaving behind inorganic residue (ash) which can be used to

quantify biomass (Liu, K., 2019). While this process is accurate, it is also expensive and time consuming. Dry weight biomass quantification is a faster but less reliable method that only involves dewatering and drying of algal samples but does not account for potential inorganic material present in cells. This can lead to an overestimation of organic biomass (Zhu & Lee, 1997). Ash removal is crucial when estimating biomass as high ash content can lower the yield and quality of desired products (Woodyward, 2009). Wet ashing methods such as total organic carbon (TOC) analysis utilize strong acids and oxidizers to purge off organic and inorganic carbon to determine carbon concentrations in a liquid sample. TOC analysis requires less sample preparation since liquid cultures can be placed directly into the analyzer for automated measuring, making it a cheaper and higher throughput alternative to AFDW (Saxena et al., 2021). Saxena et al. (2021) observed a measured and derived biomass difference of less than 2% when comparing the two techniques, demonstrating their comparability in accuracy. This streamlined process makes TOC analysis particularly appealing for high-throughput experiments or industrial applications requiring rapid biomass quantification due to its cost-effectiveness and automation capabilities. Wet ashing TOC analysis will thus be utilized to determine organic carbon concentration per cell culture batch.

Total organic carbon analysis will also allow for this system's carbon dynamics to be observed using the mass balance approach. This will help determine how carbon is being used by algal cultures since both organic and inorganic carbon is measured. (Kishi et al., 2019). The measurement of CO_2 delivered to the cultivation system via sparging, CO_2 loss, and carbon uptake by the cells will allow for the total carbon in the cultivation system to be monitored. Tracking these parameters can enable a comprehensive understanding of carbon flow through the system, identifying inefficiencies or bottlenecks in carbon utilization. Understanding the mass

balance approach in this context will enable the quantification of the algal biomass produced by each strain, providing insights into the correlation between carbon uptake and the resultant biomass yield of each strain. These insights can further inform strain selection and cultivation strategies to maximize carbon conversion efficiency and biomass productivity.

4. Enhancing microalgal traits through mutagenesis

After the growth characteristics and biomass of each high performing strain were recorded when grown with and without flue gas, two strains were further selected to undergo random mutagenesis. A random mutagenesis approach is used because natural evolution of commercially favorable traits such as disease resistance, enhanced productivity, and abiotic stress tolerance, can be both slow and untargeted. Random mutagenesis techniques have been utilized as a result to accelerate this process to generate mutants exhibiting desirable traits (Trovão et al., 2022).

A major advantage of random mutagenesis techniques is that they do not introduce foreign DNA sequences into an organism's genome, thus avoiding the regulations that would prevent large scale open cultivation (Chen and Chen, 2018; Li, X. et al., 2001). In the European Union, rigid GMO field trials and stringent regulations are capable of delaying development of a commercial-ready product by several years which increases cost long term (Zepeda & Custodio, 2018; Zimny, 2023). Chemical based mutagenesis approaches that utilize alkylating agents or ethyl methanesulfonate to induce mutation are simple and accessible but can be less stable, causing a reversal of the desired trait (Kumawat et al., 2019).

Physical mutagenesis techniques such as UV radiation in *Scenedesmus obliquus* has been demonstrated to improve traits such as CO_2 fixation and TAG accumulation (Li, X. et al., 2001; De Jaeger et al., 2014). This is done by exposing cells to an extended dose of UV radiation to

induce point mutations, deletions, and replacements (Li, X. et al., 2001; Trovão et al., 2022). Other physical mutagenesis methods utilize ionizing gamma radiation or fast neutron bombardment and have been shown to have high mutation rates (Kumawat et al., 2019; Sikora et al., 2011). As ionizing radiation interacts with cellular components such as water molecules, free radicals (hydroxyl radicals and other reactive oxygen species) are generated that damage DNA, causing both single and double-stranded breaks These ionizing mutagenesis methods result in much larger deletions and other chromosomal rearrangements than UV or chemical mutagenesis methods (Sikora et al., 2011; Hwang et al., 2015). These larger DNA breaks induced by ionizing irradiation also have slower cellular recovery than other forms of irradiation, making reversions in the mutation less likely (Hendry, 1991). Since screening mutants is a highly time-consuming process, so the higher mutation rate caused by gamma irradiation will be ideal to quickly identify mutants with significantly altered photophysiology (Liu, B. et al., 2015; Wang W. et al., 2018). Gamma irradiation mutagenesis has been successfully demonstrated in several different algal species such as *Chlamydomonas reinhardtii* and *Chlorella pyrenoidosa* with the goal of improving lipid accumulation in cells (Liu, B. et al., 2015; Wang W. et al., 2018; Baek et al., 2016). This positions gamma irradiation as an ideal mutagenesis tool for algal biotechnology that combines high mutation rates and stable genomic alterations capable of producing mutants with desirable traits for large-scale cultivation.

5. Fluorescence screening of putative mutants for altered cell photophysiology

Understanding an organism's photophysiology can provide insight into how they acquire, utilize, and convert solar energy into different usable chemical compounds. This can help gauge an organism's overall health, photosynthetic efficiency, environmental adaptation, and response to stresses (Serôdio et al., 2007; Schreiber, 2004; Tan et al., 2019; Zijffers et al., 2010). For

instance, Lee and Hsu (2009) demonstrated that sustained high temperatures caused damage to photosynthetic systems in the marine green alga *Codium edule*, leading to inhibition of photosynthetic activity. Nutrient deficiency can lead to reduced content of photosynthetic pigments such as chlorophyll and phycobilin which in turn decreases photosynthetic performance (Tan et al., 2019; Zhao, L.-S. et al., 2017). Photosynthetic systems are also susceptible to oxidative damage caused by high light leading to photoinhibition (Aro et al., 1993; Erickson et al., 2015). Microalgae are able to protect themselves from photooxidative damage by employing nonphotochemical quenching (NPQ), a photoprotective mechanism that dissipates excess absorbed light energy as heat (Cantrell et al., 2023; Erickson et al., 2015). The presence of toxic substances like triazine and phenylurea derivatives, which are Photosystem II (PSII) herbicides, can inhibit photosynthetic efficiency. Schreiber et al. previously proposed the practical usage of photophysiology measurement techniques to detect toxic pollutants that affect photosynthetic efficiency in *Phaeodactylum tricornutum* (Schreiber, et al., 2002). Each of the mentioned stressors are capable of reducing an organism's photosynthetic efficiency which can greatly affect growth rate and ultimately biomass yield, making photophysiology measurements important for monitoring organism health.

Photophysiology of algae can be observed by measuring photosynthetic quantum yield, NPQ, electron transport rate, or by conducting light response curves using pulse-amplitude-modulation (PAM) fluorometry and the saturating pulse method. PAM fluorometry is a non-invasive tool that works by modulating a measuring light that periodically pulses, exciting chlorophyll molecules without triggering electron transport. This enables the ability to distinguish between fluorescence that is emitted from photosynthesis and ambient light. A saturating pulse of high intensity light is applied to PSII in chloroplasts which causes a

temporary closure of all PSII reaction centers, allowing maximum fluorescence (Fm) to be measured. The minimum fluorescence (Fo) is then measured under dark-adapted conditions when all PSII reaction centers are open. These values are used to calculate different photophysiological parameters such as maximum quantum yield of PSII (ΦPSII), nonphotochemical quenching (NPQ), photochemical quenching coefficient (qL), and electron transport rate (ETR) (Schreiber, et al., 2002, Zuo et al., 2022).

Measuring photosynthetic quantum yield of PSII is important for quantifying the efficiency of PSII to absorb and utilize photon energy for photosynthesis. This is done by dark acclimating cells followed by a saturation pulse that excites chlorophyll *a* causing it to fluoresce which is then measured via the PAM fluorometer (Schreiber, 2004). 15-30 minutes of dark acclimation of prior to photophysiology measurements is crucial to allow for the complete oxidation of PSII and the electron transport chain, allowing for minimal fluorescence to be measured before exposing cells to a saturating light pulse to allow for maximum fluorescence to be measured (Perri et al., 2021). This is denoted as a ratio between variable fluorescence, Fv, and maximal fluorescence, Fm (Fv/Fm) which is the maximum quantum yield of PSII (Schreiber, 2004; Tan et al., 2019; Xia et al., 2023). Green algae have been shown to produce quantum yield values around 0.7 when in normal, exponential growth conditions, meaning that 70% of the absorbed light is utilized for photochemistry in PSII (Schuurmans et al., 2015/Young & Beardall, 2003; Barten et al., 2021/Li, T. et al., 2020). Genty et al. (1989) demonstrated the positive correlation between ΦPSII and quantum yield of CO_2 assimilation, suggesting that as a photosynthetic organism's efficiency of light absorption increases, the conversion into chemical energy also increases.

Light response curves are used to determine how photosynthetic efficiency varies as a function of light intensity. They can be used to determine optimal light conditions to maximize photosynthetic efficiency without causing stress and photoinhibition in cells (Ögren & Evans 1993). Cells are dark acclimated before being exposed to a series of increasing actinic red-light intensities with periodic saturating pulses using PAM fluorometry (Cantrell et al., 2023). At designated time intervals, a saturation pulse is administered, and chlorophyll fluorescence is measured (Schreiber, 2004). The PAM fluorometer records and calculates values such as Fv/Fm, NPQ, qL, ETR as well as other photosynthetic values. Light response curves are graphed as any of these photosynthetic values as the dependent variable against photosynthetically active radiation (PAR).

NPQ is a photoprotective mechanism used by plants to prevent possible damage caused by excessive light (Ruban, 2016). When an organism is overexposed to light energy, their light harvesting complexes trigger varying biochemical pathways that dissipate excess absorbed light energy in the form of heat which protects from damage to photosynthetic components (Ruban, 2016). These biochemical pathways can vary by organism but all function as photoprotective mechanisms. Measuring NPQ is therefore useful for understanding how light intensity impacts an organism's photosynthetic processes (Schreiber, 2004). Similarly, qL is the quenching coefficient for the reduction of the PSII quinone electron acceptor. Values of qL range from 0-1, indicating a percentage of open PSII reaction centers. An improved qL reflects quicker adjustments in PSII reaction center activity under light, allowing efficient photon utilization without over-reduction, and rapid reopening of reaction centers in the dark, returning qL to 1. NPQ activation under high light conditions leads to a reduction in light energy reaching PSII, reducing qL, making these two values interconnected (Schreiber, 2004).

Electron transport rate is directly related to photosynthetic components such as Photosystems I and II and its measurement can be useful in determining the efficiency of the electron transport chain during light-dependent reactions during photosynthesis (Masojidek, 2001; Takagi et al., 2022). Increased rates of electron transport have been shown to cause increased carbon assimilation rates in two symbiont-bearing phytoplankton (Takagi et al., 2022). The reliability of ETR quantification using methods that measure chlorophyll fluorescence have been questioned due to the tandem operation of both photosystems and the overall complexities that the photosynthetic process presents (Furutani et al., 2022). More advanced dual PAM fluorometers are capable of measuring both photosystems simultaneously, but these instruments calculate ETR using user-selected PAR values and a manufacturer-calculated constant which can lack specificity (Heinz Walz GmbH).

For this application, rather than growing each mutant generated, a fluorescent-based screening method demonstrated by Ware et al. (2020) was used to search for differences in photophysiological traits such as impaired electron flow, significant increases in maximum photochemical quantum yield, or altered non-photochemical quenching, which can be indicative of improved productivity. Ware et al. (2020) screened, isolated, and cultured putative mutants of interest, resulting in the discovery of three putative *Desmodesmus armatus* mutants with significantly improved biomass production compared to wild type. This is a high throughput screening approach due to its ability to detect photophysiological alterations indicative of improved productivity without having to culture each assumed generated mutant. Traditional growth-based screening methods are typically low throughput, time consuming, and expensive, as they require culturing each supposed mutant to observe growth performance.

6. Summary

The objective of this thesis was to first triage ten microalgal strains based on their productivity in a wide range of temperatures. Growth rates and biomass accumulation was measured to determine overall performance in both temperatures. The two best performing strains were selected and subjected to gamma irradiation mutagenesis. Isolated putative mutants were then screened using a novel chlorophyll fluorescence-based approach previously described by Ware et al. (2020). Putative mutants that demonstrated alterations in photophysiology that were indicative of increased photosynthetic efficiency were selected for growth performance assays to compare them with their wild type counterparts. Obtaining mutants with improved growth and biomass accumulation compared to wild type was the final goal of this thesis.

CHAPTER 1. TEMPERATURE-DEPENDENT GROWTH AND BIOMASS PERFORMANCE OF MICROALGAL STRAINS FOR LARGE-SCALE CULTIVATION

1. Introduction

Large-scale cultivation of microalgae in outdoor raceway ponds is the leading method for industrial biofuel and bioproduct production (Abdur Razzak et al., 2024). However, maximizing productivity under outdoor conditions remains a challenge due to environmental fluctuations that can influence algal productivity (Karthikeyan et al., 2016). Identifying strains capable of maintaining high productivity across a range of temperatures is essential for ensuring stable and efficient cultivation at large-scale, particularly in open raceway ponds where natural temperature fluctuations are common. Previous research has demonstrated that strains, such as *Scenedesmus acutus* and *Monoraphidium minutum*, exhibit a broad thermal tolerance and are suitable candidates for large-scale production (El-Sheekh et al., 2017; Calhoun et al., 2022). Understanding strain-specific temperature responses is important for optimizing algal cultivation strategies, particularly in regions with variable seasonal climate.

Temperature is a predominant environmental factor that drives algal growth, directly influencing metabolic activity, enzymatic function, biomass accumulation, lipid production, and protein content (Barten et al., 2021; Lee et al., 2018; El-Sheekh et al., 2017; He et al., 2018). These factors are important for determining whether a strain is suitable for industrial applications. Temperature related stress can alter cellular composition, with some strains exhibiting increased lipid accumulation under temperature stress, making them more favorable for biofuel production, while others prioritize protein synthesis, making them better suited for feedstock or other biotechnological applications (Hu et al., 2008; Renaud et al., 2002; Boussiba et al., 1987). Understanding these temperature-induced metabolic shifts can aid in the selection

of strains that not only grow efficiently in variable temperatures but also yield desirable biomass productivity for large-scale production of bioproducts.

The ability to maintain consistent biomass production under fluctuating environmental conditions is a key challenge in large-scale outdoor microalgal cultivation. While laboratory-scale studies, especially those in closed photobioreactors have demonstrated the high growth potential of many algal strains, these optimal conditions can be harder and more expensive to replicate in industrial settings (Krzemińska et al., 2015; Acién Fernández et al, 2013; Zhu, Y. et al., 2018). Open raceway ponds are among the most promising large-scale cultivation systems due to their low operational costs and ease of implementation. However, they are highly susceptible to environmental fluctuations, contamination risks, and inconsistent nutrient availability, making strain selection critical for maximizing productivity (Costa et al., 2019; Zhu, C. et al., 2022). Identifying and optimizing strains that maintain a high productivity as well as a resilience to environmental fluctuations will be essential to enhance large-scale algal cultivation.

Total organic carbon (TOC) analysis is a reliable method for quantifying biomass accumulation in algal cultures by measuring the amount of carbon present in a sample. Unlike traditional biomass measuring methods such as dry weight which is time and energy intensive, TOC analysis provides a rapid and sensitive approach to assessing the organic content of cultures, making it particularly useful for monitoring growth trends over time (Saxena et al., 2021; Liu, K. et al., 2019). This technique is especially advantageous in large-scale cultivation systems where continuous biomass monitoring can be necessary to monitor production efficiency.

The experiments conducted in this chapter aimed to assess the growth performance of selected algal strains across varying temperatures. Initial cultivation occurred in small-scale

batch cultures maintained at 18°C and 30°C to observe their specific growth rates. Subsequent experiments used larger-scale Roux flasks to evaluate scalability to observe the ability of the algal strains to maintain consistent growth performance and productivity when transitioning from small-scale batch cultures to larger cultivation systems. The strains chosen for this study were selected based on their previously established capacity for high biomass productivity and adaptability to a wide range of environmental conditions. The aim of this chapter's research was to identify candidate mutants optimally suited for scalable outdoor algal cultivation in Gillette, WY for biomass production.

2. Materials and Methods

2.1. Culture strains, conditions, and growth media

2.1.1. Selected Microalgal Strains

Picochlorum celeri TG2-CSM/EMRE, *Picochlorum renovo* NREL 39-A8, *Scenedesmus obliquus* UTEX393, *Scenedesmus acutus* LRB-AZ-0401, and *Scenedesmus rubescens* NREL 46B-D3, *Monoraphidium minutum* 26B-AM are strains characterized in the DISCOVR consortium project (Huesemann et al., 2023). SAmud7 and SRTC14 are uncharacterized strains gifted to the Peers lab by Pete Lammers. Additionally, we assayed *Nannochloropsis oceanica CCAP849/10* (gift from Sandia National Laboratory) and *Phaeodactylum tricornutum CCAP1055/1* (gifted to the Peers lab by Andy Allen, UC San Diego)

2.1.2. Growth media and culture maintenance

The first 8 algal strains are fresh- or brackish water strains. They were cultured in BG-11 pH 8 growth media modified from (Rippka et al., 1979). This recipe consists of 1L H_2O, 10ml of

100x BG-FPC stock (149.58 g/L $NaNO_3$, 7.49 g/L $MgSO_4$, 3.6 g/L $CaCl_2 \cdot 2H_2O$, 1.12 ml/L Na-EDTA, 250 mM, pH 8.0, 1ml of Fe ammonium stock (0.3 g/50 mL Fe ammonium citrate), 1 ml of 189 mM Na_2CO_3 stock, 1 ml of 175 mM K_2HPO_4 stock, and 10ml 1M TES-KOH, pH 8.2. To this, 100 mL/L trace mineral stock was added. The trace minerals stock consists of 2.86g/L H_3BO_3, 1.81g/L $MnCl_2 \cdot 4H_2O$, 0.222 g/L $ZnSO_4 \cdot 7H_2O$, 0.39 g/L $Na_2MoO_4 \cdot 2H_2O$, 0.079 g/L $CuSO_4 \cdot 5H_2O$, and 0.0494 g/L $Co(NO_3)_2 \cdot 6H_2O$ and is stored at 4°C. The media was autoclaved for 20 minutes and stored at room temperature. Solid BG-11 media was made by preparing a 500 ml 2X salts solution of liquid BG-11 with the addition of 3 g $Na_2S_2O_3 \cdot 5H_2O$, as well as a 500 ml 2X agar solution containing 15 g Fisher Scientific Agar. Both solutions were autoclaved for 20 minutes. The medium was then allowed to cool to 55°C and the 2X salts solution was added to the 2X agar solution.

N. oceanica and *P. tricornutum* were grown in F/2 media adapted from Guillard (1975). 35.95 g/L Instant Ocean™ was dissolved in deionized water, supplemented with 300 µL Proline A and Proline B micronutrient stocks (Pentair Aquatic Eco-Systems). This solution was then filtered through a sterile 0.22 µm filter and stored at room temperature.

Cultures were maintained at 25°C aside from *Phaeodactylum tricornutum* which was grown at 18°C. All cultures were grown under ~200 µmol photons m^{-2} s^{-1} constant light conditions on an orbital shaker operating at 125 rpm (VWR, Model 3500). All cultures were diluted once a week. Prior to growth experiments, cultures were diluted and allowed to grow for no more than 3 to 4 days before commencing data collection.

2.1.3. Light measurements

Light intensity was measured using a Li-Cor LI-250A light meter. Light intensities on moving surfaces such as orbital shakers were measured using the "average" function on the

device which captures 15 seconds of light intensities. A WALZ ULM-500 light meter and logger was also used to measure light intensities. These light meters differ as the Li-Cor LI-250A is a 2π meter capable of measuring light in a hemisphere while the WALZ ULM-500 is a 4π meter capable of measuring light in a full sphere The Li-Cor light meter was used to measure light intensities in growth chambers as well as the IMAGING-PAM where light was directed downwards towards cultures. The WALZ ULM-500 was used to measure light in the DUAL-PAM as it contains two light sources on either side of the sample.

2.2. Cell density and growth rate measurements

2.2.1. Hemocytometer cell density

To obtain a cell density using the hemocytometer, 10µl of well mixed cell culture was pipetted into the hemocytometer and allowed to rest for at least 5 minutes to allow cells to settle onto the slide. If the culture was too dense to accurately count, it was diluted in sterile media. A minimum of three of the nine hemocytometer squares (each is 10^{-1} µl) were counted to ensure that a consistent sample area was selected, as long as the minimum number of cells counted was greater than or equal to 100. The following equation was used to determine the density of the cultures measured in cells/µl:

(Total cells counted × Dilution factor × 10 μl^{-1}) / Number of squares counted = cells μl^{-1}

$$\text{cells } \mu l^{-1} = \frac{(\text{total cells counted} \times \text{dilution factor} \times 10^{-1})}{\text{number of squares counted}}$$

2.2.2. Flow cytometer cell density

Prior to sampling, cultures were diluted in their media to not exceed 2000 events μl^{-1} to avoid clogging the flow cell. After dilution, the culture was filtered through a 30 µm Pre-Separation Filter (Miltenyi Biotech) into a 2ml Eppendorf microcentrifuge tube. Before measuring, the microcentrifuge tube was vortexed on max speed for 3 seconds using a Scientific

Industries Vortex-Genie 2. Cultures were cell counted using a BD Accuri C6 Flow Cytometer which uses a blue 488 nm laser and a red 640 nm laser for fluorescence excitation. Particle fluorescence was obtained using the FL3 filter (>670nm). This data was gated to $>10^4$ RFU to exclude any cellular debris or dead cells. The cytometer was set to measure for 40 seconds with a flow rate of 35 µl min^{-1} and a core size of 16 µm. The gated particle data was then multiplied by the dilution factor used to obtain a cell density in cells μl^{-1}.

2.2.3 Optical density measurement

Relative cell culture density was also assayed using an Agilent Technologies Cary 60 UV-Vis Spectrophotometer that was blanked prior to measurement using 1 ml of sterile F/2 or BG-11 depending on the strain being measured. *In vivo* absorption at 680 nm (OD_{680}) was utilized and 1ml of cell culture was measured. The cell culture was diluted to achieve an OD value less than or equal to 1 as values above 1 fall outside the instrument's linear range where transmitted light can become too attenuated for accurate detection, leading to potential measurement errors. The dilution factor was then multiplied by the OD value to achieve the true OD measurement.

2.2.4 Calculating specific growth rate

Specific growth rates (μ = day $^{-1}$) were calculated by measuring the slope of the natural log of a minimum of three cell counts or optical density measurements over a period of at least two days. The slope (μ) of a least-squares regression analysis was solved with the following formula:

$$\mu(d^{-1}) = \frac{\ln(\Delta \text{ cell density})}{\ln(\Delta \text{ days})}$$

R^2 values are calculated using the method described by Motulsky & Christopoulos (2004). Growth rates were selected based on which regression line had an R^2 value closer to 1 rather than simply choosing the largest slope. This approach ensures that the selected growth rate is based on the best statistical fit rather than the highest value.

2.3. Growth screening of strains

2.3.1. Small-scale growth screening – 250ml flasks

Strains were diluted to less than 350 cells μl^{-1} in 50 ml of their growth media using the dilution equation, $(C_1 \bullet V_1) = (C_2 \bullet V_2)$. All strains were grown in duplicate sterile 250mL flasks at 18 and 30°C under 16h high light (750 µmol photons m^{-2} s^{-1}), 8 hours dark conditions while constantly shaking at 150 RPM using an orbital shaker. Cultures were cell counted via hemocytometer daily.

2.3.2. Large lab-scale growth screening – 1L Roux flasks

Strains were screened in sterile 1L Roux flasks diluted to an OD_{680} = 0.025 in 600 ml of media. After dilution, Roux flasks were assembled in a sterile environment using a size 5 silicone stopper (Cole-Parmer Instrument Co.) with three 2.5 mm holes made in the stopper. Each of these three holes contained a 3 mm wide PTFE tube with a 1 mm diameter lumen. At the top of the first tube, was an ICU Medical, Inc. C1000 Clave Connector, connected to the tubing with a flexible silicone tube. The Clave Connector allows for the sterile harvesting of cell cultures using a syringe with a Luer-Lok tip. The first tube was cut to about 26 cm in length and positioned so that the bottom of it was submerged in the cell culture. The second tube was designed for aeration and featured a Fisherbrand 0.2 µm pore size, 25mm wide filter at the top, while its bottom end was heat-sealed and punctured with a 10-gauge needle along the lower 8 cm of the tube. These smaller holes produced finer bubbles during sparging, improving gas

exchange and reducing the force exerted by the bubbles. The second tube was around 30 cm in length and positioned so that the lower 8 cm were completely submerged in the cell culture. Finally, the last tube was used as an "exhaust" to prevent an internal pressure from building up in the flask. This consisted of a 6 cm tube with no other connections on it. Roux flasks were positioned at an approximately 60° angled orthogonally towards the light source and continuously sparged at a rate of 1L air min^{-1}. The flasks were exposed to 16 hours of 800 µmol photons m^{-2} s^{-1} light and 8 hours of darkness and their positions were randomized daily. Cultures were tested at 18 and 30°C and a further experiment was performed at 30°C without air filtration. Exponential growth rates were calculated based on OD_{680} values as described above.

2.4. Assessment of biomass accumulation

2.4.1. Cell harvesting

40 ml of cell cultures were harvested directly from their Roux flasks into 50 ml Falcon tubes at days 0, 3, and 6. These samples were then centrifuged at 2500 × g for 10 min (4 °C) after harvesting. After centrifugation, the supernatant was separated into its own Falcon tube and the cell pellet was resuspended to 40 mL using 0.22 µm filtered DI water. If the pellet did not homogenize into the DI water properly and cells were visibly clustering, then the cells were sonicated using a QSonica sonicator at max power for 60 seconds to break up any cell aggregates. Resuspended cell samples were then stored at -80°C to prevent any degradation of organic carbon content.

2.4.2. Total organic carbon analyses

Total organic carbon (TOC) samples were analyzed with a Sievers InnovOx ES Laboratory TOC Analyzer. Samples were transferred to 40ml glass vials with a VWR micro stir

bar. Biomass samples were measured using the TOC measurement setting calibrated to detect a range of <5000ppm TOC. To verify the accuracy of the results, organic and inorganic carbon (OC and IC, respectively) values were cross-checked by including a 100 ppm OC and IC standard solution with each batch of samples. 6M phosphoric acid and a sodium persulfate solution (300 g/L) were prepared fresh prior to sample analysis. A 1000ppm IC standard was made by preparing solution containing 3.397g $NaHCO_3$ and 4.412g Na_2CO_3 and dissolving it with 1L DI water. A 1000ppm TOC standard was made by making a solution of 2.25g $C_8H_5NaO_4$ and dissolving it with 1L DI water. Prior to preparing the standards, all three powders were stored in a drying oven set to 50°C to allow the evaporation of any moisture in the powders that could skew mass measurements. After preparing the solution, it was stirred on a stir plate until no particulates were visible. All plastic/glassware used for TOC analyses were soaked in 1M HCl, rinsed thoroughly with DI water, and dried at 50°C prior to use to remove traces of organic carbon. The 6M phosphoric acid is used by the machine to determine ppm of inorganic carbon by reacting with carbonates and bicarbonates to produce CO_2 which is measured. The sodium persulfate solution as well as UV radiation oxidizes organic carbon compounds into CO_2 and is reported back as ppm TOC. Samples in the machine are measured four times with the average ppm of TOC or IC being calculated from the three samples with the lowest relative standard deviation. Two initial vials containing DI water are used to flush the instrument prior to measuring. Cell and supernatant samples are separated by one flush vial to prevent any crossover of liquid sample as the prior sample can have a mild influence on the sample directly after it. Flasks containing sterile BG-11 or F/2 were used as a control for this experiment for future organic and inorganic carbon measurements.

Calculating mass of carbon on a per cell basis was obtained using the following equation. This equation was also used for inorganic carbon measurements:

$$\text{pg C cell}^{-1} = \frac{(\text{ppm TOC} \times 10^3 \times \text{dilution factor})}{\text{cells } \mu\text{l}^{-1}}$$

Statistical analysis was performed using R (R Core Team). A one-way ANOVA was used to compare biomass accumulation of the tested strains with the addition of a post-hoc Tukey HSD test. Samples with $p < 0.05$ were considered statistically different.

3. Results

3.1. Evaluation of growth performance at 250ml flask scale – duplicate cultures

3.1.1 Low temperature cultivation – 18°C

To assess the low-temperature growth potential of different strains, cultures were grown in duplicate in 50 mL BG-11 media at 18°C. Testing strains under low-temperature conditions is crucial for identifying those with enhanced cold resistance, which could improve biomass productivity in cooler environments or during seasonal temperature fluctuations. At 18°C, *Phaeodactylum tricornutum* and *Scenedesmus acutus* exhibited the highest specific growth rates of 1.24 and 1.30 day^{-1}, respectively (Table 1.1). *Nannochloropsis oceanica* retained a specific growth rate above 1.0 day^{-1} with low variability between duplicate cultures. *Picochlorum renovo* and SRTC14 were the lowest performing strains, never reaching a specific growth rate higher than 0.85 day^{-1}. While counting cells with a hemocytometer, cell clumping was observed to varying degrees in several strains including *Nannochloropsis oceanica, Scenedesmus acutus, Scenedesmus obliquus,* and SAmud7.

Table 1.1: Growth rates of algal strains grown at 50 ml scale (18°C). Specific growth rates of strains grown in duplicate 250 ml flasks in 50 ml media under 16h 750 µmol photons m^{-2} s^{-1} light and 8h dark (n=2).

Strain	Specific Growth Rate Range at 18°C (day^{-1})
Phaeodactylum tricornutum	1.20 - 1.24
Nannochloropsis oceanica	1.00 - 1.04
Picochlorum celeri	0.89 - 0.92
Picochlorum renovo	0.77 - 0.80
Scenedesmus acutus	1.00 - 1.30
Scenedesmus obliquus	0.93 - 1.03
Scenedesmus rubescens	0.88 - 1.07
Monoraphidium minutum	0.83 - 0.91
SAmud7	0.88 - 0.93
SRTC14	0.85

3.1.2 High temperature cultivation – 30°C

To assess the low-temperature growth potential of different strains, cultures were grown in duplicate in 50 mL BG-11 media at 18°C. Testing strains under low-temperature conditions is crucial for identifying those with enhanced cold resistance, which could improve biomass productivity in cooler environments or during seasonal temperature fluctuations. Ten algal species were grown in 30°C under identical light and media conditions previously mentioned. Of note, *Phaeodactylum tricornutum* slowly decreased in cell density following inoculation, resulting in a negative growth rate. The two *Pichochlorum* species showed very different growth rates in the high temperature range. *Picochlorum celeri* demonstrated the highest specific growth rate range of 2.10 - 2.13 day^{-1} with *Picochloum renovo* only growing from a range of 1.46 - 1.48 day^{-1} (Table 1.2). *Scenedesmus acutus* had a specific growth rate range of 1.47 - 1.62 day^{-1} with some variation likely due to cell flocculation interfering with the accuracy of the OD_{680}

measurement. After three days of growth, *Scenedesmus obliquus* was seen forming a mild ring of cells on the edge of the flask that was shaken back into suspension daily. *Scenedesmus rubescens* had a rather low and variable specific growth rate range compared to the other *Scenedesmus* species (Table 1.1). It also was observed to form clusters of cells after a few days of growth. Similarly to the results observed at 18°C, SRTC14 had a low specific growth rate compared to the other strains tested.

Table 1.2: Growth rates of algal strains grown at 50 ml scale (30°C). Range of specific growth rates (exponential phase) of strains grown in duplicate 250 ml flasks in 50 ml media under 16h 750 µmol photons m^{-2} s^{-1} light and 8h dark (n=2).

Strain	Specific Growth Rate Range at 30°C (day^{-1})
Phaeodactylum tricornutum	-0.35 - -0.33
Nannochloropsis oceanica	1.21 - 1.22
Picochlorum celeri	2.10 - 2.13
Picochlorum renovo	1.46 - 1.48
Scenedesmus acutus	1.47 - 1.62
Scenedesmus obliquus	1.64 - 1.69
Scenedesmus rubescens	1.23 - 1.38
Monoraphidium minutum	1.04 - 1.07
SAmud7	1.48 - 1.54
SRTC14	1.00 - 1.06

Growth performance at 18°C and 30°C highlights strain suitability for specific conditions. At 18°C, *Phaeodactylum tricornutum* and *Scenedesmus acutus* excelled, while *Picochlorum renovo* and SRTC14 underperformed. At 30°C, *Picochlorum celeri* showed the highest growth rate, whereas *Phaeodactylum tricornutum* declined. *Scenedesmus obliquus* and *Scenedesmus acutus* also performed well, though cell clumping introduced variability. SRTC14

demonstrated some of the lowest growth rates across temperatures but was kept for further testing. As *Phaeodactylum tricornutum* did not survive at a higher temperature, it was cut from subsequent growth assays.

3.2. Evaluation of growth performance at roux flask scale - single cultures

3.2.1. Low temperature cultivation – 18°C

Among the tested strains, *Scenedesmus rubescens* exhibited the highest specific growth rate (1.6 day^{-1}) and OD_{680} after six days of growth (2.9), indicating its strong adaptability to the cooler end of the predicted larger-scale cultivation conditions (Table 1.3). *Scenedesmus acutus* and *Scenedesmus obliquus* were the next two high performing strains with specific growth rates of 1.1 and 1.3 day^{-1} respectively, and an OD_{680} of 2.0 for both. *Monoraphidium minutum* followed behind with a specific growth rate of 0.8 day^{-1} and an OD_{680} of 1.8.

In contrast, *Picochlorum celeri* and *Picochlorum renovo* struggled to grow effectively at 18°C, with their growth rates not exceeding 0.5 day^{-1}. SAmud7 and SRTC14 demonstrated similar or slightly reduced specific growth rates and OD_{680} measurements compared to the smaller scale tests described in Table 1.1. *Picochlorum renovo,* SAmud7, and SRTC14 were cut from future experiments due to their poor performance at low temperature.

Table 1.3: Specific growth rates (day^{-1}) and optical densities (OD_{680}) of selected algal strains grown at single 600 ml scale (18°C). Cultures were grown for 6 days in single roux flasks under 16h 800 µmol photons m^{-2} s^{-1} light and 8h dark (n=1).

Strain	Specific Growth Rate at 18°C (day^{-1})	OD_{680} after 6 days of growth
Nannochloropsis oceanica	1.0	1.0
Picochlorum celeri	0.4	0.5
Picochlorum renovo	0.5	0.3
Scenedesmus acutus	1.1	2.0
Scenedesmus obliquus	1.3	2.0
Scenedesmus rubescens	1.6	2.9
Monoraphidium minutum	0.8	1.8
SAmud7	0.7	0.8
SRTC14	0.6	0.9

3.2.2. High temperature cultivation – 30°C

Roux flasks represent a different growth environment than Erlenmeyer flasks and are used because they provide a larger surface area-to-volume ratio, allowing for enhanced gas exchange and light exposure. The nine remaining strains were grown in Roux flasks to assess growth performance at a larger scale in both 18°C and 30°C. In 30°C conditions, *Picochlorum celeri* had an equally as fast specific growth rate as *Scenedesmus rubescens* (1.9 day^{-1}) but *Picochlorum celeri* achieved a higher OD_{680} after six days of growth, making it the overall best performing strain in this test (Table 1.4). The OD_{680} of *Scenedesmus obliquus* after six days of growth was 6.4 but the Roux flask had noticeable evaporation, as there were salt deposits surrounding the exhaust port and the liquid level was visibly lower compared to the other flasks

at the time. So this high OD is likely due to factors other than superior growth characteristics. *Scenedesmus acutus* had the overall lowest growth performance, growing at a maximum specific growth rate of 1.2 day^{-1} and only achieving a day six OD_{680} of 2.2. SAmud7 and SRTC14 demonstrated adequate growth in both conditions but ultimately did not outperform any of the other high performing characterized strains included in this experiment. Specific growth rates were calculated using the natural log of OD_{680} as well as the natural log of cell density values and were determined to be comparable (Table S1). From here on, specific growth rates were calculated using the natural log of OD_{680} values.

Table 1.4: Specific growth rates (day^{-1}) and optical densities (OD_{680}) of selected algal strains grown at single 600 ml scale (30°C). Cultures were grown for 6 days in single roux flasks under 16h 800 µmol photons m^{-2} s^{-1} light and 8h dark (n=1). (*) Denotes high levels of evaporation noticed.

Strain	Specific Growth Rate at 30°C (day^{-1})	OD_{680} after 6 days of growth
Nannochloropsis oceanica	1.4	4.2
Picochlorum celeri	1.9	4.2
Picochlorum renovo	1.4	4.3
Scenedesmus acutus	1.2	2.2
Scenedesmus obliquus	1.6	6.4*
Scenedesmus rubescens	1.9	3.2
Monoraphidium minutum	1.0	3.2
SAmud7	1.3	4.2
SRTC14	1.2	4.0

3.3. Evaluation of growth performance at roux flask scale – triplicate cultures

3.3.1. High temperature cultivation – 30°C

The remaining 6 species were grown in triplicate Roux flasks diluted to an OD_{680} = 0.035 and grown for six days to assess specific growth rate. maximum OD_{680} and TOC (Total Organic Carbon). Despite having the highest exponential growth rate, *Scenedesmus acutus* exhibited the lowest final OD_{680} of 2.8 ± 1.5. In contrast, *Monoraphidium minutum* achieved the highest final OD_{680} of 4.8 ± 0.3 but displayed a more moderate exponential growth rate of 1.0 day^{-1}. *Nannochloropsis oceanica* also had a maximum specific growth rate of 1.0 day^{-1} but only reached a final OD_{680} of 3.9 ± 0.3. *Scenedesmus obliquus* also performed well, achieving a final OD_{680} of 4.3 ± 0.6 with a specific growth rate of 1.6 ± 0.1 day^{-1}, similar to *Scenedesmus rubescens*, which reached an OD_{680} of 3.9 ± 1.1. *Picochlorum celeri*, demonstrated a moderate specific growth rate of 1.4 ± 0.1 day^{-1} and a final OD_{680} of 3.7 ± 0.7.

Table 1.5: Average specific growth rates (day^{-1}) and optical densities (OD_{680}) of selected algal strains grown at triplicate 600 ml scale (30°C). Cultures were cultivated for 6 days in roux flasks under 16h 800 μmol photons m^{-2} s^{-1} light and 8h dark. Values reported are averages ± 1 standard deviation (n=3).

Strain	Average Specific Growth Rate at 30°C (day^{-1})	OD_{680} after 6 days of growth
Nannochloropsis oceanica	1.0 ± 0.1	3.9 ± 0.3
Picochlorum celeri	1.4 ± 0.1	3.7 ± 0.7
Scenedesmus acutus	1.8 ± 0.0	2.8 ± 1.5
Scenedesmus obliquus	1.6 ± 0.1	4.3 ± 0.6
Scenedesmus rubescens	1.6 ± 0.1	3.9 ± 1.1
Monoraphidium minutum	1.0	4.8 ± 0.3

3.3.2. Total organic carbon (TOC) biomass quantification

40 ml from each culture was removed on days 0, 3, and 6 of growth for biomass quantification via total organic carbon (TOC) analysis. *Scenedesmus rubescens* accumulated the most organic carbon by day 6 (1285 ± 322 ppm TOC). *Monoraphidium minutum* accumulating 836 ± 49 ppm TOC, making it the second most productive strain tested (Figure 1.1). *Scenedesmus rubescens* also had a relative standard deviation of 25.1% making it the highest in terms of biomass accumulation variability. *Nannochloropsis oceanica* was the third most productive strain with 682 ± 16 ppm TOC accumulated. Its consistent growth rate and optical density resulted in one of the smallest variations in day six biomass accumulation. *Picochlorum celeri* accumulated the lowest amount of carbon (281 ± 5 ppm TOC) of the six strains tested. A one-way ANOVA and post-hoc Tukey HSD test was performed and determined *S. rubescens* to be significantly higher than the othe strains tested while *M. minutum* was only significantly higher than *P. celeri* ($p < 0.05$).

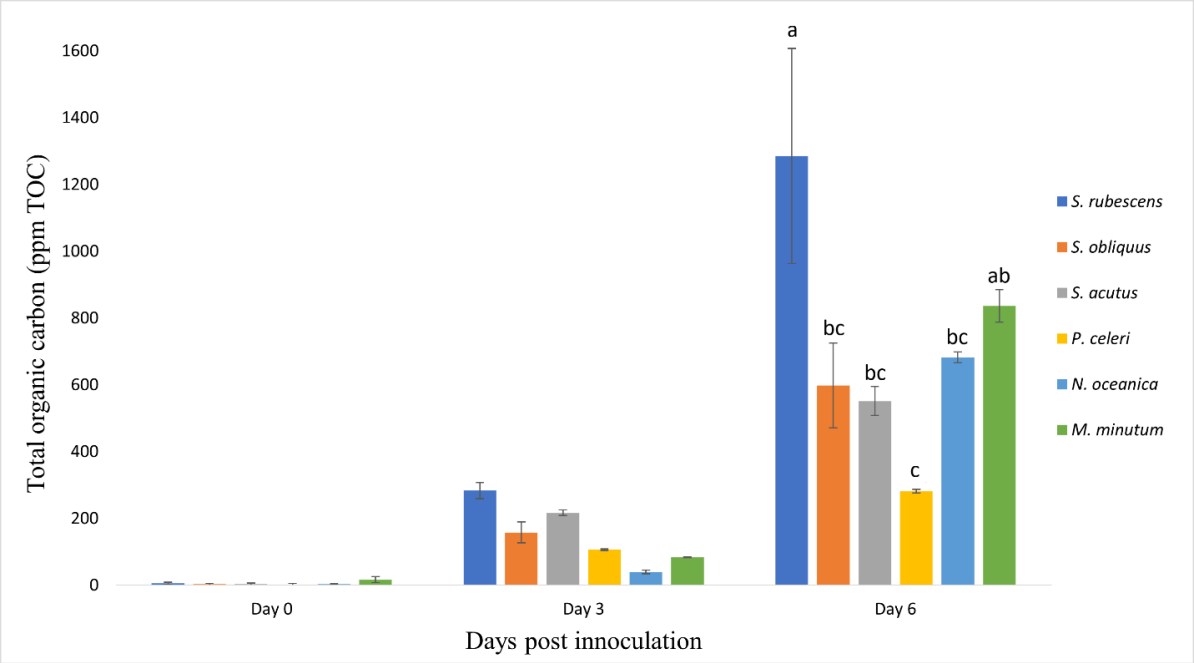

Figure 1.1: Total Organic Carbon Content of Algal Pellets from Cultures Grown at 30°C Under High Light. Cultures were grown for 6 days in triplicate roux flasks under 16h 800 µmol photons m^{-2} s^{-1} light and 8h dark. 40 ml aliquots were taken on days 0, 3, and 6 and processed for TOC analyses. Values represent averages ± 1 standard deviation (n=3). A single factor ANOVA and post-hoc Tukey HSD was performed for the results of day 6.

3.3.2. Estimation of carbon content per cell

Lastly, mass of organic carbon was calculated on the cellular level using the cell counts taken at the time of aliquots and the TOC results shown in Figure 1.1. The findings shown in Figure 1.2 suggest that *Nannochloropsis oceanica* accumulated 5.7 ± 0.7 pg TOC $cell^{-1}$ after six days of growth. *Scenedesmus rubescens* demonstrated the largest mass of organic carbon with an average of 149 ± 29 pg TOC $cell^{-1}$ after six days of growth. *Picochlorum celeri* cells accumulated the lowest amount of TOC, only averaging 1.0 ± 0.1 pg TOC $cell^{-1}$ on day 6. Lastly, *Scenedesmus obliquus* and *Scenedesmus acutus* accumulated 15.8 ± 2.7 pg TOC $cell^{-1}$ and 32.9 ± 8.0 pg TOC $cell^{-1}$ by day 6. Overall, mass of TOC per cell could be seen increasing from day 0 to 6 aside from *Monoraphidium minutum* which contained 45.0 ± 6.5 pg TOC $cell^{-1}$ following inoculation. A one-way ANOVA and post-hoc Tukey HSD test was performed and

determined *S. rubescens* to be significantly higher than the othe strains tested while *M. minutum* was only significantly higher than *P. celeri* ($p < 0.05$).

Scenedesmus rubesens and *Monoraphidium minutum* were chosen out of the final six strains to be mutagenized due to their high average biomass accumulation and their ability to thrive in a wide range of temperatures.

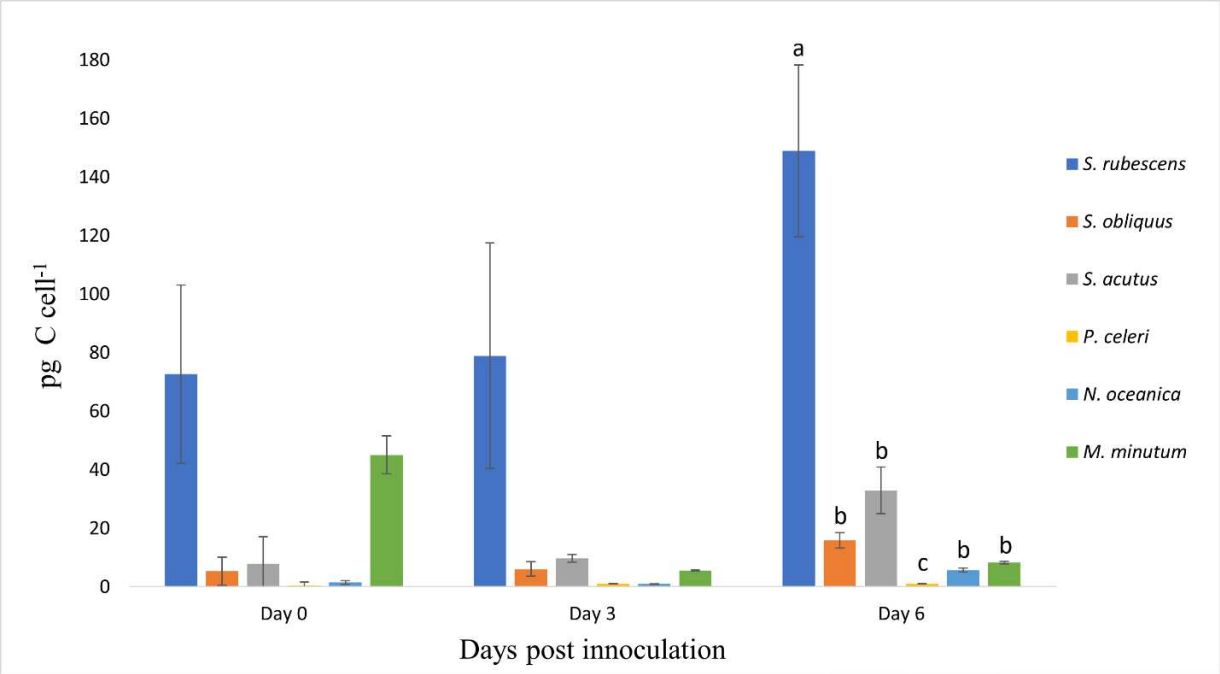

Figure 1.2: Carbon content (pg of carbon cell^{-1}) from algal cultures grown at 30°C under high light. TOC values shown in figure 1.1 were used to calculate mass of carbon with cell counts of triplicate cultures taken on days 0, 3, and 6. Values represent averages ± 1 standard deviation (n=3). A single factor ANOVA and post-hoc Tukey HSD was performed for the results of day 6.

4. Discussion

4.1. Evaluation of growth performance at 250ml flask scale – duplicate cultures

Ten algal strains were initially grown in duplicates in 50 mL of media in both 18 and 30°C to assess growth performance at a wide range of temperatures. Seasonal temperature fluctuations for commercial scale outdoor growth are important to consider as a strain might perform well in the spring/fall months but not in the summer and vice versa. However, the goal of this experiment was to identify an algal strain capable of tolerating a wide range of outdoor temperatures in Gillette, WY (National Weather Service, n.d.). So the first task of this thesis was to triage strains based on these criteria.

4.1.1. Low temperature cultivation – 18°C

The highest average specific growth rate being demonstrated by *Phaeodactylum tricornutum* was expected as optimal growth rates for this species have been shown in temperatures ranging from 18-21°C, making it an ideal winter strain for large scale cultivation. (Ova Ozcan & Ovez, 2020 / Pereira et al., 2021). *Scenedesmus acutus* has previously been shown to grow and remain productive across a temperature range of 15-40°C (El-Sheekh et al., 2017). While *Scenedesmus acutus* achieved a maximum growth rate of 1.3 day^{-1}, its variability shown between the duplicate cultures resulted in an overall lower average specific growth rate compared to *Phaeodactylum tricornutum*. Despite *Phaeodactylum tricornutum's* excellent performance in colder temperatures, due to its inability to grow at 30°C, it was cut from future experiments.

Cell counting with the hemocytometer revealed notable variation in cell size and frequent cell clumping in some strains. The wide growth rate variation seen in *Scenedesmus acutus* was attributed to one of the two cultures clumping more than the other which skewed cell counting

results. The flask seen flocculating yielded a higher cell count of one of the hemocytometer squares than was likely not representative of the true cell density. This posed as a potential source of error when cell counting non-homogenized strains via hemocytometer. SAmud7 was observed both flocculating and having drastically varying cell sizes throughout the first four days of growth which could have impacted the accuracy of cell counts. *Nannochloropsis oceanica* displayed a mix of cell sizes and shapes, with some retaining a uniform circular structure while others appeared irregular and oblong during the first five days of growth. Flocculation was also observed in *Nannochloropsis oceanica* to a minor degree but growth performance between duplicates remained comparable. Variations in cell morphology were observed in *Nannochloropsis oceanica* and may have resulted from light, temperature, or salinity induced stress (Kholssi et al, 2023). Wang & Jia, (2020) demonstrated that light levels exceeding 500 μmol photons m^{-2} s^{-1} significantly impacted the morphology of *Nannochloropsis oceanica* by altering lipid body sizes and fatty acid composition which makes up various organelle membranes that provide internal structure. Wei and Huang (2017) observed morphological changes in *Nannochloropsis oculata* when exposed to multiple different stressors, one of which being high light irradiation. Understanding how high light irradiation affects microalgal physiology reveals fundamental mechanisms of stress responses and cellular adaptation. This concept can be applied to improve growth performance, productivity, and environmental resilience, across various species.

Cell clumping can be a symptom caused by different environmental stressors such as light, temperature, nutrient deficiency, or pollutants. Two studies involving *Scenedesmus acutus* noticed significant cell clumping in the presence of different environmental pollutants (Chandrashekaraiah et al., 2021 A; Chandrashekaraia et al., 2021 B). While pollutants were not

the causative agent in this study, flocculation of cells could also be caused by high light, sub-optimal temperature, or nutrient limitation (Richmond, 2004; Matter et al., 2019). In addition to cell flocculation, occasionally cells were seen adhering to the sides of flasks. Microalgae are known to secrete extracellular polysaccharides (EPS) which enable them to adhere to surfaces especially under stressful abiotic conditions such as nutrient stress or in light limiting or saturating conditions (Gerbersdorf et al., 2009; Babiak & Krzemińska, 2021; Patwal & Baranwal, 2021). It may be that these strains secrete EPS. This could be a beneficial trait in production of microbial algae biomass as flocculating cells would sink faster and reduce harvesting costs (Li, Tianrui et al., 2021; Tran et al., 2017).

4.1.2. High temperature cultivation – 30°C

Phaeodactylum tricornutum's fatal growth performance in 30°C has been previously demonstrated by Cui, et al. 2020, where *Phaeodactylum tricornutum* was unable to grow effectively in temperatures 30°C and higher. *Picochlorum celeri* demonstrating a high specific growth rate was in line with previous research that showed it to be a high-temperature tolerant strain, capable of thriving at 25-35°C and could quickly adapt to extremely high light (2000 μmol photons m^{-2} s^{-1}) (Huesemann et al., 2023; Weissman et al., 2018). In a previous study, *Picochlorum renovo* was the most productive strain tested in a summer climate-simulated photobioreactor (Huesemann et al., 2023) but only had the 5th highest maximum specific growth rate in this experiment (Table 1.1). No cell flocculation or adhesion was observed in *Picochlorum renovo* during cultivation under these conditions.

The variability in the estimations of specific growth rate was likely caused by cell flocculation. One of the *Scenedesmus acutus* cultures was noticed intensely clumping near day 3 of growth while the other culture showed some mild cell flocculation (cells in groups of 2-4)

beginning on day 2 of growth. The culture with the higher growth rate was observed to be the one where flocculation was the highest. Hemocytometer counts became more variable on day three as a result of large cell clumps being present while counting. Since *Scenedesmus acutus* demonstrated a high growth rate, it was kept to see whether larger scale cultivation would alleviate cell clumping. Likewise, though SRTC14 grew at some of the lowest rates observed, the specific growth rates weren't necessarily as detrimental as the inability for *Phaeodactylum tricornutum* to grow at all at a high temperature, thus being kept in the experiment.

4.2. Evaluation of growth performance at Roux flask scale – single cultres

To assess the scalability of the selected algal strains, they were cultivated in single Roux flasks. Flasks were sparged with ambient air which provides more effective culture mixing than orbital shaking and allows more CO_2 to enter the system. Additionally, cultures in Roux flasks achieve a higher incident light due to their flat, wide dimensions relative to light sources. This provides the ability for cultures to achieve a higher productivity and density compared to cultivation in 250 ml flasks. Optical density was used to calculate growth rate and monitor cell density as it is typically the choice of measurement at large scale cultivation due to its ease of use and ability to be automated (Novoveská et al., 2023). Additionally, in the event of cell flocculation, optical density measurements are easier to acquire compared to manually counting cells via hemocytometer.

4.2.1. Low temperature cultivation – 18°C

The highest three specific growth rates and optical densities were observed in the three *Scenedesmus* species tested, with *Monoraphidium minutum* growing at a slower specific growth rate but still maintaining a comparatively high OD_{680}. This is due to *Monoraphidium minutum* remaining in exponential growth phase for a longer period than strains with similar maximum

specific growth rates such as *Nannochloropsis oceanica* or SAmud7, allowing it to excel in density when grown over a longer period of time (Figure S1). The DISCOVR consortium project tested *S. acutus, S. obliquus,* and *M. minutum,* as well as seven other strains in simulated winter conditions in a photobioreactor and found that *M. minutum* had the highest areal productivity (Huesemann et al., 2023). The simulated winter conditions utilized by Huesemann et al. (2023) consisted of sinusoidal light and water temperatures ranging from 5 to 15°C.

In Roux flask-scale cultivation at 18°C, both *Picochlorum* species drastically struggled to maintain an adequate growth rate despite growing at a much higher rate on a smaller scale. This discrepancy can be seen in Tables 1.1 and 1.3. It could be attributed to *Picochlorum celeri* and *Picochlorum renovo* cells adhering to the sides of the Roux flasks and no longer being suspended in the growth medium. As this started to occur, the cells seemed to develop a yellow-ish pigmentation which was most likely an indicator of stress caused by both temperature and cells going in and out of suspension (Cano et al., 2021). Without consistent cell suspension in the medium, cell desiccation could occur, leading to a decline in growth and possibly cell death. This was a common issue that was noticed to some degree during Roux flask cultivation of each strain, as flasks would have to be shaken daily to resuspend cells into the media. The DISCOVR consortium project classifies the *Picochlorum* strains as warm weather strains that are optimal for outdoor cultivation in the late spring and summer (Gao et al., 2023). *Picochlorum celeri* and *Picochlorum renovo* both struggled to grow at low temperatures and experienced cell adhesion. Their specific growth rates (0.4 and 0.5 day^{-1} respectively) were much lower than other cold-tolerant strains such as *Monoraphidium minutum, Scenedesmus acutus, Scenedesmus obliquus,* and *Scenedesmus rubescens* (0.8, 1.1, 1.3, and 1.9 day^{-1} respectively) as seen in Table 1.3. The consistent outperformance of *Picochlorum celeri* across both low and high temperature

conditions (Tables 1.1, 1.2, and 1.4) highlight its superior adaptability to thermal tolerance compared to *Picochlorum renovo*. Under low temperature conditions, *Picochlorum celeri* achieved a higher maximum growth rate than *Picochlorum renovo* (Table 1.1), and its advantage became even more pronounced at elevated temperatures (Table 1.2). Importantly, *Picochlorum celeri* maintained this dominance in its average growth rates without compromising biomass density (Table 1.4), suggesting better performance in higher temperatures. For this reason, *Picochlorum celeri* was selected for further testing. This also positions it as a more viable candidate for outdoor cultivation in warmer climates, where thermal fluctuations demand consistent growth and productivity.

SAmud7 and SRTC14 are newly isolated and uncharacterized strains. Their overall growth performance did not warrant their selection for further experimentation. This decision was made to futureproof the results of this thesis for further research. Even for unmodified algal strains, outdoor cultivation has regulatory requirements to have taxonomic information on the organism which costs additional time and money (Glass, 2015). Additionally, these strains lack established genomic information which makes forward or reverse genetic screening impossible. This decision ensures that future research aiming to identify any genes associated with improved biomass productivity can be conducted without additional genomic characterization.

4.2.2. High temperature cultivation – 30°C

Scenedesmus rubescens achieving a maximum specific growth rate equal to *Picochlorum celeri* was surprising as the maximum specific growth rate of *Picchlorum celeri* was described to be double that of *Scenedesmus rubescens* by the DISCOVER consortium project (Huesemann et al., 2023). The main difference observed was the difference of an OD_{680} of 1.0 between the two strains, likely due to *Scenedesmus rubescens* reaching stationary phase earlier (Figure S2). A

noticeable amount of evaporation took place in *Scenedesmus obliquus'* Roux flask leading to the high OD_{680} observed on day six of growth. For that reason, this OD_{680} value should be ignored when considering the growth performance of this strain. In retrospect, the solution to this problem would be to measure the amount of evaporation that has occurred and replace it with sterile DI water throughout the growth assay.

Scenedesmus acutus struggled at larger scale at 30°C as aggressive foaming of the cell culture, multiple instances of the bubbling rate decreasing (flow rates were measured daily due to potential clogging of filters), and cell clumping plagued this growth test. This could have been the cause of both the specific growth rate and OD_{680} being lower than expected. Aggressive shaking of the flask to resuspend the cells did not seem to help all the time as some of the cells were dried and sticking to the sides of the flask. This issue was also noticed in both *Scenedesmus obliquus* and *Scenedesmus rubescens* but to a less debilitating degree and there were no issues with the bubbling rate decreasing. This might have allowed cells that were adhering to the sides of the flask to remain more hydrated. As the cells were diluted to an OD_{680} of 0.025, the prolonged exposure of high light as well as potential carbon limitation could have been stressful to the cells, causing EPS secretion to occur (Gerbersdorf et al., 2009). Additionally, carbon limitation has been shown to induce auto-flocculation in *Nannochloropsis oculata* (Tran et al., 2017). As the selected strain would eventually be grown with the addition of flue gas, which will contain roughly 12% CO_2, this issue was not a deciding factor whether a strain would be cut from the experiment or not.

4.3. Evaluation of productivity at Roux flask scale – triplicate cultures

Future outdoor performance tests are targeting summer conditions in Gillette, WY. So, the final biomass accumulation experiments were conducted at 30°C. Measurements of organic carbon accumulation were added at this stage of strain evaluation.

4.3.1. High temperature cultivation – 30°C

Similar to the findings based on the results from Table 2.1, *Scenedesmus acutus* once again produced the lowest average optical density of the strains tested in 30°C. This strain demonstrated the highest specific growth rate with no variability, but its final optical density had the highest variability. High amounts of cell adhesion to the sides of the flask were to blame for this which was further reinforced by previous observations of cell adhesion to the flask surface. This occurred 48h after initial dilution and persisted for the remainder of the experiment despite routine shaking, suggesting that certain environmental factors may have influenced EPS secretion and led to adhesion on the sides of the flasks. The highest specific growth rates for *Scenedesmus acutus* were calculated within the first two days of growth (an average of 1.8 day^{-1}), before cell adhesion was observed. Cell adhesion was particularly problematic on day 6 of growth which caused the highest variation of OD_{680} values seen during triplicate growth of *Scenedesmus acutus* (Figure S3). All three *Scenedesmus* species had issues involving cells sticking to the sides of the flask and all required vigorous shaking, which likely caused the high variability in OD_{680} between triplicates. This issue however was most debilitating in *Scenedesmus acutus* as the other *Scenedesmus* species had lower comparative variations and still maintained a higher optical density at the end of cultivation (Table 1.5). This suggests that *Scenedesmus acutus* is less thermotolerant compared to the other strains tested.

Monoraphidium minutum had a comparatively low growth rate but high OD_{680} which reaffirmed previous observations that it did not have the fastest exponential growth rate; but maintained steady and consistent growth of cells over time, which led to a superior optical density by the end of the cultivation period.

Nannochloropsis oceanica demonstrated similar results to *Monoraphidium minutum*. While observing growth performance, its cells tended to be in lag phase during its first day of growth while *Monoraphidium minutum* was not, likely leading to its overall lower OD_{680} (Figure S4).

Picochlorum celeri's rather average performance was intriguing. While this strain had shown rapid growth in previous trials, its lower specific growth rate and final OD_{680} greatly decreased this time around. Cell adhesion was noticed around day four of growth, but cells were able to be resuspended by manually shaking the flask. Overall, these findings highlight the variability in performance among strains when transitioning from small to larger-scale cultivation systems.

4.3.2. Total organic carbon (TOC) biomass quantification

The use of TOC analysis to derive biomass productivity has been demonstrated by (Saxena et al., 2021) to be cheaper, quicker, and as reliable as conventional methods of biomass measurement that use ash free dry weight (AFDW) as the metric. The cultures were centrifuged, and the pellet was separated from the supernatant and washed to remove any exogenous carbon present in the media. This means that any secreted carbon was not included in the assay. Strains that produced the most organic carbon by day six were determined to have the highest productivity.

Scenedesmus rubescens and *Monoraphidium minutum* had the highest overall average TOC on day 6 of growth, making them the two most productive strains tested (Figure 1.1). Both *Scenedesmus rubescens* and *Monoraphidium minutum* were however significantly higher than the strain with the next highest average TOC, *Nannochloropsis oceanica* (Student's t-test: $p < 0.05$). This solidified them as the most productive strains tested. The alleviation of cell adhesion would have likely not hindered growth performance in some of the flasks, resulting in a significant increase in TOC compared to *Monoraphidium minutum.* The overall TOC standard deviation of each strain appeared increased from days three to six, presumably a result of culture adhesion to the flasks becoming more prominent around this time. Sonication was used to attempt to homogenize aliquots harvested for TOC analysis. Sonication ensures that the TOC analyzer will have a homogenized sample to measure from, eliminating potential variability caused by auto-flocculated cells that aren't distributed equally.

Other factors to consider are cell size and composition as molecules such as lipids are more carbon dense than carbohydrates, proteins, or pigments (Polsten and Walter, 2012). Cellular carbon allocation is driven by a dynamic interaction of physiological, environmental, and genetic factors. For instance, lipids are more carbon-dense than carbohydrates, proteins, or pigments (Polsten and Walter, 2012), meaning that strains allocating more carbon to lipid synthesis may exhibit higher TOC content even if their growth rates are similar. Smaller cells, such as *Picochlorum celeri*, which had the lowest TOC content at day 6, may have higher surface-area-to-volume ratios, enhancing nutrient uptake but limiting storage capacity for carbon-rich molecules (Liu X. et al., 2023). This is relevant as *Picochlorum celeri* had an average optical density at day 6 that was comperable to both *Nannochloropsis oceanica* and

Scenedesmus rubescens but greatly underperformed at accumulating biomass (Table 1.5; Figure 1.1).

Physiological responses to environmental conditions, such as nutrient availability, light intensity, and temperature, further affect carbon allocation. For example, observations of *Scenedesmus obliquus* and *Nannochloropsis salina* cultivated in nitrogen-replete conditions typically favored protein synthesis, while nitrogen limitation as well as temperature variation shifted allocation toward lipids and carbohydrates (Fakhry and El Maghraby, 2015; Shen et al., 2015; Li et al., 2020). Additionally, *Picochlorum celeri* has shown to have a dry biomass composition of 50% protein, 12% carbohydrate, and 11% lipid under nitrogen replete conditions. The dry weight lipid compositions of *Scenedesmus rubescens* and *Monoraphidium sp.* have been reported as 25.44% and 28.92% respectively under nitrogen replete conditions (Anbalagan et al., 2023; Tsarenko et al., 2020). This difference in lipid accumulation between *Picochlorum celeri, Scenedesmus rubescens,* and *Monoraphidium sp.* grown in nitrogen replete BG-11 could explain the difference in average TOC described in Figure 1.1 since *Picochlorum celeri's* optical density was similar to other strains such as *Scenedesmus rubescens* and *Nannochloropsis oceanica* which accumulated more TOC.

4.3.3. Calculation of mass of organic carbon on a cellular level

Cellular organic carbon mass was calculated on a per cell basis using cell counts during cultivation and TOC measurements. This calculation allows us to link TOC measurements to cellular physiology, providing insights into how carbon is accumulated at the individual cell level, which is essential for understanding strain-specific differences in carbon accumulation. Additionally, it acted as a verification to compare calculated TOC cell^{-1} mass to the known size or mass of other species.

Nannochloropsis cells can range from 2-4 µm in diameter and have been shown to have dry weights of 3.5-6 pg cell^{-1} (Borowitzka, 2018; Daniel & Srivastava, 2016). At day 6 of growth, *Nannochloropsis oceanica* cells contained 5.7 pg C cell^{-1} which corresponds to previous findings. While there is not much information on the cellular mass of each of these species, the results of Figure 1.2 indicate a clear correlation between cell size and organic carbon mass per cell. Larger species like *Scenedesmus rubescens* (capable of exceeding 10+ µm in diameter) accumulate significantly more carbon (148.9 pg C cell^{-1}) compared to smaller species like *Picochlorum celeri* (1–3 µm in diameter, 1 pg C cell^{-1}) (Huesemann et al., 2023; Cardoso et al., 2022; LaPanse et al., 2024). This highlights an important trade-off in microalgal physiology where cell size affects carbon storage capacity (Finkel et al., 2010).

The high variability of TOC per cell mass observed in day 0 of *Monoraphidium minutum* is likely due to the 1:20 sample dilution prior to TOC measurement. The unexpectedly high TOC value recorded for *Monoraphidium minutum* on day 0 may have resulted from incomplete pellet washing, leading to residual BG-11 medium contamination, which contains organic carbon. The decision to make a high dilution for day 0 was to preserve enough sample in the event they had to be remeasured.

As cell densities increased from days 3 and 6, variability decreased, suggesting that analyzing undiluted day 0 samples in future analyses could improve measurement consistency. A statistically significant increase in TOC per cell from day 3 to day 6 (student's t-test: $p < 0.05$) was observed in all strains except *Picochlorum celeri*, which remained at approximately 1 pg C cell^{-1}, and *Scenedesmus obliquus*, which showed an increase in pg C cell^{-1} from day 3 to day 6 but with too much variation to be statistically significant. From days 3 to 6 of growth, the cultures were transitioning out of exponential phase into stationary phase, where individual cell

size and biomass accumulation tends to increase (Guschina & Harwood, 2006; Ren et al., 2013). From a large-scale cultivation perspective, the increase in TOC per cell during the transition to stationary phase is crucial as it reflects greater carbon accumulation in the form of lipids or carbohydrates, which are valuable for various bioproducts. Harvesting during this phase maximizes yield of biomass.

4.4. Rationale for strain selection for mutagenesis

Scenedesmus rubescens and *Monoraphidium minutum* were the two strains down selected for mutagenesis as they frequently demonstrated high growth and productivity performance in both low and high temperatures. These traits are vital for large-scale outdoor cultivation, as they must withstand fluctuating environmental conditions such as seasonal temperature changes and varying light intensities.

Scenedesmus rubescens NREL 46B-D3 was down selected in this thesis due to its competitive growth performance and high biomass accumulation capabilities. This is a relatively new, halotolerant strain isolated from brackish waters and has been shown to have a maximum lipid and carbohydrate composition of both 40% of its dry cell weight (Calhoun et al., 2021). This strain has shown to have other beneficial traits such as having the highest post cell division biomass accumulation of currently studied halotolerant strains and its overall size which allows rapid natural settling of cells for improved harvesting (Calhoun et al., 2021). Dahlin et al., (2018) tested *Scenedesmus rubescens* 46B-D3 and two other down selected halotolerant algal strains in outdoor raceway ponds in winter climate (0-20ºC) and found that *Scenedesmus rubescens* 46B-D3 had the highest carbohydrate content (34% of biomass) but the lowest lipid content of around 11% of its dry weight while the other two strains both exceeded 22%. They

suggested that this strain under winter conditions would be best for carbohydrate-based bioproducts or applications requiring easy harvesting due to its settling abilities.

Monoraphidium minutum 26B-AM was also down-selected because of its high biomass accumulation capabilities and wide temperature tolerance. Previous research has highlighted *Monoraphidium minutum's* dominant biomass productivity in colder climates (Caloun et al., 2021; Gao et al., 2023). Its lipid composition has also been shown to range from 23.58% to 39.06% when tested in mixotrophic conditions (Patidar et al., 2014). This places *Monoraphidium minutum* in a competitive position to become a more frequently utilized outdoor scale winter crop.

The traits exhibited by both *Scenedesmus rubescens* and *Monoraphidium minutum* are characteristic of those observed in commercially favorable strains. *Chlorella vulgaris, Nannochloropsis spp*., *Scenedesmus obliquus, Dunaliella salina,* and *Haematococcus pluvialis* are highly utilized algal strains in commercial outdoor cultivation due to their unique physiological traits, adaptability to varying environmental conditions, and potential for high-value applications. Specifically, they are ideal for applications such as biofuel production, pigment synthesis, wastewater treatment, and carbon sequestration. These strains have been extensively studied and optimized for industrial-scale cultivation, making them ideal candidates for sustainable biomass production.

Chlorella vulgaris is a well-known and commercially favored species for its rapid growth rates and high protein content, and wide temperature tolerance, making it excellent for food and feedstock production (Lee et al., 2018). Additionally, *Chlorella vulgaris* is known to accumulate a high lipid content under nutrient stress which makes it a desirable candidate for biofuel production (Guccione et al., 2014).

Various *Nannochloropsis* species such as *N. oceanica, N. salina, N. oculata,* and *N. gaditana* are most notable for their high lipid content, reaching over 60% of its dry weight in nitrogen depleted conditions (Chen et al., 2024; Chiu et al., 2009). This makes it one of the most popular genera for biofuel production at large, outdoor scale (Corcoran et al., 2024). The widespread interest in *Nannochloropsis spp.* has made it into a model organism for microalgal studies, prompting an expansion of synthetic biology research for value added products (Ma et al., 2016; Du et al., 2023).

Similar to the strains previously mentioned, *Scenedesmus obliquus* is a well-researched strain that is proven to have high biomass yields and lipid production in large scale outdoor cultivation (Pereira et al., 2017). *Scenedesmus obliquus* has also been shown to effectively remove nutrients from wastewater, which treats the wastewater while acting as a low-cost nutrient source for cultivation (Arif et al., 2020).

Both *Dunaliella salina* and *Haematococcus pluvialis* are popular algal strains for outdoor cultivation due to their high biomass productivity and carotenoid composition. Specifically, *Dunaliella salina* is a halotolerant strain and is commonly used in nutritional supplements and aquatic feedstocks additives because of its high β-carotene content capable of reaching over 7% of its dry mass (Hermawan et al., 2018; Xi et al., 2020). *Haematococcus pluvialis* is used in similar applications but contains a high astaxanthin content of 2-5% of its dry weight (Teng et al., 2023; Oslan et al., 2021)

These characteristics coincide with the favorable growth, adaptability, and biomass acumulation observed in *Scenedesmus rubescens 46B-D3* and *Monoraphidium minutum*, positioning them as strong candidates for large-scale outdoor cultivation and diverse bioproduct applications.

5. Conclusion

This series of experiments presented in this chapter provided insight into how temperature and scale affected the growth and biomass accumulation performance of ten selected algal strains. Strains would be down-selected based on their ability to maintain high productivity in both temperature conditions. First, strains were each grown in duplicate small-scale flasks at both 18 and 30ºC under high light to observe their specific growth rates in exponential phase. During growth, strains were also monitored for any signs of stress in the form of autoflocculation, cell adhesion to surfaces, or altered cell morphology. After small-scale cultivation, *Phaeodactylum tricornutum* was determined to not grow in 30ºC, eliminating it from further trials. Next, cultivation of the remaining nine strains was scaled up using Roux flasks, where cultures would be exposed to both temperature conditions with the addition of bubbling and higher light irradiance. This time, optical density was measured to observe the maximum density that cultures could achieve after six days of cultivation in addition to monitoring specific growth rate. This offered an idea of how productive strains were across different growth phases, as specific growth rates were used to capture a strain's growth performance in exponential phase. Cultures grown in industrial settings typically grow to densities exceeding exponential phase, making optical density monitoring more practical. *Picochlorum renovo* was eliminated from the experiment due to its poor performance at 18ºC. Both SRTC14 and SAmud7 were eliminated because they demonstrated average performance compared to the other strains and were not characterized, making potential future research involving genetic screening more difficult. Triplicate growth in Roux flasks of the remaining six strains at 30ºC to measure growth and biomass accumulation revealed the three *Scenedesmus* species to have the highest specific growth rates, while *Monoraphidium minutum* achieved the highest final optical density. TOC

analysis of aliquots taken from Roux flasks showed *Scenedesmus rubescens* and *Monoraphidium minutum* to have 88.5% and 22.6% higher average TOC accumulation compared to the next highest performing strain, *Nannochloropsis oceanica.* Lastly, calculation of the mass of TOC per cell yielded results that generally corresponded with known cell sizes and masses. This calculation also enabled an initial assessment of how carbon accumulation differed between the tested species.

In summary, these experiments underscore how temperature and cultivation scale can alter algal growth performance and biomass accumulation. Down-selection of ten initially selected strains pinpointed *Scenedesmus rubescens* and *Monoraphidium minutum* as having the most robust performance under the tested conditions, highlighting their potential for large-scale cultivation. High performance liquid chromatography could give further insights on the detailed biochemical profile of each strain to determine the appropriate application for bioproduct development.

CHAPTER 2. IDENTIFYING HIGH-PRODUCTIVITY MUTAGENIZED MICROALGAL STRAINS USING A FLUORESCENCE-BASED SCREENING APPROACH

1. Introduction

Large-scale outdoor cultivation of microalgae requires strains that can not only tolerate fluctuations in environmental conditions but also maintain high photosynthetic efficiency and biomass productivity. Industrial systems, such as open raceway ponds or photobioreactors, subject cells to dynamic stressors such as changes in light intensity between excess surface irradiance and near-darkness during mixing. Algae containing enlarged light-harvesting antennae can exacerbate self-shading and over 80% of absorbed light is typically lost to

protective mechanisms like non-photochemical quenching (Peers, 2014; Melis, 2009). Simultaneously, photoinhibition, CO_2 depletion, and elevated oxygen levels further limit productivity by inducing photorespiration and oxidative stress (Aro et al., 1993; Peers, 2014). To overcome these inefficiencies, strains must be optimized for fluctuating environment, ideally with smaller antennae, regulated NPQ, and enhanced carbon fixation pathways.

While the findings of Chapter 1 identified *Scenedesmus rubescens* and *Monoraphidium minutum* as promising candidates for their thermal tolerance and biomass accumulation, further strain optimization is needed to meet industrial demands. This chapter focuses on enhancing these strains through mutagenesis and fluorescence-based screening to develop mutants with improved photophysiological traits that are suggestive of improved productivity. There were three main objectives of this chapter. The first objective was to establish optimal mutagenesis protocols using gamma irradiation to generate *Scenedesmus rubescens* and *Monoraphidium minutum* mutants. The second objective was to screen supposed mutants for improved photophysiology using pulse amplitude modulation (PAM) fluorometry, enabling the identification of strains with improved energy utilization and stress resilience. Lastly, the third objective was to grow down-selected mutants to identify any improvements in growth rate and productivity.

Mutagenesis is an effective approach utilized in microbial biotechnology research that offers a pathway to enhance desirable traits such as growth rates, stress tolerance, and biochemical composition. In microalgae, random mutagenesis via ionizing irradiation has successfully generated strains with increased lipid yields, thermotolerance, and pigment content, demonstrating its potential for industrial applications (Liu et al., 2016; Fan et al., 2021; Wang et al., 2018; Baek et al., 2016; Ma, Y. et al., 2013). Gamma irradiation was selected over chemical

mutagens like EMS due to its ability to induce larger-scale DNA damage, including single and double-stranded breaks, which are more likely to result in significant phenotypic changes compared to the small point mutations caused by EMS (Sikora et al., 2011; Hwang et al., 2015). Gamma irradiation generates free radicals that interact with cellular components, leading to slower cellular recovery and reduced likelihood of mutation reversions, making it ideal for generating stable mutants (Hendry, 1991). Additionally, gamma irradiation has been shown to produce higher mutation rates (Kumawat et al., 2019), which is critical for efficiently isolating strains with improved traits, such as enhanced lipid production, as demonstrated in species like *Chlamydomonas reinhardtii, Chlorella pyrenoidosa,* and *Scenedesmus sp.* (Liu, B., 2015; Wang, W., 2018; Baek, 2016).

Fluorescence-based screening of mutants enabled high-throughput analysis of altered photophysiology in mutagenized strains (Ware et al., 2020). Traditional growth-based screening methods, while effective, are time and resource intensive. In contrast, chlorophyll fluorescence measurements provide immediate insights into the functional state of photosystem II, including parameters such as maximum quantum yield, non-photochemical quenching, and the redox state of the plastoquinone pool (Schreiber, 2004; Baker, 2008). These parameters are critical for evaluating how efficiently mutants convert light energy into biomass under dynamic conditions. The IMAGING-PAM and DUAL-PAM fluorometry systems utilized enabled the rapid, non-destructive screening of thousands of colonies, revealing mutants with altered fluorescence relaxation kinetics, elevated Fv/Fm, or enhanced NPQ induction, traits which can be indicative of improved photosynthetic performance (Ware et al., 2020).

The integration of fluorescence-based screening with mutagenesis addresses a central challenge in algal biotechnology: linking genetic changes to functional improvements in

photosynthesis. For example, mutants exhibiting delayed NPQ relaxation or increased qL recovery may better balance light harvesting and energy dissipation, minimizing photodamage while maximizing carbon fixation (Niyogi et al., 1997; Peers, 2014). Such traits are particularly advantageous in outdoor systems, where fluctuating light intensities and temperature shifts can destabilize productivity.

The overall goal of this chapter was to identify prospective mutants via fluorescence screening that demonstrated altered photophysiology indicative of improved growth performance. These putative mutants were cultivated at lab-scale to assess growth rate and biomass accumulation to identify ones with improved productivity compared to wild type.

2. Methods

2.1. Culture growth conditions

2.1.1. Growth media

Scenedesmus rubescens NREL 46B-D3 and *Monoraphidium minutum* 26B-AM, both of which are fresh or brackish water strains characterized in the DISCOVR consortium project, were cultured in BG-11 pH 8 growth media modified from Rippka et, al. 1979 [Huesemann et al., 2023 / Rippka et al., 1979]. This recipe consists of 1L H_2O, 10ml of 100x BG-FPC stock (149.58 g/L $NaNO_3$, 7.49 g/L $MgSO_4$, 3.6 g/L $CaCl_2 \cdot 2H_2O$, 1.12 ml/L Na-EDTA, 250 mM, pH 8.0, 1ml of Fe ammonium stock (0.3 g/50 mL Fe ammonium citrate), 1 ml of 189 mM Na_2CO_3 stock, 1 ml of 175 mM K_2HPO_4 stock, and 10ml 1M TES-KOH, pH 8.2. To this, 100 mL/L trace mineral stock was added. The trace minerals stock consists of 2.86g/L H_3BO_3, 1.81g/L $MnCl_2 \cdot 4H_2O$, 0.222 g/L $ZnSO_4 \cdot 7H_2O$, 0.39 g/L $Na_2MoO_4 \cdot 2H_2O$, 0.079 g/L $CuSO_4 \cdot 5H_2O$, and 0.0494 g/L $Co(NO_3)_2 \cdot 6H_2O$ and is stored at 4°C. The media was autoclaved for 20 minutes and

stored at room temperature. Solid BG-11 media was made by preparing a 500 ml 2X salts solution of liquid BG-11 with the addition of 3 g $Na_2S_2O_3$•$5H_2O$, as well as a 500 ml 2X agar solution containing 15 g Fisher Scientific Agar. Both solutions were autoclaved for 20 minutes. The medium was then allowed to cool to 55°C and the 2X salts solution was added to the 2X agar solution. Strains were grown at 25ºC under ~200 µmol photons m^{-2} s^{-1} constant light conditions on an orbital shaker operating at 125 rpm (VWR, Model 3500). All cultures were diluted 1:50 once a week. Prior to growth experiments, cultures were diluted and allowed to grow for no more than 3-4 days before commencing data collection so that cells were in exponential growth phase.

2.1.2. Pre-mutagenesis cell plating

To obtain distinct, well-isolated colonies suitable for accurate counting before mutagenesis, 100-400 total *Monoraphidium minutum* cells and 50-200 total *Scenedesmus rubescens* cells were spread onto BG-11 agar plates and allowed to grow for 10-14 days in 25°C under 50-200 µmol photons m^{-2} s^{-1} continuous light conditions until colonies formed.

2.2. Mutagenesis

2.2.1. Irradiation lethal dosage curve and gamma irradiation mutagenesis

Cells were subject to gamma irradiation to induce mutations. Briefly, a J. L. Shephered Mark-I 68A ^{137}Cs sealed source irradiator containing an original activity of 6000 Ci was used to expose liquid cell samples to ionizing radiation. The irradiator was designed so that multiple samples can be exposed to varying dose rates of radiation simultaneously. During radiation exposure, a rotating carousel was used to better provide a homogenous dose distribution.

A radiation dosimetry assessment was completed prior to experimentation. Specifically, in accordance with ISO/ATSM 51261 protocols, Fricke dosimeters dosimetry solution was

prepared, and dosimeters were created that were representative of the dimensions and physical characteristics of samples that were irradiated in 15 ml 17x120 mm Falcon tubes (Corning Science) (ATSM International, 2004). At the designated sample location within the chamber, an initial dose rate of 7.25 Gy min^{-1} was determined. Accordingly, the decay of the radiation source was accounted for prior to each exposure to radiation so that sampled received the same absorbed radiation dose by increasing the exposure duration.

A range of ^{137}Cs γ radiation dosages were chosen to generate a lethal dosage curve to determine an optimal LD_{90} dosage. Dosages of 50, 100, 200, 250, 300, 350, and 400 Gy and dosages of 25, 50, 75, 100, and 150 Gy were used to test for lethality in *S. rubescens* and *M. minutum* respectively. Selection of initial dosage ranges were based off of findings from previous studies on microalgae (Liu et al., 2015 and Wang et al., 2018). A 0 Gy control was included for each experiment. 200 *S. rubescens* and 400 *M. minutum* cells were plated in triplicates on BG-11 agar plates after receiving each irradiated dosage. Percent survival was calculated by dividing the average colony count of each dosage treatment by the average colony count of the 0 Gy control. 300 Gy for *S. rubescens* and 75Gy for *M. minutum* yielded a ~10% survival rate and was used for subsequent mutagenesis experiments.

2.2.2. Optimal irradiation dosage for mutagenesis

Following liquid cell culture irradiation of 300 Gy for *S. rubescens* and 75 Gy for *M. minutum*, 1000-1500 cells are plated onto BG-11 plates and allowed to grow at 25°C in constant low light (~150 μmol photons m^{-2} s^{-1}) for 14 days. Once visible colonies were observed, they were picked and streaked out onto pre-labeled 6x6 grid square BG-11 agar plates. A WT control is plated onto each plate as a positive control. After 7-10 days of growth, plates were screened

for photophysiological traits as described below. Putative mutants of interest were re-streaked in triplicates on new plates and reanalyzed to verify phenotypes.

2.3. Fluorescence based screening of putative mutants

2.3.1. Chlorophyll fluorescence dynamics screening – imaging pulse amplitude modulated fluorescence (IMAGING-PAM)

Plates were dark adapted for 15 minutes prior to screening. An IMAGING-PAM (MAXI version Walz GmbH, Effeltrich, Germany) equipped with an LED-array illumination unit IMAG-MAX/L and an IMAG-K6 CCD camera with a K6-MAX objective was used for all plate screening experiments (WALZ, H., 2019). Measuring light intensities were adjusted in each experiment to achieve an Fo of ~0.2 (Int 1-8, frequency 1, gain 1-5). A custom light script was created to replicate one used previously (Ware et al., 2020) which identifies mutants with impaired photoprotection or alternative electron transport. During this script, the pulse modulated measuring light pulses for 100 μsec at a frequency of 1Hz. Fluorescence measurements are taken twice per second. The custom script takes an initial Fv/Fm measurement. Fv/Fm is the maximal PSII quantum yield calculated from chlorophyll *a* fluorescence after dark adaptation using the maximal and minimal fluorescence measurements. Calculation of chlorophyll *a* fluorescence parameters are mentioned below. This is then followed by darkness and then a low light period (303 μmol photons m^{-2} s^{-1}) for three minutes. Samples were then exposed to thirty seconds of darkness followed by 1749 μmol photons m^{-2} s^{-1} for three minutes. Lastly, samples were exposed to darkness for four minutes. Plates were exposed to saturating pulses every 30-60 seconds. Specific details on saturating pulse events are shown below in Table A.

Table A: IMAGING-PAM mutant photophysiology screening script details.

Measurement #	Total Time (seconds)	Light Intensity (μmol photons m^{-2} s^{-1})
1	0	0
2	35	0
3	155	303
4	205	303
5	265	303
6	295	0
7	355	1749
8	415	1749
9	475	1749
10	535	0
11	595	0
12	655	0
13	715	0

2.3.2. Dual-PAM Chlorophyll Fluorescence Assays

Photophysiological measurements were taken with a Dual-PAM-100 Chlorophyll Fluorescence & P700 Photosynthesis Analyzer (Walz GmbH, Effeltrich, Germany). It was equipped with a DUAL-E measuring head (P700 dual-wavelength emitter measuring light and a 720 nm and 635 nm actinic light) as well as a DUAL-DB measuring head with detector (460 nm LED actinic light and fluorescence measuring light). All cell samples were dark acclimated for at least 15 minutes prior to measurement. At least five milliliters of cell cultures in late exponential or early stationary phase were filtered onto a Millipore-Sigma glass fiber prefilter

using a 5 ml syringe with Luer-Lok tip (BD Biosciences). Measuring mode was set to "Fluo" which only utilizes the DUAL-DB measuring head and analysis mode was set to SP-Analysis. The "Fluo" gain was set to 5 (high) and the damping was set to 1 ms (high). F-ML (Fluorescence Measuring Light) is toggled on, and the measuring light is adjusted to achieve a basal F_o level of around 0.2 V. A separate custom light script similar to the IMAGING-PAM light script with saturating pulse details is mentioned below in Table 2. The measuring light frequency range was set to 20-2000 Hz and fluorescence measurements were taken every 10 ms for the duration of the script.

Table B: DUAL-PAM mutant physiology screening script details

Measurement #	Total Time (seconds)	Light Intensity (µmol photons m^{-2} s^{-1})
1	0	0
2	35	0
3	155	303
4	205	303
5	265	303
6	295	0
7	355	1735
8	415	1735
9	475	1735
10	535	0
11	595	0
12	655	0
13	715	0

Putative mutants were screened via IMAGING-PAM for drastic increases in Fv/Fm, variations in non-photochemical quenching (NPQ), rapid changes in coefficient of photochemical quenching (qL) and altered fluorescence kinetics patterns similar to the ones mentioned in (Ware et al., 2020). F represents the steady-state fluorescence, Fm is the maximum fluorescence when dark adapted, Fm' represents the light adapted maximum fluorescence, Fo is the minimum fluorescence when dark adapted, and Fo' is the minimum fluorescence when light adapted.

$$\mathrm{Fv/Fm} = \frac{(F_m - F_o)}{F_m}$$

$$\mathrm{NPQ} = \frac{(F_m - F_m{}')}{F_m{}'}$$

$$\mathrm{qL} = \frac{(F_m' - F)}{(F_m' - F_o')} \times \frac{F_o{}'}{F}$$

Additionally, mutants containing alterations in their pigment were visually screened for and selected for further testing of growth performance. It has been shown that accumulation of pigments such as astaxanthin can increase biomass productivity in green algae (Cazzaniga et al., 2022). Any mutants that continued to demonstrate improvements in photophysiology were then selected for lab scale growth assessment.

2.4. Putative mutant growth assays and biomass accumulation

Selected prospective *S. rubescens* and *M. minutum* mutants were grown in triplicate 250 ml flasks diluted to 50 cells/µl in 50 ml of BG-11 and grown under 278 ± 10 µmol photons m^{-2} s^{-1} 16h light 8h dark cycle in 25°C while shaken at 130 rpm. WT triplicates were included in each experimental run as a control. Growth rates were calculated using the methods described above. Growth rates of mutants were compared to WT as either a percentage increase or

decrease. A Student's t-test was used to determine significance ($p < 0.05$) between suspected mutants and WT.

High performing mutants and their corresponding WT strains were then grown in 500 ml of BG-11 media in 2 L flasks, under 700 ± 8 μmol photons m^{-2} s^{-1} 16h light 8h dark cycle at 25°C while shaken at 100 rpm. The air composition of the growth chamber was altered to have 1% CO_2 to prevent carbon limitation, but the strains were not directly bubbled. Strains were diluted to an $OD_{680} = 0.5$ and grown for three days, with 40 ml aliquots taken at days 0 and 3. These samples were then centrifuged at 2500 × g for 10 min (4 °C) after harvesting. After centrifugation, the supernatant was separated into its own Falcon tube and the cell pellet was resuspended to 40 mL using 0.22 μm filtered DI water. If the pellet did not homogenize into the DI water properly and cells were visibly clustering, then the cells were sonicated at max power for 60 seconds to break up any cell aggregates.

Samples were transferred to 40ml glass vials with a VWR micro stir bar. Biomass samples were measured using the TOC measurement setting calibrated to detect a range of <5000 ppm TOC. To verify the accuracy of the results, organic and inorganic carbon (OC and IC, respectively) values were cross-checked by including a 100 ppm OC and IC standard solution with each batch of samples. 6M phosphoric acid and a sodium persulfate solution (300 g/L) were prepared fresh prior to sample analysis. A 1000ppm IC standard was made by preparing solution containing 3.397g $NaHCO_3$ and 4.412g Na_2CO_3 and dissolving it with 1L DI water. A 1000ppm TOC standard was made by making a solution of 2.25g $C_8H_5NaO_4$ and dissolving it with 1L DI water. Prior to preparing the standards, all three powders were stored in a drying oven set to 50°C to allow the evaporation of any moisture in the powders that could skew mass measurements. After preparing the solution, it was stirred on a stir plate until no

particulates were visible. All plastic/glassware used for TOC analyses were soaked in 1M HCl, rinsed thoroughly with DI water, and dried at 50°C prior to use to remove traces of organic carbon. The 6M phosphoric acid is used by the machine to determine ppm of inorganic carbon by reacting with carbonates and bicarbonates to produce CO_2 which is measured. The sodium persulfate solution oxidizes organic carbon compounds into CO_2 and is reported back as ppm TOC. Samples in the machine are measured four times with the average ppm of TOC or IC being calculated from the three samples with the lowest relative standard deviation. Two initial vials containing DI water are used to flush the instrument prior to measuring. Cell and supernatant samples are separated by one flush vial to prevent any crossover of liquid sample as the prior sample can have a mild influence on the sample directly after it. Flasks containing sterile BG-11 or F/2 were used as a control for this experiment for future organic and inorganic carbon measurements.

Calculating mass of carbon on a per cell basis was obtained using the following equations. This equation was also used for inorganic carbon measurements.

$$\text{pg C cell}^{-1} = \frac{(\text{ppm TOC} \times 10^3 \times \text{ dilution factor})}{\text{cells } \mu\text{l}^{-1}}$$

3. Results

3.1. Establishing an optimal gamma irradiation dosage for mutagenesis of Scenedesmus rubescens and Monoraphidium minutum

3.1.1. ^{137}Cs gamma irradiation lethal dose assay

To establish an optimal gamma irradiation dosage for mutagenesis, a lethal dose assay was conducted on *Scenedesmus rubescens* and *Monoraphidium minutum* to identify irradiation levels that effectively induce mutations while maintaining sufficient cell viability for further

study. A lethal dose assay was conducted on *Scenedesmus rubescens* and *Monoraphidium minutum* to determine an optimal dosage to effectively generate mutants. Initial irradiation dosages of 50, 100, 200, and 400 Gy, as well as a 0 Gy control were first selected to be tested on both strains. The first test yielded favorable results for *Scenedesmus rubescens* with 400 Gy yielding an average 98.5% lethality (Figure 2.1). For 200 Gy, an average 73.8% lethality was observed, indicating that the LD_{90} was between 200 and 400 Gy. A second test was conducted with 250, 300, and 350 Gy doses. 300 and 350 Gy doses yielded lethality averages of 87.7% and 90.9% respectively. Because 250 Gy had a lethality of only 64.3%, the overall survivability of this group of dosages was higher than anticipated. Because of this, 350 Gy was suspected to likely yield a higher percent lethality if tested again. Therefore, 300 Gy was selected as the target dose.

The initial dose range mentioned above yielded no growth on some of the plates with *Monoraphidium minutum* cells (100% lethality), so the dose range was adjusted down to 25, 50, 75, 100, and 150 Gy with a 0 Gy control. A dose of 75 Gy yielded an average 90.5% lethality, making it ideal for mutagenesis (Figure 2.2).

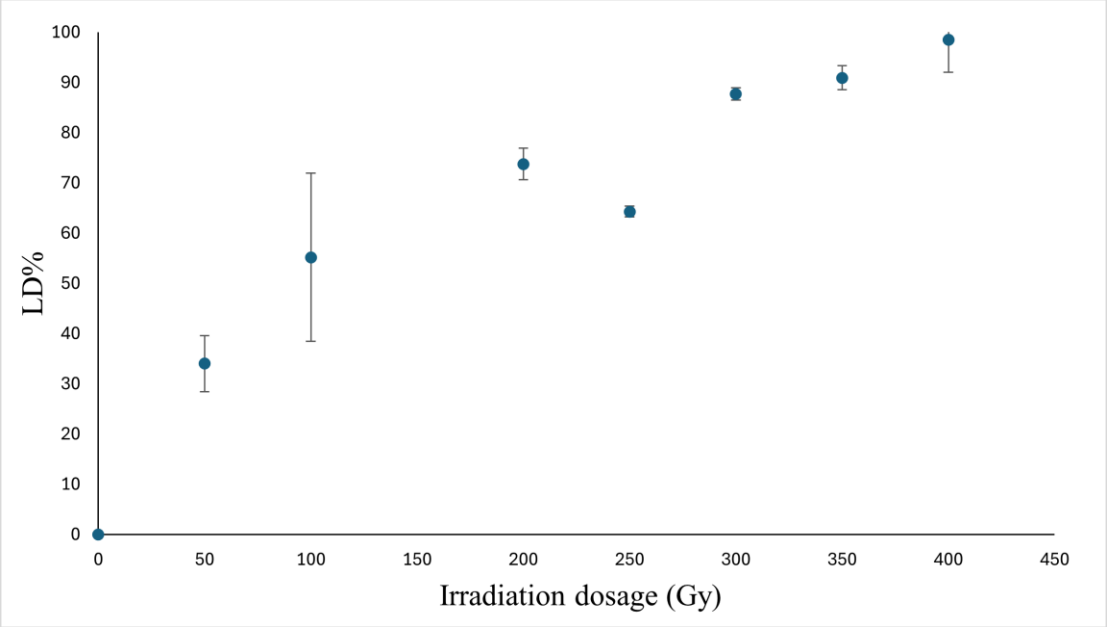

Figure 2.1: *Scenedesmus rubescens* gamma irradiation lethal dose (LD) curve. An equal number of cells were plated on BG-11 agar plates and grown under continuous light (175 µmol photons m^{-2} s^{-1}) at 25°C until visually distinct colonies formed (n=3). Values represent averages ± 1 standard deviation.

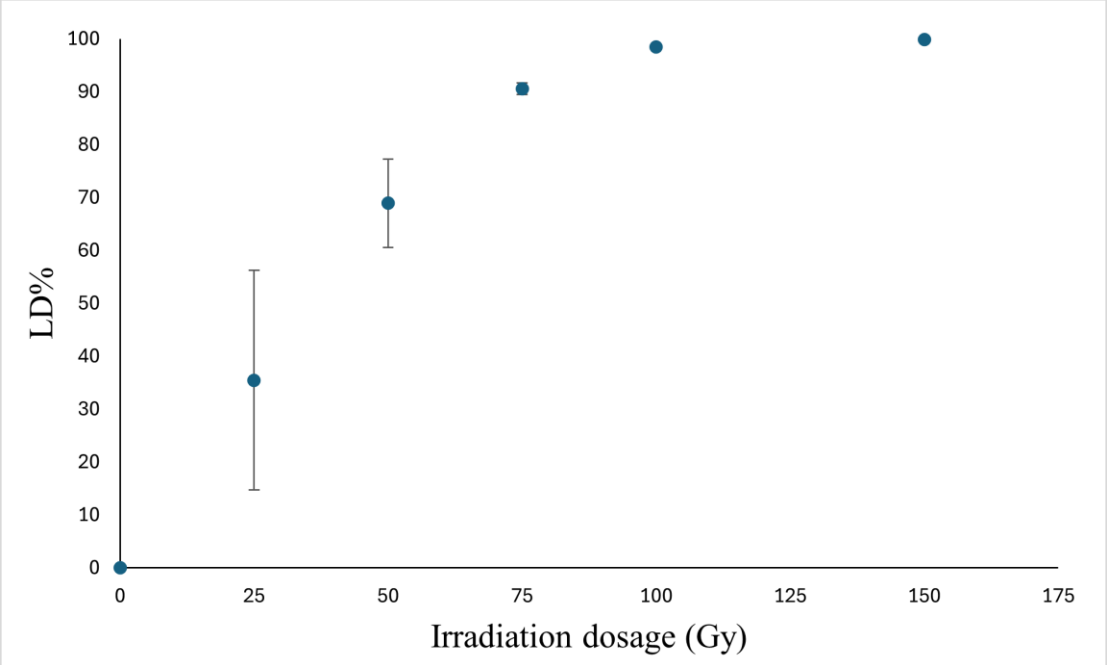

Figure 2.2: *Monoraphidium minutum* gamma irradiation lethal dose (LD) curve. Equal volume of cell culture was plated on BG-11 agar plates and grown under continuous light (175 µmol photons m^{-2} s^{-1}) at 25°C until visually distinct colonies formed (n=3). Values represent averages ± 1 standard deviation.

3.2. Fluorescence-based screening of mutagenized strains

3.2.1. Observations of putative Scenedesmus rubescens and Monoraphidium minutum mutants with altered chlorophyll fluorescence kinetics

To identify strains with altered photosynthetic efficiency, *Scenedesmus rubescens* and *Monoraphidium minutum* mutants were screened for changes in chlorophyll fluorescence kinetics, revealing distinct groups of mutants with alterations in photosynthetic performance. Exponentially growing WT *Scenedesmus rubescens* and *Monoraphidium minutum* cells were treated with LD90 doses of ^{137}Cs gamma irradiation. Following recovery, cell colonies were picked and streaked onto 6x6 square plates containing BG-11 agar. Each plate contained 35 isolated mutants and a WT control. A brief summary of the strategy used to screen suspected mutants can be seen in Figure S6.

Single cell colonies for 3135 *Scenedesmus rubescens* mutants and 3356 *Monoraphidium minutum* mutants were screened during this process and 20 and 24 mutants were identified for *Scenedesmus rubescens* and *Monoraphidium minutum* respectively to have appreciably altered chlorophyll fluorescence kinetics. For *Scenedesmus rubescens,* two groups of altered fluorescence kinetics (AFK) mutants were identified, and five groups of AFK mutants were identified for *Monoraphidium minutum.*

Scenedesmus rubescens mutants were observed to have two distinct types of alterations to their fluorescence kinetics. The first group of mutants, represented by *SR G-46* in Figure 2.3, were characterized as having altered relaxation kinetics, specifically under dark periods following illumination. Relative fluorescence could be seen increasing contrary to WT, where fluorescence tended to decrease when transitioning from light to darkness. 14 of the 20 AFK mutants were observed to have this phenotype. The second group of AFK mutants observed in

Scenedesmus rubescens, represented by *SR I-202,* were mutants containing a dip in fluorescence in low or high light followed by an increase to a higher level than was initially noticed at the start of the light period. This is phenotype was not observed in WT. 6 of the 20 AFK mutants were observed with this phenotype.

Only four mutants retained their altered fluorescence kinetics when regrown in triplicate. *SR 83, SR 89,* and *SR L-1* contained altered fluorescence kinetics similar to *SR G-46* in Figure 2.3. *SR C-10* contained altered fluorescence kinetics similar to *SR I-202* in Figure 2.3.

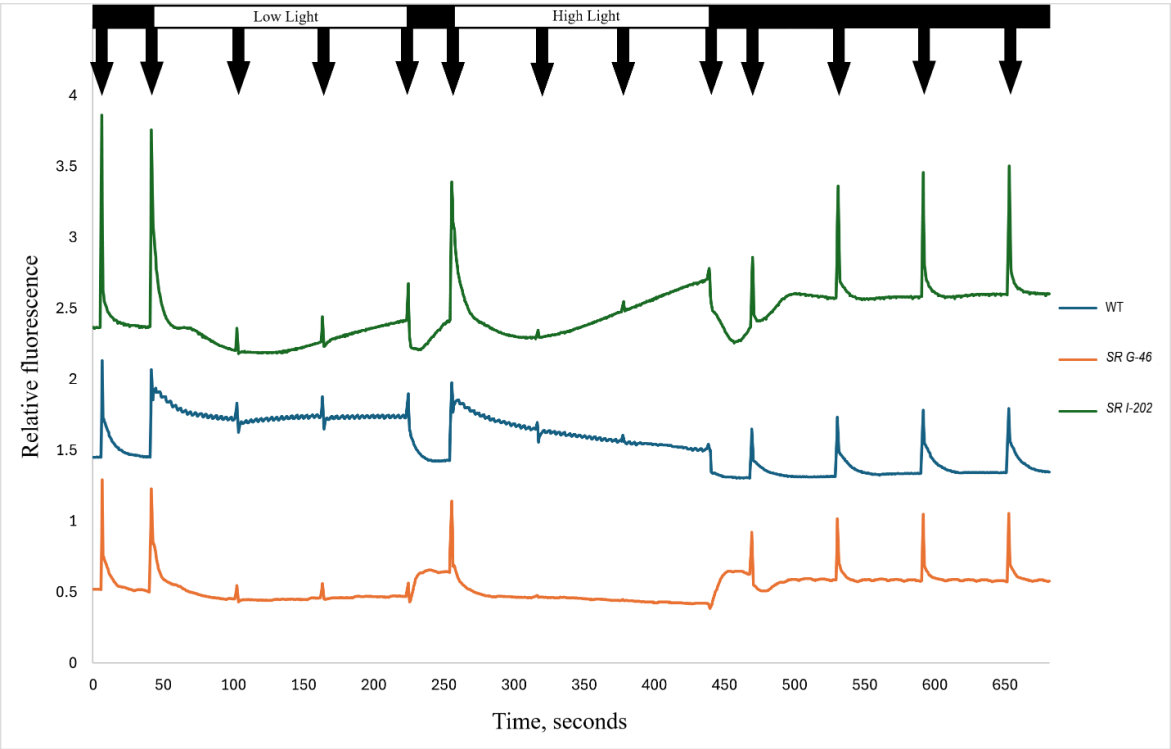

Figure 2.3: *Scenedesmus rubescens* chlorophyll fluorescence trace kinetics observed using the IMAGING-PAM assays of isogenic strains on agar plates. Black bars depict dark exposure, Low Light indicates actinic light levels of 186 µmol photons m^{-2} s^{-1}, High Light shows timing of actinic light levels of 1076 µmol photons m^{-2} s^{-1}. Arrows indicate timing of saturating light pulses. WT indicates a single replicate of WT *Scenedesmus rubescens. SR G-46* and *SR I-202* were mutants with observed alterations to their chlorophyll fluorescence trace kinetics. Relative fluorescence of individual strains were offset manually for ease of pattern comparison.

There were four distinct types of AFK mutants identified in *Monoraphidium minutum*. The first group was similar to *SR G-46* described Figure 2.3, where relative fluorescence increased in dark periods that immediately followed illumination periods which is not seen in WT. This is represented as *MRM 347* in Figure 2.4. Of the 24 AFK mutants found, 6 of them contained this phenotype. The second group of mutants were ones that exhibited increased fluorescence in low light saturation, these mutants' fluorescence increased noticeably and then began to decrease shortly after. The general fluorescence kinetics of this mutant are represented as *MRM I-121* in Figure 2.4. This was the most common type of AFK mutant observed, with 16 of the 24 mutants exhibiting this phenotype. The third group, represented by *MRM J-63*, contained one mutant that demonstrated perturbed saturation pulses under low light conditions where fluorescence dropped following saturating pulses rather than increased. The last group, represented by *MRM L-367*, contained one mutant that demonstrated noticeably decreased fluorescence, resulting in a muted fluorescence trace.

Overall, the only mutants that demonstrated repeated AFK when grown in triplicates were *MRM 307, MRM 308, MRM 312, MRM 323, MRM 343,* and *MRM 347.* These mutants were kept for future growth assays.

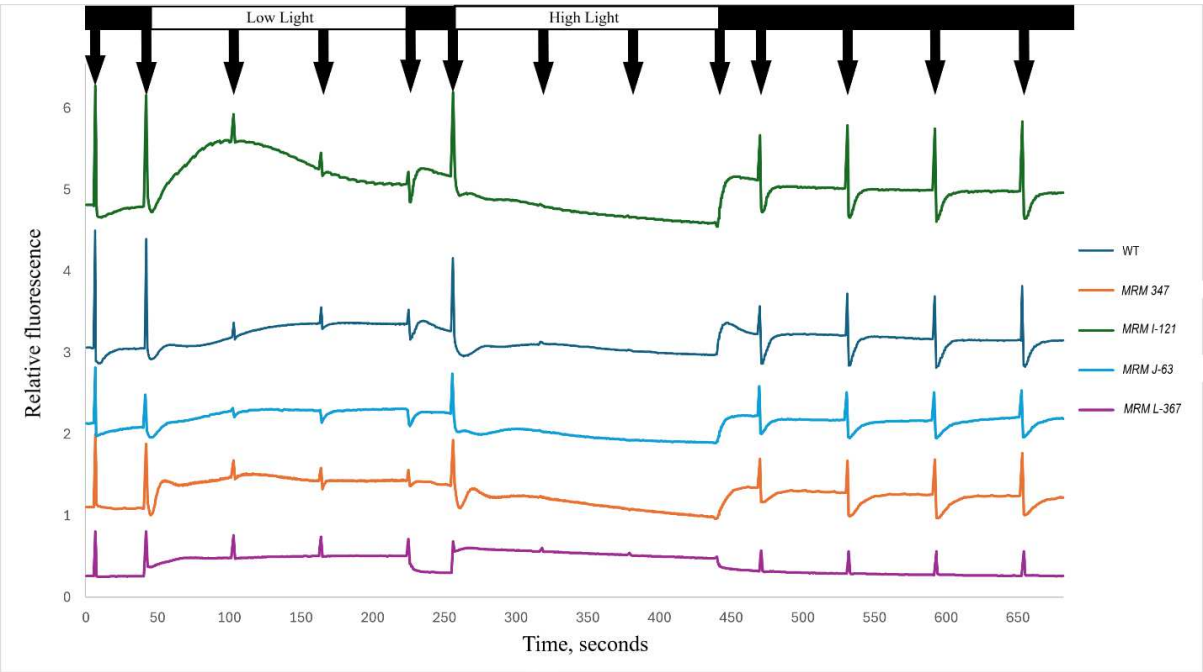

Figure 2.4: *Monoraphidium minutum* chlorophyll fluorescence trace kinetics observed using the IMAGING-PAM assays of isogenic strains on agar plates. Black bars depict darkness, Low Light = 186 µmol photons m^{-2} s^{-1}, High Light = 1076 µmol photons m^{-2} s^{-1}, and arrows are saturating light pulses. WT indicates a single replicate of WT *Monoraphidium minutum. MRM 347, MRM I-121, MRM J-63,* and *MRM L-367* were mutants with observed alterations to their chlorophyll fluorescence trace kinetics. Relative fluorescence of individual strains were offset manually for ease of pattern comparison.

3.2.2. Screening of scenedesmus rubescens and Monoraphidium minutum mutants with altered physiology

In addition to looking for mutants with altered chlorophyll fluorescence kinetics, mutants were also screened for general alterations to their photophysiology. Parameters such as increased Fv/Fm, altered non-photochemical quenching (NPQ), and faster induction and relaxation of photochemical quenching (qL) were observed. Fv/Fm is the maximum quantum yield of PSII, representing the efficiency of light energy conversion in photosynthesis. NPQ is a photoprotective mechanism that dissipates excess light energy as heat to protect the photosynthetic apparatus. qL reflects the fraction of open PSII reaction centers, indicating the capacity for light-driven electron transport. Mutants that demonstrated traits indicative of

potentially improved photophysiology were regrown in triplicates to observe if their phenotypes remained. Many mutants with alterations in these photosynthetic parameters did not have alterations in their chlorophyll fluorescence kinetics similar to the ones mentioned in Figures 2.3 and 2.4. Mutants that were not labeled as AFK in these figures retained chlorophyll fluorescence kinetics similar to their WT counterparts.

A total of 149 *Scenedesmus rubescens* mutants were initially identified to have photophysiological alterations such as improved Fv/Fm, altered NPQ, or higher qL after light exposure. After triplicate screening of these mutants, 22 mutants retained their photophysiological alterations and were thus kept for liquid cultivation (Table 1.1). 8 of the 149 mutants have yet to be rescreened in triplicates. Six mutants demonstrated a wide range of increased qL under low light illumination. These values were demonstrated as a range rather than as averages due to one of the triplicate plates demonstrating overall lower Fv/Fm values, indicating stressed cultures. Mutants *SR 83, SR 89,* and *SR L-1* were identified to have altered fluorescence kinetics similar to *SR-G46* in Figure 2.3. *SR 83, SR 89,* and *SR L-1* demonstrated increased qL at the start of low light, with *SR 89* and *SR L-1* also demonstrating an increased NPQ at the end of the high light period. *SR C-10,* which had altered fluorescence kinetics resembling *SR I-202* in Figure 2.1, had an increased Fv/Fm and low light qL compared to WT.

Table 2.1: Summary of changes in *Scenedesmus rubescens* chlorophyll fluorescence kinetics parameters used to downselect strains for liquid culture assay. A percentage range taken from duplicate cultures was indicated by (*) (n=2). All other strains are grown in triplicates and displayed as averages ± 1 standard deviation (n=3). qL averages were calculated based on the qL values measured at the first saturating pulse during low light illumination. NPQ averages are calculated based on the last saturating pulse of the high light illumination period. Mutants labeled with AFK were ones that were identified to have alterations in their fluorescence kinetics.

Mutant	Photosynthetic Parameter	Percent Change in Parameter Vs. WT
SR 83	Increased low light qL (AFK)	51.8 ± 24.2%
SR 89	Increased low light qL; high light NPQ (AFK)	128 ± 55.1%; 71.3 ± 17.9%
SR 218	Increased low light qL	11.5 – 78.3%*
SR 222	Increased low light qL	32.1 – 95.2%*
SR 225	Increased low light qL	19.1 – 119.3%*
SR 249	Increased low light qL	52.0 – 141.0%*
SR 260	Increased low light qL	43.0 – 124.1%*
SR 261	Increased low light qL	34.4 – 102.4%*
SR C-6	Increased Fv/Fm	10.5 ± 2.3%
SR C-10	Increased Fv/Fm; Increased low light qL (AFK)	18.0 ± 2.5%; 63.1 ± 5.6%
SR I-148	Increased Fv/Fm	6.2 ± 1.8%
SR I-158	Increased Fv/Fm	7.4 ± 1.3%
SR I-164	Increased Fv/Fm	9.8 ± 1.2%
SR I-241	Increased Fv/Fm	12.7 ± 0.4%
SR I-299	Increased Fv/Fm	8.0 ± 1.3%
SR I-305	Increased Fv/Fm	8.4 ± 1.0%
SR I-310	Increased Fv/Fm	7.8 ± 0.3%
SR I-349	Increased Fv/Fm	15.8 ± 1.2%
SR K-223	Increased Fv/Fm	11.5 ± 2.0%
SR K241	Increased Fv/Fm	12.0 ± 2.9%
SR-L233	Increased Fv/Fm	6.9 ± 1.2%
SR L-1	Increased high light NPQ; Increased low light qL (AFK)	150.4 ± 61.4%; 39.9 ± 9.2%
SR L-45	Increased high light NPQ	63.2 ± 44.5%

A total of 135 *Monoraphidium minutum* mutants were initially identified to have photophysiological alterations such as improved Fv/Fm, altered NPQ, or higher qL during light exposure were found and eight were selected after triplicate growth for liquid cultivation (Table 1.2). 9 of the 135 mutants have yet to be rescreened in triplicates. Half of the mutants found demonstrated large increases in NPQ. Only one mutant was found to have higher qL in low light and one mutant was found to have increased Fv/Fm when screened again in triplicates. *MRM K-25* and *MRM K-29* mutants showed improved Fv/Fm during initial screening but not in triplicate growth. The 6 AFK mutants that retained their chlorophyll fluorescence kinetics alterations, *MRM 307, MRM 308, MRM 312, MRM 323, MRM 343,* and *MRM 347,* did not show alterations in these photophysiological parameters.

Table 2.2: Summary of changes in *Monoraphidium minutum* chlorophyll fluorescence kinetics parameters used to downselect strains for liquid culture assay. Mutants are grown in triplicates and displayed as averages ± 1 standard deviation (n=3). Results that were obtained by a single datapoint are indicated by (*) (n=1). NPQ averages are obtained from the values measured during the last saturating pulse of the high light illumination period. The qL average is calculated based on the first saturating pulse during the low light illumination period.

Mutant	Reason for Selection	Percent Change in Parameter Vs. WT
MRM J-48	Increased low light qL	22.0 ± 3.1%
MRM J-325	Increased Fv/Fm	12.3 ± 0.7%
MRM K-25	Increased Fv/Fm	9.5%*
MRM K-29	Increased Fv/Fm	11.9%*
MRM 273	Increased high light NPQ	35.1 ± 3.1%
MRM 310	Increased high light NPQ	47 ± 3.9%
MRM 342	Increased high light NPQ	53.4 ± 4.2%
MRM 346	Increased high light NPQ	37.5 ± 2.3%

3.2.3. Visual screening of Scenedesmus rubescens mutants with altered pigmentation

In addition to screening for altered photophysiology, mutant colonies were also visually screened for any changes in their pigmentation following irradiation. Colonies that demonstrated any pigmentation changes were streaked onto plates for isolation. Figure 2.3-A offers a visual demonstration of what streaked out pigment mutants looked like next to WT *Scenedesmus rubescens* when growing on BG-11 agar. Figure 2.3-B shows a higher magnification perspective of pigment mutant colonies growing next to a mutant that either lost or did not have this mutation. Figure 2.3-C shows how these pigment mutants grew when streaked out onto a BG-11 square plate next to WT cultures. Lastly, Figure 2.3-D is a side-by-side comparison of the isolated pigment mutants growing in 5 ml of BG-11. Cultures that grew well when transferred to liquid culture were kept to measure their growth rates. A total of 14 mutants were isolated due to their suspected pigment alterations and subsequently kept to be tested for their growth performance in liquid culture. Mutants demonstrating this phenotype were initially labeled as "SRB" standing for *Scenedesmus rubescens* brown as colonies initially appeared to have a brownish hue to them. Three other mutants with altered pigmentation (SR J-16, SR J-35, SR J-64) were isolated but were named based on the alphanumeric naming scheme that was used for most of the screening process.

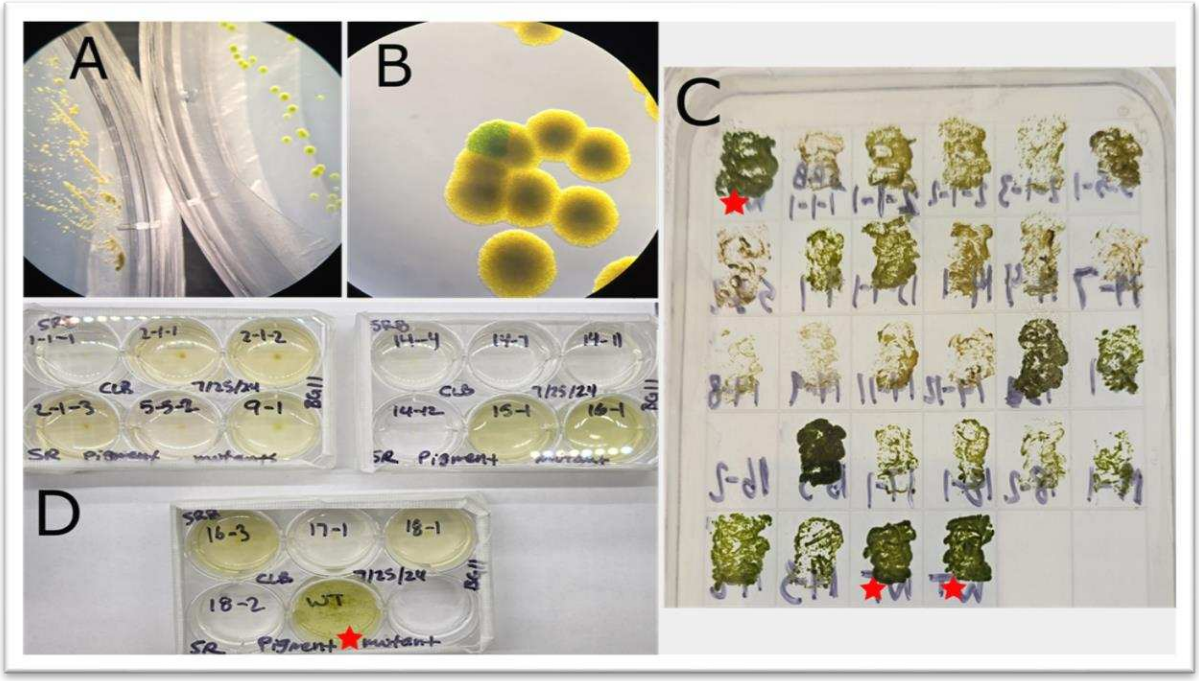

Figure 2.3: Examples of altered pigmentation observed in *Scenedesmus rubescens.* A) Microscopy image (8x magnification) comparing suspected pigment mutants (left) and WT *Scenedesmus rubescens* (right) growing on BG-11 agar plates. B) Microscopy image (~60x magnification) of suspected pigment mutant colonies growing next to a mutant with WT-like pigmentation. C) Isolated pigment mutants growing on a BG-11 agar plate. WT cultures are denoted with a red star. D) Isolated pigment mutants inoculated in BG-11 liquid culture in 6-well plates under ~200 µmol photons m^{-2} s^{-1} light. Cultures growing in the wells are not OD-normalized.

3.3. Evaluation of growth performance of selected Scenedesmus rubescens and Monoraphidium minutum mutants

3.3.1. Initial growth performance screening of selected Scenedesmus rubescens mutants

A total of 37 *Scenedesmus rubescens* mutants were grown in duplicate cultures that were diluted to 50 cells μl^{-1} in 50 ml BG-11. Wild type *Scenedesmus rubescens* growth ranges ranged from from 1.1 to 1.3 day^{-1}. Mutants selected based on observed alterations in their fluorescence kinetics, namely *SR 83, SR 89, SR C-10,* and *SR L-1,* grew poorly, not exceeding a maximum specific growth rate of 0.75 day^{-1}. *SR 83, SR 89,* and *SR L-1* had fluorescence kinetics similar to *SR G-46* in Figure 2.3 and demonstrated repeated increases in qL at the start of the low light

period. *SR C-10,* which had fluorescence kinetics similar to *SR I-202* in Figure 2.3*,* had an 18% higher Fv/Fm than WT on average. Despite this, none of these mutants had comparable growth rates to WT. Of the mutants selected based on their increased Fv/Fm, high qL in low light, and altered NPQ, only one mutant, *SR I-148* outperformed WT, achieving a maximum specific growth rate of 1.33 day^{-1}. Pigment mutants *SRB 1-1, SRB 9-1,* and *SRB 18-1* were selected to be grown in triplicate due to their robust initial performance in duplicate growth. *SRB 1-1* was the slowest of these mutants with a maximum specific growth rate of 0.8 day^{-1}. *SRB 9-1* and *SRB 18-1* had better maximum specific growth rates of 0.93 day^{-1} and 1.2 day^{-1} respectively. No other mutant demonstrated adequate specific growth rates to warrant triplicate growth.

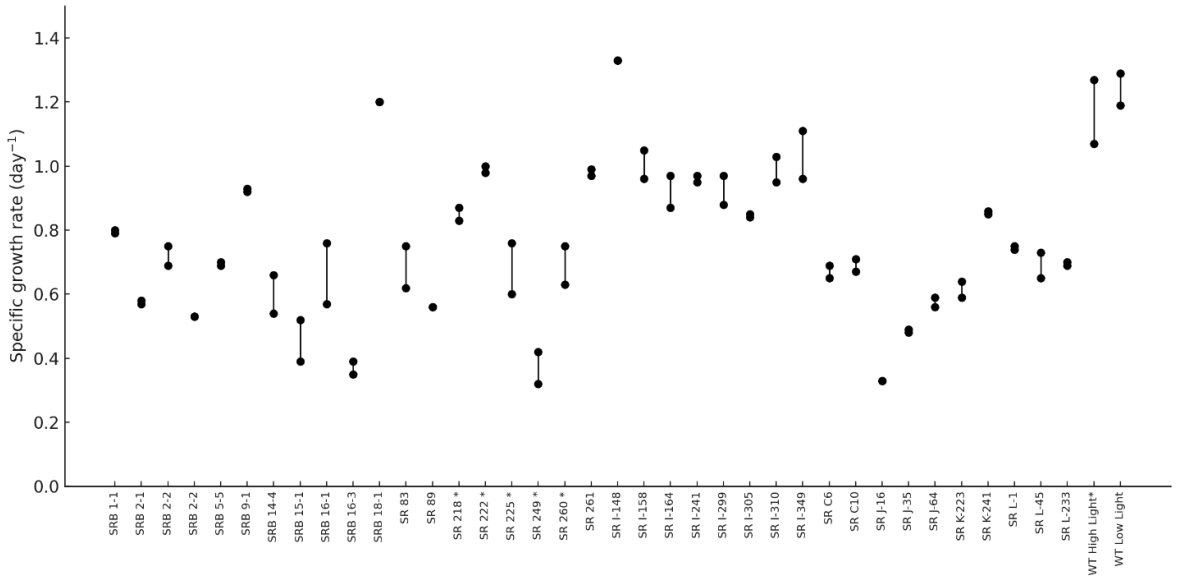

Figure 2.4: Range of specific growth rates for down-selected *Scenedesmus rubescens* mutants. Mutants with (*) represent strains assayed in high light (~750 µmol photons m^{-2} s^{-1} 16h light 8h dark) while mutants without an asterisk were assayed in low light (~280 µmol photons m^{-2} s^{-1} 16h light 8h dark) at 25°C in duplicate.

3.3.2. Initial growth performance screening of selected Monoraphidium minutum mutants

14 total *Monoraphidium minutum* mutants were selected for duplicate growth screening. 6 of the 14 mutants, *MRM 307, MRM 308, MRM 312, MRM 323, MRM 343,* and *MRM 347* contained altered fluorescence kinetics similar to *MRM 347* in Figure 2.4 and the other 8 mutants were described in Table 2.2. Most of the mutants had lower maximum specific growth rates compared to WT such as *MRM 343, MRM 308,* and *MRM 310. MRM J-325, MRM K-25* and *MRM K-29* had maximum specific growth rates (1.45 day^{-1}, 1.26 day^{-1} and 1.42 day^{-1} respectively) higher than the maximum specific growth rate observed in low light WT (1.25 day^{-1}). *MRM J-48* had a maximum specific growth rate that was 0.01 day^{-1} lower than WT, so it was not grown in triplicates.

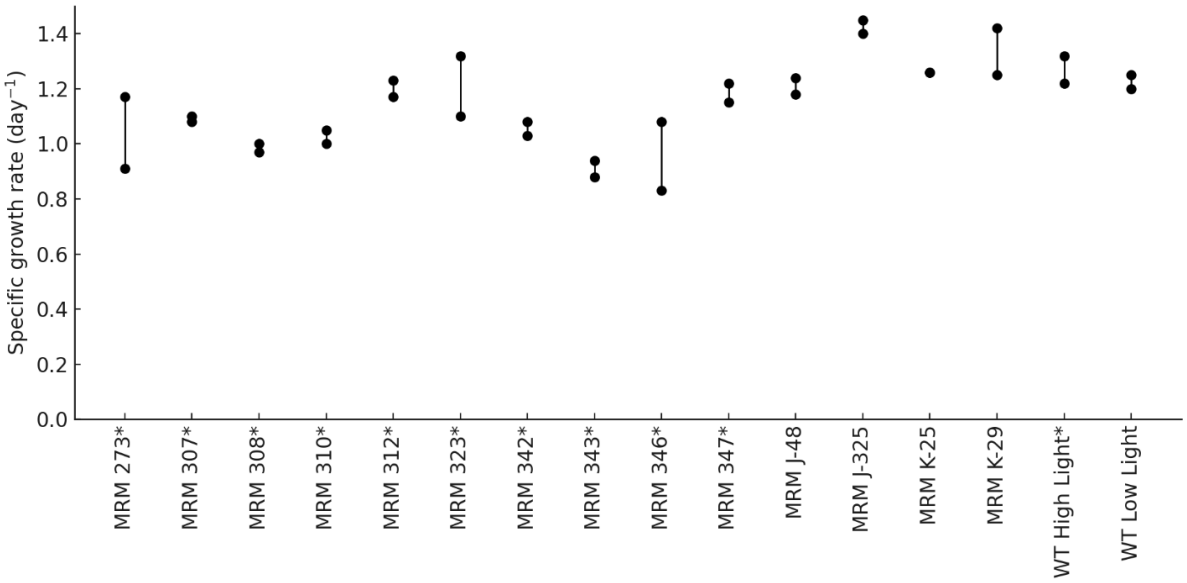

Figure 2.5: Range of specific growth rates for down-selected *Monoraphidium minutum* mutants. Mutants with (*) represent strains assayed in high light (~750 µmol photons m^{-2} s^{-1} 16h light 8h dark) while mutants without an asterisk were assayed in low light (~280 µmol photons m^{-2} s^{-1} 16h light 8h dark) at 25°C in duplicate.

3.3.3. Triplicate growth performance screening of Scenedesmus rubescens mutants

SRB 1-1, SRB 9-1, SRB 18-1, and *SR I-148* were grown in triplicates under low light conditions mentioned in Figures 2.6 and 2.7. In Figure 2.6 the only strain that surpassed the average specific growth rate observed in WT *Scenedesmus rubescens* (1.2 day^{-1}) was *SR I-148* with a specific growth rate of 1.24 day^{-1}. This was only a 3% increase in growth and was not significantly higher than WT (Student's t-test: $p \geq 0.05$). This strain was held onto, but further tests have not been conducted on it yet. *SRB 9-1* and *SRB 18-1* had comparable growth rates to WT but did not surpass it. Overall, none of these strains presented significant improvements in specific growth rate compared to WT.

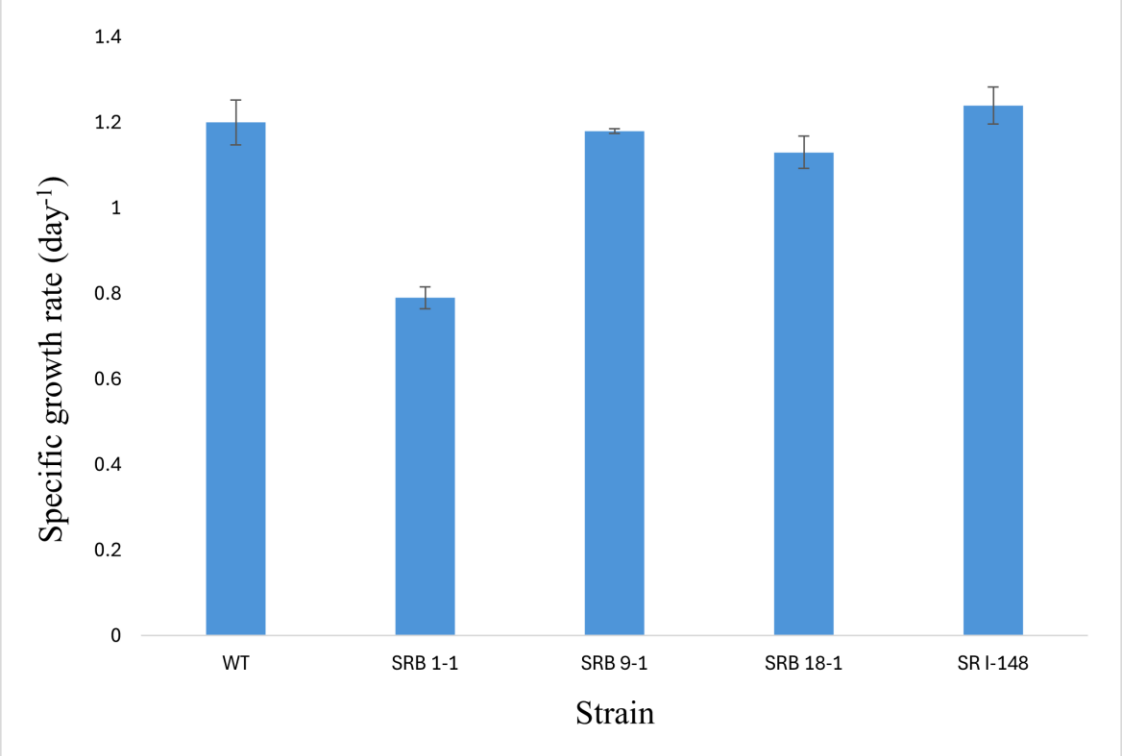

Figure 2.6: Average specific growth rates for down-selected *Scenedesmus rubescens* mutants. Strains were grown in triplicate flasks diluted to 50 cells μl^{-1} in 50 ml BG-11 grown in 250 ml flasks. They were exposed to ~280 µmol photons m^{-2} s^{-1} 16h light 8h dark at 25°C and continuously shaken.

3.3.4. Triplicate growth performance screening of Monoraphidium minutum mutants

MRM J-325, MRM K-25, and *MRM K-29* were grown in triplicates with WT and only *MRM J-325* outperformed it, demonstrating an average 23 ± 9.4% increase in specific growth rate over WT (Figure 2.7). *MRM J-325* was further selected to test biomass accumulation to see whether it outperforms WT. *MRM K-25* and *MRM K-29* both showed decreased specific growth rates compared to WT and were not further selected.

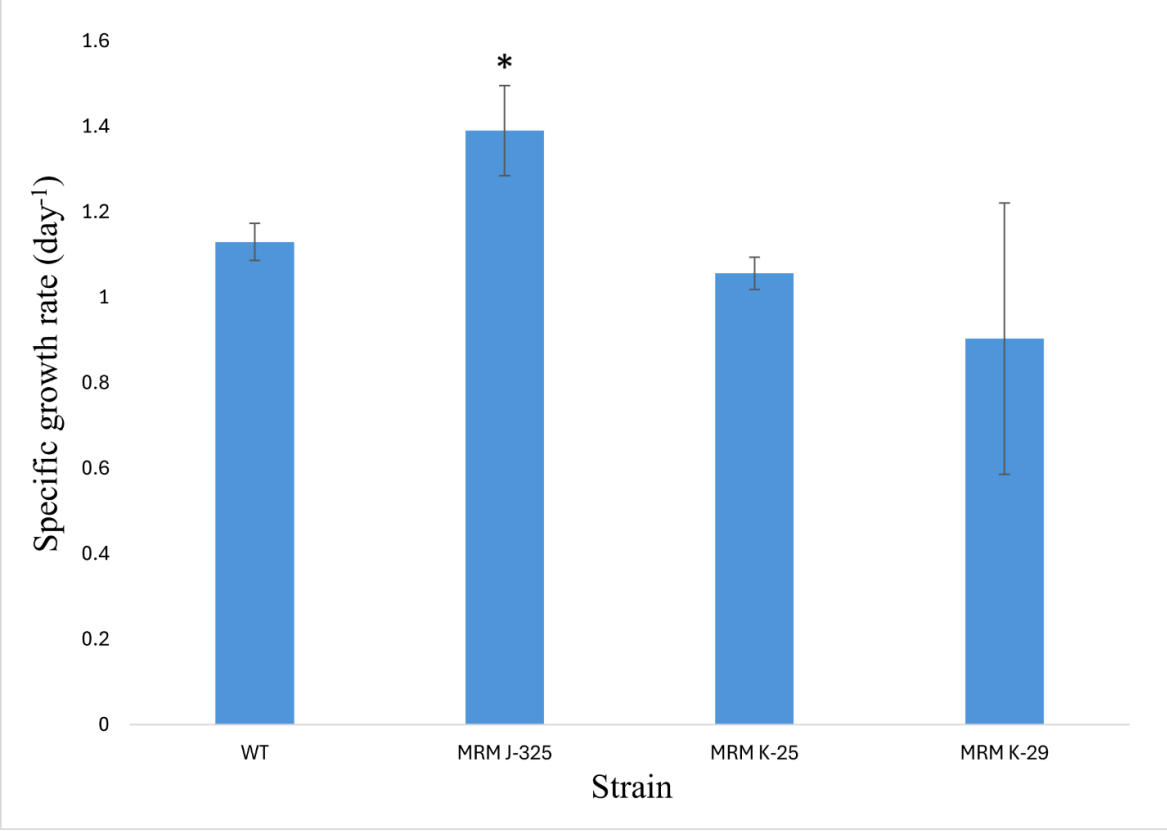

Figure 2.7: Average specific growth rates of down-selected *Monoraphidium minutum* mutants. Strains were grown in triplicate flasks diluted to 50 cells μl^{-1} in 50 ml BG-11 grown in 250 ml flasks. They were exposed to ~280 µmol photons m^{-2} s^{-1} 16h light 8h dark at 25°C and continuously shaken. (*) indicates Student's t-test = $p < 0.05$.

4. Discussion

4.1. Mutagenesis of down selected strains

Mutagenesis has been demonstrated as a useful tool in plant and microbial biotechnology, offering a variety of methods to generate mutants with improved traits for industrial applications (Sikora et al., 2011; Kumawat et al., 2019). Mutagenesis has been a particularly transformative resource in terms of enhancing growth performance and biomass accumulation. Generated mutant libraries also serve as a powerful resource for algal biotechnology research by helping to reveal the functional roles of specific genes and pathways that result in increased biomass production as well as improved stress tolerance and photosynthetic efficiency (Bleisch et al., 2022; Cecchin et al., 2020; Trovão et al., 2022).

Mutagenesis has also played a pivotal role in advancing algal biotechnology, leading to the development of strains with improved lipid and carotenoid content, increased thermotolerance, and chlorophyll deficiency. In *Nannochloropsis gaditana,* ethylmethane sulfonate (EMS) mutagenesis revealed a mutant with decreased chlorophyll content and an increased lipid content (Cecchin et al., 2020). Ong et al., (2010), identified *Chlorella sp.* mutants via EMS mutagenesis with improved thermotolerance compared to WT. A *Phaeodactylum tricornutum* mutant generated via heavy-ion irradiation showed a 25% higher fucoxanthin content compared to WT (Fan et al., 2021). These successes demonstrate how mutagenesis can improve value-added product content and stress tolerance. In this thesis, the use of gamma irradiation mutagenesis of *Scenedesmus rubescens* and *Monoraphidium minutum* aimed to build on these achievements and explore new ways to optimize algal strains for large scale cultivation.

4.1.1. ^{137}Cs gamma irradiation lethal dose dssay

Prior to mutagenesis, a lethal dose curve had to be established to determine the effects that a wide range of ^{137}Cs gamma irradiation dosages would have on cell lethality of both *Scenedesmus rubescens* and *Monoraphidium minutum*. When mutagenizing an organism, it is generally ideal to select a dosage that yields a 10-20% survival rate (De Jaeger et al., 2014; Bleisch et al., 2022). Selecting a dosage that results in a high survival rate might not induce significant genetic changes which would lead to a lower probability of desired traits occurring. Additionally, strains that are only mildly mutated have a higher probability to revert to their original phenotypes (Ward, 1988). Alternatively, selecting a dosage that has an extremely low survival rate can cause excessive cell death, with surviving cells having potentially detrimental mutations caused by widespread DNA damage (Sikora et al., 2011).

Initial irradiation dosages of 50, 100, 200, and 400 Gy, as well as a 0 Gy control were initially selected based on previous research of ionizing radiation effects on *Chlamydomonas reinhardtii* which found 400 Gy to be the upper limit of survivability (Baek et al., 2016; Koo et al., 2017). Similarly, Liu et al., (2015) tested a dosage range from 0 to 3000 Gy and found that 500 Gy yielded a 2% survivability. The selected range worked for *Scenedesmus rubescens* as 300 Gy was selected as the optimal dose (Figure 2.1) but was too high for *Monoraphidium minutum,* which caused some of the triplicate plates to not grow at all. Colonies were only seen forming at 50 and 100 Gy, so the range of dosages was adjusted to 0-150 Gy which yielded growth on plates, resulting in a 75 Gy dose being selected for its ~90% lethality of cells (Figure 2.2). Dosage ranges can vary based on the selected species. Ma Y. et al., (2013), utilized a dosage range of 20 to 160 Gy in *Nannochloropsis oceancica* to generate mutants with increased lipid productivity. On the other end of the spectrum, the polyextremophile bacteria *Deinococcus*

radiodurans was shown to survive up to 5000 Gy (Cox and Battista, 2005). The difference in optimal dosages between *Scenedesmus rubescens* and *Monoraphidium minutum* is not out of the ordinary.

4.2. Fluorescence-based screening of mutagenized strains

The use of a fluorescent-based screening method provides a higher-throughput alternative for identifying potential high-productivity algal mutants, compared to traditional growth-based selection approaches. Growth-based selection methods require the culturing of individual strains to select for improved growth and biomass productivity performance. This method is both time consuming and resource intensive as culturing strains can take anywhere from several days to weeks depending on the organism and growth conditions. Additionally, the cost of growth media, lab equipment, and labor increase as a result. The benefit of a growth-based selection process is the direct quantitative measurement of growth performance or biomass productivity.

Fluorescence-based techniques also enable a greater understanding of how each mutant functions at a photophysiological level, revealing changes in photosystem efficiency, photoprotective mechanisms and energy dissipation (Schreiber, 2004). By screening for these traits, it is possible to identify algal mutants with optimized photosynthetic performance, ultimately leading to improved biomass productivity as enhanced photosynthesis increases the rate of carbon fixation and energy conversion, resulting in greater production organic compounds that drive cell growth and biomass accumulation (Ware et al., 2020). This approach increases throughput and eliminates the need to grow out each strain individually as many reports of microalgal mutagenesis have generated well over a thousand mutants (Ware et al., 2020; Ma et al., 2013; Baek et al., 2016).

The ecophysiology of mass algal cultures focuses on understanding how algae adapt to the dynamic and stressful conditions of large-scale cultivation. Under industrial scale cultivation, cells encounter a combination of dynamic environmental stressors, such as fluctuations in light levels and temperatures, nutrient limitation, and high cell densities that can result in lost energy via processes like NPQ, damage from oxidative stress, and metabolic shifts (Peers, 2014). All of these factors slow down electron transport and carbon fixation and ultimately hinder growth and productivity. The goal of this screening process is to alleviate energy drains while maintaining efficient photosynthesis by recognizing certain fluorescence phenotypes with altered NPQ capabilities, improved Fv/Fm, and elevated qL recovery rates associated with greater adaptability to those conditions. This phenomenon corresponds with what Peers, (2014) stressed in the convergence of ecophysiology and systems biology concepts, which is the development of algal strains that can withstand large scale production while still being able to maintain high productivity under changing and usually unfavorable conditions. A brief summary of the strategy used to screen suspected mutants can be seen in Figure S6.

4.2.1. Observations of altered fluorescence kinetics in putative Scenedesmus rubescens and Monoraphidium minutum mutants

The fluorescence trace kinetics and other photophysiological parameters of mutants were measured via IMAGING-PAM using a custom light script. This light script is similar to the one described by Ware et al., (2020) used to assess photophysiological parameters such as Fv/Fm, redox state of the plastoquinone pool, and the reversibility of ΔpH-dependent processes, including NPQ, alternative electron transport (AET), and state transitions, to identify mutants with altered chlorophyll fluorescence kinetics (AFK).

The first group of *Scenedesmus rubescens* AFK mutants were characterized as having altered relaxation kinetics, specifically under dark periods following illumination. Relative fluorescence could be seen increasing contrary to WT, where fluorescence tended to decrease when transitioning from light to darkness. This phenotype suggests the impairment of the AET component, plastid terminal oxidase-2 (PTOX2), which is a plastoquinol oxidase that transfers electrons from the PQ pool to molecular oxygen, playing a crucial role in protecting photosynthetic mechanisms from over-reduction. (Houille-Vernes et al., 2011). Ultimately, PTOX2 is important during stressful conditions such as continuous high light or temperature to help manage excess electrons and reduce oxidative damage. It was previously observed that these mutants possessed higher NPQ levels in low and high light intensities compared to WT. This could be a cellular response to enhance NPQ in the absence of PTOX2 in order to manage excess excitation energy and maintain redox balance (Levin et al., 2024). NPQ is a photoprotective mechanism that dissipates excess light energy as heat, preventing photodamage to the photosynthetic machinery. Selecting for mutants with altered NPQ dynamics can enhance photosynthetic efficiency and biomass productivity especially under variable light conditions. Mutants capable of rapidly inducing and relaxing NPQ can better balance photoprotection with light utilization, preventing energy loss under low light and minimizing photodamage under high light (Niu et al., 2023). Additionally, improved NPQ regulation may work synergistically with other photoprotective mechanisms, such as Flavodiiron (FLV) proteins, which help dissipate excess electrons and reduce oxidative stress, further contributing to improved productivity under dynamic light conditions (Allahverdiyeva et al., 2013). Initially, 14 of the 20 total *Scenedesmus rubescens* AFK mutants possessed this phenotype, but after triplicate screening, only 3 of them,

SR 31, SR 83, and *SR L-1* retained it. This suggests that some mutants potentially reverted back to the WT phenotype.

The second group of AFK mutants observed in *Scenedesmus rubescens* were mutants containing a sharp dip in fluorescence in low or high light followed by an increase to a higher base fluorescence level than was observed at the start of the light period. In Figure 2.3, WT *Scenedesmus rubescens* exhibited stable or gradually decreasing Fm' and F values during prolonged light exposure, indicating consistent photochemical quenching and a steady rate of electron transport. In contrast, *SR I-202* showed a distinct pattern in which Fm' and F values initially decreased upon light exposure but then increased with each subsequent saturating pulse. This suggests that *SR I-202* undergoes dynamic changes in its photosynthetic efficiency which could be due to altered regulation of energy dissipation of electron transport. During this period of increased fluorescence under light saturation, NPQ values of this group of mutants could be seen decreasing as illumination continued. This suggests that the initial rise in NPQ upon light exposure reflects the activation of energy-dependent quenching (qE), and the subsequent decrease in NPQ under prolonged illumination indicates a dynamic regulation of excess energy dissipation rather than a failure to induce photoprotective mechanisms. (Peers, 2009). However, a sustained decrease in NPQ under prolonged illumination was observed, pointing towards a potential impairment in downstream processes, such as electron transport. More specifically, there are potential electron flow disruptions in the cytochrome b_6f complex, plastoquinone pool, or photosystem I (PSI) which likely caused photoprotective issues in these mutants (Tikkanen et al., 2014; Malone et al., 2021). This type of impairment could lead to over-reduction of the electron transport chain, limiting the buildup of the proton gradient required to sustain NPQ, resulting in increased fluorescence under light stress (Johnson & Barry, 2021). Initially, damage

to photoprotection mechanisms was suspected but impairments in a photoprotective mechanism such as the xanthophyll cycle show overall decreases in NPQ rather than alterations in the induction or relaxation kinetics of NPQ in response to light (Niyogi et al., 1997). When grown in triplicates, none of these mutants retained their fluorescence phenotypes.

Four groups of *Monoraphidium minutum* AFK mutants were observed during the screening process. The first group was described as having increased fluorescence in the dark, similar to what was described with the supposed PTOX2 mutants found in *Scenedesmus rubescens.* However, further screening revealed that WT *Monoraphidium minutum* can exhibit a slight increase in fluorescence in the dark following high light. The main difference between this group of mutants and the one observed in *Scenedesmus rubescens* was that fluorescence does not increase in the darkness following low light as it does with *Scenedesmus rubescens*. Following triplicate growth of these mutants, they all retained their supposed phenotypic change and were kept for future growth comparisons with WT *Monoraphidium minutum.* These mutants would not be considered not true AFK mutants as cultures on this batch of plates were photosynthetically underperforming at the time based on their Fv/Fm (~0.5-0.53) which likely caused fluorescence kinetics to be different than they would under non-stressful conditions (Baker, 2008). This was likely due to light or nutrient related stress caused by the algae cultures being too old at the time of screening (Erickson et al., 2015). Initially, mutagenized cell colonies were picked and plated as soon as they appeared on the plates, which meant that cells had to grow on the square plates for 1 to 2 weeks to achieve sufficient density and coverage for accurate PAM fluorometry measurements. However, this extended growth period on plates likely led to nutrient limitations and a decline in photosynthetic health, potentially affecting the reliability of the screening results. Typically, when plates were grown for 2 weeks, their Fv/Fm values would

be noticeably lower than the Fv/Fm values of healthy, unstressed cells which usually ranged from (0.6 to 0.7). To address this issue, the protocol was adjusted to allow mutagenized colonies to grow longer prior to plating. This ensured that cells plated onto the square plates were already at a higher density, which reduced the time required to achieve adequate coverage and minimizing the risk of nutrient depletion or photosynthetic decline.

The second group of mutants observed in *Monoraphidium minutum* were high chlorophyll fluorescence (HCF) mutants. These mutants exhibited an increase in fluorescence in low light after a saturating pulse followed by a steady decrease as illumination continued. Fm' values steadily decreased as light exposure progressed whereas WT kinetics demonstrated either a slight increase or maintenance of F and Fm'. HCF mutants have been characterized in *Arabidopsis thaliana* previously and are thought to have defects in PSII machinery as well as the electron transport chain, leading to reduced photochemistry efficiency (Schult et al., 2007; Meurer et al., 1996). These reports correspond to what was generally observed in the mutants, as one suspected HCF mutant had a 45% decrease in Fv/Fm compared to WT cultures grown on the same plate in triplicates (Figure S5). Lin et al., (2016) has discussed the three fates of photon energy absorption going towards photochemistry, heat dissipation via photoprotective mechanisms, or fluorescence. These mutants are likely releasing most of the energy absorbed in the form of fluorescence. Meurer et al., (1996) reported that photoautotrophic growth of the HCF *Arabidopsis thaliana* mutants was hindered due to their severely impaired photosynthetic performance. They followed up by cultivating the HCF mutants in a sucrose-supplemented agar medium, where the majority of the mutants grew normally, demonstrating the mutant's growth defect was due to photosynthetic deficiency (Meurer et al., 1996). Because of this it was determined that these supposed mutants were likely to be severely impaired in photochemistry

and did not warrant future growth or screening experiments. Of the 16 putative mutants discovered, 11 were tested in triplicates and 3 retained their phenotype.

The third group of AFK mutants observed, previously classified by Ware et al. (2020) as "perturbed saturation pulse" demonstrated a decrease in fluorescence following low light saturating pulses rather than an increase seen in WT cultures. Ware et al., (2020) observed six of these mutants while screening and was under the suspicion that this was a measurement error in the IMAGING-PAM. Further screening revealed them to not retain their original phenotype. Due to these previous findings, this mutant has not been yet tested in triplicates.

The last group of AFK mutants observed contained a decrease in chlorophyll fluorescence. While screening, it was not uncommon to see strains that had lower overall chlorophyll fluorescence, but these tended to be less dense as they had not fully grown. While screening, one mutant grew visibly as dense as the rest but had a noticeably lower F and Fm compared to other mutants and WT on the plate. The fluorescence kinetics of this mutant are similar to the WT kinetics aside from its decrease in fluorescence in both dark periods. This was classified by Ware et al., (2020) to be retarded oxidation in the dark and was characterized by minimal changes in fluorescence during dark periods. The *Chlamydomonas reinhardtii* mutant, *stm6,* which contained a similar phenotype, was tested by (Uhmeyer et al., 2017) and found that it exhibited an impairment in mitochondrial gene regulation. They observed a significant growth defect of the mutant under heterotrophic conditions, but it grew similarly to WT under photoautotrophic and mixotrophic conditions. This mutant has not yet been retested to confirm these physiological changes, but it is unlikely to grow better than WT as poor performance in the dark over multiple day-night cycles could reduce its overall productivity. An impairment in

mitochondrial respiration can decrease mitochondrial ATP production at night when photosynthesis stops, ultimately leading to reduced productivity (Uhmeyer et al., 2017).

Overall, this screeening approach had its benefits and flaws. I believe that finding a rapid way to standardize the number of cells that are plated would fix the issue that arose where some putative mutant cultures would be much denser than the others, resulting in it likely being more nutrient limited, and thus had a decreased photosynthetic efficiency. These strains were likely not performing at their true healthy state and would be selected as having AFK but were likely false positives.

4.2.2. Observations of improved or altered photophysiology in putative Scenedesmus rubescens and Monoraphidium minutm mutants

While screening supposed algal mutants for altered photophysiology, observing photosynthetic parameters such as increased Fv/Fm, higher qL under illumination, and altered NPQ can potentially have increased photosynthetic performance. Fv/Fm is a critical indicator of photosynthetic health and efficiency. Putative mutants with higher Fv/Fm values often exhibit enhanced light conversion efficiency, suggesting a greater capacity for energy utilization and potentially higher biomass accumulation (Gorbunov & Falkowski, 2021; Zhu et al., X. 2010; Singh et al., 2019). Altered NPQ mechanisms can play an important role in managing excess light energy and minimizing photoinhibition while maximizing light harvesting under differing light conditions (Ruban, 2016). Lastly, qL reflects the proportion of PSII reaction centers that are available for photochemistry. Faster qL recovery rates indicate improved electron transport efficiency and reduced photodamage, which can lead to sustained photosynthetic activity under varying light conditions and potentially contribute to increased biomass yields (Baker, 2008; Maxwell & Johnson, 2000).

Screening of *Scenedesmus rubescens* revealed 13 mutants that demonstrated repeatable increases in Fv/Fm, with the highest performing mutants, SR C-10 and SR I-349, having an increase of 18.0 ± 2.5% and 15.8 ± 1.2% respectively (Table 2.1). Values were presented in Tables 2.1 and 2.2 as percentage increases over WT as WT cells performed differently on each plate. Two mutants were identified with increased NPQ over WT. SR L-1 and SR L-45 had average NPQ increases of 150.4 ± 61.4% and 63.2 ± 44.5% respectively. Despite the high variability, the lowest increases in NPQ out of the SR L-1 and SR L-45 triplicates were 101% and 20% respectively. The high NPQ averages were calculated using the values obtained from the last saturating pulse under high light as NPQ is typically highest at this point. Lastly, six mutants demonstrated increased qL in low light conditions with SR 249 and SR 260 having percent increases over WT ranging from 52.0 – 141.0% and 43.0 – 124.1%. These values were not averaged as cultures on one of the triplicate plates suggested overall worse photophysiological health due to low Fv/Fm. For that reason, the results obtained from this plate were disregarded. Data used to calculate improvements in qL came from the first saturating pulse in low light as this is useful to show what percentage of PSII reaction centers are available for photochemistry immediately after being exposed to light. This value was not generated from the qL measurements obtained during high light as most of the reaction centers were closed which typically yielded qL values of 0.

Overall, noticeable alterations in photophysiology were harder to come by when screening Monoraphidium minutum mutants. Only three mutants containing improved Fv/Fm were selected for growth assays. MRM J-325 demonstrated an increase of 12.3 ± 0.7% compared to WT and MRM K-25 and MRM K-29 showed increases of 9.5% and 9% respectively (Table 2.2). Despite not showing these improvements when grown in triplicates, MRM K-25 and MRM K-29

were selected as there was available space and resources to grow two extra cultures for growth analysis. Because of this, their initial screening improvements were presented in Table 1.2. Four mutants exhibiting increased NPQ were discovered with the highest being MRM 342 having a 53.4 ± 4.2% increase over WT. Only one mutant, MRM J-48 demonstrated repeatable increases in qL under low light conditions. A 22.0 ± 3.1% higher qL compared to WT was noticed at the start of the low light period.

4.2.3. Visual screening of putative Scenedesmus rubescens mutants with altered pigmentation

Mutants with altered chlorophyll content or carotenoid profiles, which often manifest as distinct color changes, may exhibit improved light-harvesting capabilities or better stress tolerance, both of which can contribute to higher productivity. Cazzaniga et al., (2022) found that engineering astaxanthin accumulation in *Chlamydomonas reinhardtii* resulted in a significant increase in biomass under high light conditions as well as reduced photoinhibition. Shin et al., (2016) identified a mutant with an altered chlorophyll *a, b,* and carotenoid profile to have a truncated light antenna which has been shown to reduce the self-shading effect resulting in increased light penetration in dense cultures. While decreased pigment content reduces light-harvesting efficiency per cell, it can improve overall culture productivity in dense, outdoor systems by allowing deeper light penetration and reducing energy losses through NPQ as highlighted by Peers, (2014), where smaller antennae mutants showed higher photosynthetic efficiency under high light and dense culture conditions. This is important for large scale cultivation where cultures need to grow dense in raceway ponds to achieve high areal productivities. A common issue with raceway ponds is the effective distribution of light to the culture. Even though sunlight can provide up to ~2000 μmol photons m^{-2} s^{-1}, only a portion of

this light will penetrate the surface of the pond, resulting in the average cell receiving less than 300 μmol photons m^{-2} s^{-1} (Karthikeyan et al., 2016; Zhu C. et al., 2022).

While screening, only *Scenedesmus rubescens* revealed these alterations in pigmentation. A total of 14 mutants were identified to have suspected pigment alterations. While screening irradiated colonies, brownish colonies could be seen forming on occasion, the majority of them were much smaller than other colonies and did not grow when streaked onto square plates. Colonies that were similar in size to the other mutants were streaked out onto separate plates to isolate single colonies containing no green cells. Figure 2.3-B demonstrates the process of identifying colonies with uniform alterations in pigmentation. These isolated colonies were then streaked out onto the plate shown in Figure 2.3-C where there is a mix of mutants that either kept their altered pigmentation or appeared as a more visibly green culture. These mutants were then diluted into 6-well plates and those that grew visibly dense were kept for growth performance screening. Some cultures failed to grow well when transferred to a liquid culture and were not screened for growth performance.

Identifying mutants with alterations in pigmentation is typically rare. After screening over 6600 *Desmodesmus armatus* mutants that were exposed to EMS mutagenesis, Ware et al., (2020) only found 7 mutants with altered pigmentation. The increased ratio of pigment mutants discovered in *Scenedesmus rubescens* stoked intrigue into why this occurred. Jo et al., (2020) demonstrated the capability for *Scenedesmus rubescens* to enhance carotenoid production by applying salinity, high light, and nitrogen deficiency stress, suggesting that these stress responses can redirect metabolic pathways towards the synthesis of carotenoids. The upregulation of the methylerythritol phosphate (MEP) and phytoene synthase (PSY) pathways could be responsible for the increase in carotenoid biosynthesis as they have been shown to produce more carotenoid

precursors and convert them into carotenoids under stressful conditions (Steinbrenner & Linden, 2001; Perez-Gil et al., 2024). These findings, paired with the increased number of *Scenedesmus rubescens* mutants identified with pigment alterations, suggest that these mutations are likely caused by upregulating these metabolic pathways that normally trigger under cellular stress.

4.3. Evaluation of growth performance of selected putative Scenedesmus rubescens and Monoraphidium minutum mutants

4.3.1. Initial growth performance screening of selected putative Scenedesmus rubescens mutants

Duplicate growth of mutants revealed very few with growth rates comparable to WT. For the most part, specific growth rates exhibited by mutants with altered pigmentation were generally much slower than WT, with the only pigment mutant coming relatively close being *SRB 18-1*. However, it was noticed that this mutant quickly lost its altered pigmentation prior to duplicate growth. *SRB 1-1* and *SRB 9-1* grew well during duplicate growth and were selected for triplicate growth tests. Many selected pigment mutants severely underperformed and struggled to exceed maximum specific growth rates of 0.75 day^{-1}. This was not unexpected as some of these mutants were seen struggling to grow dense enough on BG-11 agar plates to properly screen with the IMAGING-PAM (Figure 2.3-C).

The mutants with an asterisk next to their names grew in high light rather than low light. The decision to switch to low light was made early on in consideration of mutants likely being grown in outdoor raceway ponds where they would encounter self-shading and overall lower light exposure.

4.3.2. Initial growth performance screening of selected putative Monoraphidium minutum mutants

14 total *Monoraphidium minutum* mutants were selected for duplicate growth screening. 6 of the 14 mutants, *MRM 307, 308, 312, 323, 343,* and *347* contained altered fluorescence kinetics similar to Mutant 1 in Figure 2.2 and the other 8 mutants possessed photophysiological alterations such as increased Fv/Fm, altered NPQ, and increased qL in low light (Table 1.2). Most of the mutants had lower maximum specific growth rates compared to WT such as *MRM 343, MRM 308,* and *MRM 310. MRM 323* had an identical maximum specific growth rate compared to high light WT (1.32 day^{-1}) but has a much larger range, so it was not kept for triplicate growth. *MRM J-325, MRM K-25* and *MRM K-29* had maximum specific growth rates higher than low light WT (1.45 day^{-1}, 1.26 day^{-1} and 1.42 day^{-1} respectively). These mutants all displayed increased Fv/Fm during the fluorescence screening process, indicating higher quantum efficiencies (Table 1.2).

4.3.3. Triplicate growth performance screening of putative Scenedesmus rubescens mutants

Triplicate growth of selected *Scenedesmus rubescens* mutants revealed no significant increases in specific growth rate. *SR I-148,* a strain with observed increases in Fv/Fm, came close but only achieved a 3% increase in average specific growth rate compared to WT. *SRB 1-1* had the lowest average specific growth rate but to no surprise as it grew similarly in duplicate growth tests. It was included at the time as there was extra space and materials to grow another mutant in triplicates. *SRB 9-1* and *SRB 18-1* had similar average specific growth rates to WT but did not outperform it. From these results, no strain was selected to compare biomass accumulation with its WT counterpart.

4.3.4. Triplicate growth performance screening of putative Monoraphidium minutum mutants

MRM J-325, MRM K-25, and *MRM K-29* were grown in triplicates with WT and only *MRM J-325* outperformed it, demonstrating an average 23 ± 9.4% increase in specific growth rate over WT. This was the only mutant observed to have repeatable increases in Fv/Fm during fluorescent screening (Table 2.2) and was selected for future assessment biomass accumulation.

5. Conclusion

The experiments conducted in this chapter aimed to utilize gamma irradiation mutagenesis to generate high performing microalgal mutants for industrial-scale cultivation. Optimal dosages were identified for both *Scenedesmus rubescens* and *Monoraphidium minutum* to generate mutations that were screened via a fluorescence-based approach performed by Ware et al. (2020). Another key objective was to further expand the application of this novel screening approach by using it on different strains not tested by Ware et al., (2020). *Scenedesmus rubescens* and *Monoraphidium minutum* mutants were screened for alterations in their photophysiology and selected based on traits indicative of improved photosynthetic performance. Selected mutants were then grown under conditions mimicking mass culture conditions to identify any mutants with improved growth and biomass productivity. *MRM J-325* was identified as the only mutant with repeated increased specific growth rate comapred to WT and will be tested for improved biomass capabilities.

SUMMARIZING DISCUSSION

1. Experimental Approach

Large-scale outdoor cultivation of microalgae requires strains with a wide temperature tolerance as environmental conditions constantly fluctuate. This is due to temperature directly impacting metabolic activity, enzymatic function, and overall biomass accumulation which can have negative impacts on crop yield (Barten et al., 2021; Lee et al., 2018). Ten strains were initially selected based on their previously identified high productivity and cultivated at a wide temperature range (Huesemann et al., 2023). Rather than immediately choosing two of these strains, they were subjected to a series of growth performance tests tailored to the temperature conditions of Gillette, WY, where the down-selected strains would be eventually cultivated. Optical density and cell density derived specific growth rates were used to calculate growth performance instead of doubling time as specific growth rate provides a more dynamic assessment of growth across different cellular growth phases (Richmond, 2004). To quantify biomass productivity, TOC analysis was selected as it has been demonstrated by (Saxena et al., 2021) to be cheaper, quicker, and as reliable as conventional methods of biomass measurement that use ash free dry weight (AFDW) as the metric. Efficiency and optimization of each step of the industrial cultivation and processing of microalgae is critical to increasing its commercial viability. Expanding general knowledge by employing these tools can hopefully lead to increased adoption of them.

The two highest performing strains were selected for gamma irradiation mutagenesis rather than other forms such as EMS mutagenesis due to its ability to induce larger-scale DNA damage, including single and double-stranded breaks, which are more likely to result in

significant phenotypic changes compared to the small point mutations caused by EMS (Sikora et al., 2011; Hwang et al., 2015). Ionizing based mutagenesis methods however are already commonly utilized to generate mutants of interest in microalgae (See Chapter 2 introduction). More broadly, random mutagenesis was utilized rather than more targeted genetic engineering approaches as mutagenesis generated mutants are not considered GMOs, which do not require regulatory approval to grow outdoors, overall reducing cost and time investments (Zepeda & Custodio, 2018; Zimny, 2023). The screening of the generated mutants utilized a fluorescence based approach using PAM fluorometry to screen for alterations in photophysiology that were indicative of improved photosynthetic performance (Ware et al., 2020). This is a novel and high-throughput screening method compared to growth performance based screening that cultures each mutant and compared them to WT growth dynamics. As mutagenesis methods can generate thousands of putative mutants in a short period of time, the fluorescence based screening approach can quickly identify mutants with decreases in photosynthetic performance that can be immediately removed from further trials, making it a more efficient screening method.

2. Summary of Findings

Initial experiments provided insight into how temperature and scale affected the growth and biomass accumulation performance of ten selected algal strains. First, strains were each grown in duplicate small-scale flasks at both 18 and 30ºC under high light to observe their specific growth rates in exponential phase. *Phaeodactylum tricornutum* was determined to not grow in 30ºC and was eliminated from further trials. The remaining nine strains were scaled up using Roux flasks, where cultures would be exposed to both temperature conditions with the addition of bubbling and higher light irradiance. *Picochlorum renovo* was eliminated from the experiment due to its poor performance at 18ºC. Both SRTC14 and SAmud7 were eliminated

because they demonstrated average performance compared to the other strains and were not characterized, making potential future research involving genetic screening more difficult. Triplicate growth in Roux flasks of the remaining six strains at 30ºC to measure growth and biomass accumulation revealed the three *Scenedesmus* species to have the highest specific growth rates, while *Monoraphidium minutum* achieved the highest final optical density. TOC analysis of aliquots taken from Roux flasks showed *Scenedesmus rubescens* and *Monoraphidium minutum* to have 88.5% and 22.6% higher average TOC accumulation compared to the next highest performing strain, *Nannochloropsis oceanica.* Surprisingly, *Picochlorum celeri*, a strain widely regarded for its rapid cell growth, produced the least amount of total organic carbon after cultivation in high temperature despite demonstrating a comparatively high specific growth rate and final optical density (See Chapter 1 results). It was speculated that this strain's cellular metabolism prioritized protein synthesis for growth rather than lipid accumulation. Lastly, calculation of the mass of TOC per cell yielded results that generally corresponded with known cell sizes and masses. This calculation also enabled an initial assessment of how carbon accumulation differed between the tested species.

The results from Chapter 1 pinpointed *Scenedesmus rubescens* and *Monoraphidium minutum* as having the most robust performance under the tested conditions, highlighting their potential for large-scale cultivation. High performance liquid chromatography could give further insights into the detailed biochemical profile of each strain to determine the appropriate application for bioproduct development.

The experiments conducted in this chapter aimed to utilize gamma irradiation mutagenesis to generate high performing microalgal mutants for industrial-scale cultivation. Optimal dosages were identified for both *Scenedesmus rubescens* and *Monoraphidium minutum*

to generate mutations that were screened via a fluorescence-based approach performed by Ware et al. (2020). Another key objective was to further expand the application of this novel screening approach by using it on different strains not tested by Ware et al., (2020). Putative *Scenedesmus rubescens* and *Monoraphidium minutum* mutants were screened for alterations in their photophysiology and selected based on traits indicative of improved photosynthetic performance. Selected mutants were then grown under conditions mimicking mass culture conditions to identify any mutants with improved growth and biomass productivity. *MRM J-325* was identified to have increased specific growth rate compared to WT and will be tested for improved biomass capabilities.

3. Future Direction

Future research could build upon the high productivity mutants generated by exploring the use of industrial flue gas as a nutrient source and as a carbon capturing method. Additionally, next steps could involve quantifying carbon dynamics using the mass balance approach by analyzing organic and inorganic carbon in biomass and media to evaluate strain efficiency in carbon assimilation. By pairing these two techniques together, future research can assess how strains utilize available carbon sources in industrially relevant conditions. This would bridge the gap between lab-scale mutant screening and industrial-scale cultivation by revealing how strain performance characteristics developed under controlled conditions translate to productivity gains in carbon-intensive, large-scale outdoor cultivation environmetns. Future testing of mutants identified with high productivity at the lab-scale will involve them being sent to the WITC in Gillette, WY to test their performance capabilities at industrial-scale.

REFERENCES

Abdur Razzak, S., Bahar, K., Islam, K. M. O., Haniffa, A. K., Faruque, M. O., Hossain, S. M. Z., & Hossain, M. M. (2024). Microalgae cultivation in photobioreactors: Sustainable solutions for a greener future. *Green Chemical Engineering, 5*(4), 418–439.

Acién Fernández, F. G., Fernández Sevilla, J. M., & Molina Grima, E. (2013). Photobioreactors for the production of microalgae. *Reviews in Environmental Science and Bio/Technology, 12*(2), 131–151.

Allahverdiyeva, Y., Mustila, H., Ermakova, M., Bersanini, L., Richaud, P., Ajlani, G., Battchikova, N., Cournac, L., & Aro, E.-M. (2013). Flavodiiron proteins Flv1 and Flv3 enable cyanobacterial growth and photosynthesis under fluctuating light. *Proceedings of the National Academy of Sciences, 110*(10), 4111–4116.

Amaro, H. M., Guedes, A. C., & Malcata, F. X. (2011). Advances and perspectives in using microalgae to produce biodiesel. *Applied Energy, 88(10)*, 3402–3410.

Anbalagan, L., Serri, N. A., & Kassim, M. A. (2023). Investigation of different environmental conditions: Influence on lipid accumulations by Halochlorella rubescens. *040004*.

Arif, M., Bai, Y., Usman, M., Jalalah, M., Harraz, F. A., Al-Assiri, M. S., Li, X., Salama, E.-S., & Zhang, C. (2020). Highest accumulated microalgal lipids (polar and non-polar) for biodiesel production with advanced wastewater treatment: Role of lipidomics. *Bioresource Technology, 298*, 122299.

Aro, E.-M., Virgin, I., & Andersson, B. (1993). Photoinhibition of Photosystem II. Inactivation, protein damage and turnover. *Biochimica et Biophysica Acta (BBA) - Bioenergetics, 1143*(2), 113–134.

Araújo, R., Vázquez Calderón, F., Sánchez López, J., Azevedo, I. C., Bruhn, A., Fluch, S., Garcia Tasende, M., Ghaderiardakani, F., Ilmjärv, T., Laurans, M., Mac Monagail, M., Mangini, S., Peteiro, C., Rebours, C., Stefansson, T., & Ullmann, J. (2021). Current Status of the Algae Production Industry in Europe: An Emerging Sector of the Blue Bioeconomy. *Frontiers in Marine Science*, *7*, 626389.

Assunção, J., Batista, A. P., Manoel, J., Da Silva, T. L., Marques, P., Reis, A., & Gouveia, L. (2017). CO 2 utilization in the production of biomass and biocompounds by three different microalgae. *Engineering in Life Sciences, 17(10),* 1126–1135.

ASTM International. (2004). Standard practice for using the Fricke reference-standard dosimetry system (E 1026–04). ASTM International.

Babiak, W., & Krzemińska, I. (2021). Extracellular Polymeric Substances (EPS) as Microalgal Bioproducts: A Review of Factors Affecting EPS Synthesis and Application in Flocculation Processes. *Energies, 14(13)*, 4007.

Baek, J., Choi, J., Park, H., Lim, S., & Park, S. J. (2016). Isolation and Proteomic Analysis of a Chlamydomonas reinhardtii Mutant with Enhanced Lipid Production by the Gamma Irradiation Method. *Journal of Microbiology and Biotechnology, 26*(12), 2066–2075.

Baker, N. R. (2008). Chlorophyll Fluorescence: A Probe of Photosynthesis In Vivo. *Annual Review of Plant Biology, 59*(1), 89–113.

Barten, R., Djohan, Y., Evers, W., Wijffels, R., & Barbosa, M. (2021). Towards industrial production of microalgae without temperature control: The effect of diel temperature fluctuations on microalgal physiology. *Journal of Biotechnology, 336*, 56–63.

Benedetti, M., Vecchi, V., Barera, S., & Dall'Osto, L. (2018). Biomass from microalgae: The potential of domestication towards sustainable biofactories. *Microbial Cell Factories, 17(1)*, 173.

Blanco, A. M., Moreno, J., Del Campo, J. A., Rivas, J., & Guerrero, M. G. (2007). Outdoor cultivation of lutein-rich cells of Muriellopsis sp. In open ponds. Applied Microbiology and Biotechnology, 73(6), 1259–1266.

Bleisch, R., Freitag, L., Ihadjadene, Y., Sprenger, U., Steingröwer, J., Walther, T., & Krujatz, F. (2022). Strain Development in Microalgal Biotechnology---Random Mutagenesis Techniques. *Life, 12*(7), 961.

Borowitzka, M. A. (2018). Biology of Microalgae. In *Microalgae in Health and Disease Prevention* (pp. 23–72). Elsevier.

Boussiba, S., Vonshak, A., Cohen, Z., Avissar, Y., & Richmond, A. (1987). Lipid and biomass production by the halotolerant microalga Nannochloropsis salina. *Biomass, 12*(1), 37–47.

Calhoun, S., Bell, T. A. S., Dahlin, L. R., Kunde, Y., LaButti, K., Louie, K. B., Kuftin, A., Treen, D., Dilworth, D., Mihaltcheva, S., Daum, C., Bowen, B. P., Northen, T. R., Guarnieri, M. T., Starkenburg, S. R., & Grigoriev, I. V. (2021). A multi-omic characterization of temperature stress in a halotolerant Scenedesmus strain for algal biotechnology. *Communications Biology, 4*(1), 333.

Cano, M., Karns, D. A. J., Weissman, J. C., Heinnickel, M. L., & Posewitz, M. C. (2021). Pigment modulation in response to irradiance intensity in the fast-growing alga Picochlorum celeri. *Algal Research, 58*, 102370.

Cantrell, M., Ware, M. A., & Peers, G. (2023). Characterizing compensatory mechanisms in the absence of photoprotective qE in Chlamydomonas reinhardtii. *Photosynthesis Research, 158(1)*, 23–39.

Cardoso, L. B. (2022). Development of novel Scenedesmus rubescens mutants with improved pigmentation and protein contents. (Thesis).

Cazzaniga, S., Perozeni, F., Baier, T., & Ballottari, M. (2022). Engineering astaxanthin accumulation reduces photoinhibition and increases biomass productivity under high light in Chlamydomonas reinhardtii. *Biotechnology for Biofuels and Bioproducts, 15*(1), 77.

Cecchin, M., Berteotti, S., Paltrinieri, S., Vigliante, I., Iadarola, B., Giovannone, B., Maffei, M. E., Delledonne, M., & Ballottari, M. (2020). Improved lipid productivity in Nannochloropsis gaditana in nitrogen-replete conditions by selection of pale green mutants. *Biotechnology for Biofuels, 13*(1), 78.

Celi, C., Fino, D., & Savorani, F. (2022). Phaeodactylum tricornutum as a source of value-added products: A review on recent developments in cultivation and extraction technologies. *Bioresource Technology Reports, 19*, 101122.

Chandrashekaraiah, P.S., Sanyal, D., Dasgupta, S., & Banik, A. (2021). Cadmium biosorption and biomass production by two freshwater microalgae Scenedesmus acutus and Chlorella pyrenoidosa: An integrated approach. *Chemosphere, 269*, 128755.

Chandrashekaraiah, P.S., Sanyal, D., Dasgupta, S., & Banik, A. (2021). Phycoremediation and photosynthetic toxicity assessment of lead by two freshwater microalgae Scenedesmus acutus and Chlorella pyrenoidosa. *Physiologia Plantarum, ppl.13368*.

Chen, X., Khatiwada, J. R., Chio, C., Shrestha, S., Kognou, A. L. M., Fan, L., & Qin, W. (2024). Low-cost cultivation of Nannochloropsis oceanica in newly designed photobioreactors and its productivity trends in semi-continuous cultivation under inland outdoor conditions. *Bioresource Technology, 402*, 130829.

Chen, Y., & Chen, R. (2018). Physical Mutagenesis in Medicago truncatula Using Fast Neutron Bombardment (FNB) for Symbiosis and Developmental Biology Studies. In L. A. Cañas & J. P. Beltrán (Eds.), *Functional Genomics in Medicago truncatula* (*Vol. 1822*, pp. 61–69). Springer New York.

Cheng, J., Zhu, Y., Zhang, Z., & Yang, W. (2019). Modification and improvement of microalgae strains for strengthening CO2 fixation from coal-fired flue gas in power plants. *Bioresource Technology, 291*, 121850.

Cheng, P., Wang, Y., Liu, T., & Liu, D. (2017). Biofilm Attached Cultivation of Chlorella pyrenoidosa Is a Developed System for Swine Wastewater Treatment and Lipid Production. *Frontiers in Plant Science, 8,* 1594.

Chiu, S.-Y., Kao, C.-Y., Chen, C.-H., Kuan, T.-C., Ong, S.-C., & Lin, C.-S. (2008). Reduction of CO2 by a high-density culture of Chlorella sp. In a semicontinuous photobioreactor. *Bioresource Technology, 99*(9), 3389–3396.

Chiu, S.-Y., Kao, C.-Y., Tsai, M.-T., Ong, S.-C., Chen, C.-H., & Lin, C.-S. (2009). Lipid accumulation and CO2 utilization of Nannochloropsis oculata in response to CO2 aeration. *Bioresource Technology, 100*(2), 833–838.

Corcoran, A. A., Alvarez, M. S., Cornell, T., Echenique-Subiabre, I., Gerber, J., Getto, S., Jebali, A., Martinez, H., Nalley, J. O., O'Kelly, C. J., Ryan, A., Shurin, J. B., & Starkenburg, S. R. (2024). Long-Term Outdoor Cultivation of Nannochloropsis in California, Hawaii, and New Mexico. *Data, 9*(11), 126.

Costa, J. A. V., Freitas, B. C. B., Santos, T. D., Mitchell, B. G., & Morais, M. G. (2019). Open pond systems for microalgal culture. In *Biofuels from Algae* (pp. 199–223). Elsevier.

Cox, M. M., & Battista, J. R. (2005). Deinococcus radiodurans---The consummate survivor. *Nature Reviews Microbiology, 3*(11), 882–892.

Cui, Y., Skye R., Thomas-Hall, Peer M. Schenk (2020) Isolation and Cultivation of a Phaeodactylum tricornutum Strain from the East Coast of Australia for EPA Production. *Geol Earth Mar Sci Volume 2*(2): 1–7.

Dahlin, L. R., Gerritsen, A. T., Henard, C. A., Van Wychen, S., Linger, J. G., Kunde, Y., Hovde, B. T., Starkenburg, S. R., Posewitz, M. C., & Guarnieri, M. T. (2019). Development of a high-productivity, halophilic, thermotolerant microalga Picochlorum renovo. *Communications Biology, 2*(1), 388.

Dahlin, L. R., Van Wychen, S., Gerken, H. G., McGowen, J., Pienkos, P. T., Posewitz, M. C., & Guarnieri, M. T. (2018). Down-Selection and Outdoor Evaluation of Novel, Halotolerant Algal Strains for Winter Cultivation. *Frontiers in Plant Science, 9*, 1513.

Daniel, R. S., & Srivastava, A. (2016). Cell productivity of Nannochloropsis gaditana CCAP 849/5 in varied reactor types with different culture light paths and light regimes. *Journal of Algal Biomass Utilization*. ISSN: 2229 – 6905 12

De Jaeger, L., Verbeek, R. E., Draaisma, R. B., Martens, D. E., Springer, J., Eggink, G., & Wijffels, R. H. (2014). Superior triacylglycerol (TAG) accumulation in starchless mutants of Scenedesmus obliquus: (I) mutant generation and characterization. *Biotechnology for Biofuels, 7*(1), 69.

De Vree, J. H., Bosma, R., Janssen, M., Barbosa, M. J., & Wijffels, R. H. (2015). Comparison of four outdoor pilot-scale photobioreactors. *Biotechnology for Biofuels, 8*(1), 215.

Demirbas, M. F. (2011). Biofuels from algae for sustainable development. *Applied Energy, 88(10)*, 3473–3480. https://doi.org/10.1016/j.apenergy.2011.01.059

Dogaris, I., Welch, M., Meiser, A., Walmsley, L., & Philippidis, G. (2015). A novel horizontal photobioreactor for high-density cultivation of microalgae. *Bioresource Technology, 198*, 316–324. https://doi.org/10.1016/j.biortech.2015.09.030

Du, Z., Bhat, W. W., Poliner, E., Johnson, S., Bertucci, C., Farre, E., & Hamberger, B. (2023). Engineering Nannochloropsis oceanica for the production of diterpenoid compounds. *mLife, 2*(4), 428–437.

El-Sheekh, M., Abomohra, A. E.-F., El-Azim, M. A., & Abou-Shanab, R. (2017). Effect of temperature on growth and fatty acids profile of the biodiesel producing microalga Scenedesmus acutus. *BASE, 233–239*.

Erickson, E., Wakao, S., & Niyogi, K. K. (2015). Light stress and photoprotection in Chlamydomonas reinhardtii. *The Plant Journal, 82*(3), 449–465.

Fakhry, E. M., & El Maghraby, D. M. (2015). Lipid accumulation in response to nitrogen limitation and variation of temperature in Nannochloropsis salina. *Botanical Studies, 56(1)*, 6.

Fan, Y., Ding, X.-T., Wang, L.-J., Jiang, E.-Y., Van, P. N., & Li, F.-L. (2021). Rapid Sorting of Fucoxanthin-Producing Phaeodactylum tricornutum Mutants by Flow Cytometry. *Marine Drugs, 19*(4), 228.

Feng, P., Yang, K., Xu, Z., Wang, Z., Fan, L., Qin, L., Zhu, S., Shang, C., Chai, P., Yuan, Z., & Hu, L. (2014). Growth and lipid accumulation characteristics of Scenedesmus obliquus in semi-continuous cultivation outdoors for biodiesel feedstock production. *Bioresource Technology, 173*, 406-414.

Finkel, Z. V., Beardall, J., Flynn, K. J., Quigg, A., Rees, T. A. V., & Raven, J. A. (2010). Phytoplankton in a changing world: Cell size and elemental stoichiometry. *Journal of Plankton Research*, *32*(1), 119–137.

Furutani, R., Ohnishi, M., Mori, Y., Wada, S., & Miyake, C. (2022). The difficulty of estimating the electron transport rate at photosystem I. *Journal of Plant Research, 135(4)*, 565–577.

Gao, S., Edmundson, S., Huesemann, M., Gutknecht, A., Laurens, L. M. L., Van Wychen, S., Pittman, K., & Greer, M. (2023). DISCOVR strain screening pipeline – Part III: Strain evaluation in outdoor raceway ponds. *Algal Research, 70*, 102990.

Gao, S., Zhou, L., Yang, W., Wang, L., Liu, X., Gong, Y., Hu, Q., & Wang, G. (2022). Overexpression of a novel gene (Pt2015) endows the commercial diatom Phaeodactylum tricornutum high lipid content and grazing resistance. *Biotechnology for Biofuels and Bioproducts, 15(1)*, 131.

Genty, B., Briantais, J.-M., & Baker, N. R. (1989). The relationship between the quantum yield of photosynthetic electron transport and quenching of chlorophyll fluorescence. Biochimica et Biophysica Acta (BBA) - *General Subjects, 990(1)*, 87–92.

Gerbersdorf, S. U., Westrich, B., & Paterson, D. M. (2009). Microbial Extracellular Polymeric Substances (EPS) in Fresh Water Sediments. *Microbial Ecology, 58*(2), 334–349.

Glass, D.J. (2015). Government Regulation of the Uses of Genetically Modified Algae and Other Microorganisms in Biofuel and Bio-based Chemical Production. In: Prokop, A., Bajpai, R., Zappi, M. (eds) *Algal Biorefineries.* Springer, Cham.

Gong, Y., & Jiang, M. (2011). Biodiesel production with microalgae as feedstock: From strains to biodiesel. *Biotechnology Letters, 33(7)*, 1269–1284.

Gorbunov, M. Y., & Falkowski, P. G. (2021). Using chlorophyll fluorescence kinetics to determine photosynthesis in aquatic ecosystems. *Limnology and Oceanography, 66*(1), 1–13.

Guccione, A., Biondi, N., Sampietro, G., Rodolfi, L., Bassi, N., & Tredici, M. R. (2014). Chlorella for protein and biofuels: From strain selection to outdoor cultivation in a Green Wall Panel photobioreactor. *Biotechnology for Biofuels, 7*(1), 84.

Guillard, R.R.L. (1975). Culture of phytoplankton for feeding marine invertebrates. In Smith W.L. and Chanley M.H (Eds.) *Culture of Marine Invertebrate Animals* (pp. 26–60). Plenum Press, New York, USA.

Guschina, I. A., & Harwood, J. L. (2006). Lipids and lipid metabolism in eukaryotic algae. *Progress in Lipid Research, 45*(2), 160–186.

He, L., Subramanian, V. R., & Tang, Y. J. (2012). Experimental analysis and model-based optimization of microalgae growth in photo-bioreactors using flue gas. *Biomass and Bioenergy, 41*, 131–138.

He, Q., Yang, H., & Hu, C. (2018). Effects of temperature and its combination with high light intensity on lipid production of Monoraphidium dybowskii Y2 from semi-arid desert areas. *Bioresource Technology, 265*, 407–414.

Hendry, J. H. (1991). The Slower Cellular Recovery after Higher-LET Irradiations, Including Neutrons, Focuses on the Quality of DNA Breaks. *Radiation Research, 128(1)*, S111.

Hermawan, J., Masithah, E. D., Tjahjaningsih, W., & Abdillah, A. A. (2018). Increasing β-carotene content of phytoplankton Dunaliella salina using different salinity media. *IOP Conference Series: Earth and Environmental Science, 137*, 012034.

Hess, D., Wendt, L. M., Wahlen, B. D., Aston, J. E., Hu, H., & Quinn, J. C. (2019). Techno-economic analysis of ash removal in biomass harvested from algal turf scrubbers. *Biomass and Bioenergy, 123*, 149–158.

Houille-Vernes, L., Rappaport, F., Wollman, F.-A., Alric, J., & Johnson, X. (2011). Plastid terminal oxidase 2 (PTOX2) is the major oxidase involved in chlororespiration in Chlamydomonas. *Proceedings of the National Academy of Sciences, 108*(51), 20820–20825.

Hu, Q., Sommerfeld, M., Jarvis, E., Ghirardi, M., Posewitz, M., Seibert, M., & Darzins, A. (2008). Microalgal triacylglycerols as feedstocks for biofuel production: Perspectives and advances. *The Plant Journal, 54*(4), 621–639.

Hu, W. (2014). Dry weight and cell density of individual algal and cyanobacterial cells for algae research and development (Thesis).

Huang, G., Chen, F., Kuang, Y., He, H., & Qin, A. (2016). Current Techniques of Growing Algae Using Flue Gas from Exhaust Gas Industry: A Review. *Applied Biochemistry and Biotechnology, 178(6)*, Article 6.

Huesemann, M., Edmundson, S., Gao, S., Negi, S., Dale, T., Gutknecht, A., Daligault, H. E., Carr, C. K., Freeman, J., Kern, T., Starkenburg, S. R., Gleasner, C. D., Louie, W., Kruk, R., & McGuire, S. (2023). DISCOVR strain pipeline screening -- Part I: Maximum specific growth rate as a function of temperature and salinity for 38 candidate microalgae for biofuels production. *Algal Research, 71*, 102996.

Huesemann, M., Gao, S., Edmundson, S., Laurens, L. M. L., Van Wychen, S., Beirne, N., Gutknecht, A., Kruk, R., Pittman, K., Greer, M., Graham, S., & Mueller, T. (2023). DISCOVR strain pipeline screening -- Part II: Winter and summer season areal productivities and biomass compositional shifts in climate-simulation photobioreactor cultures. *Algal Research, 70*, 102948.

Hwang, W. J., Kim, M. Y., Kang, Y. J., Shim, S., Stacey, M. G., Stacey, G., & Lee, S.-H. (2015). Genome-wide analysis of mutations in a dwarf soybean mutant induced by fast neutron bombardment. *Euphytica, 203*(2), Article 2.

Infante, P., Moore, K., Hurburgh, C., Scott, P., Archontoulis, S., Lenssen, A., & Fei, S. (2018). Biomass Production and Composition of Temperate and Tropical Maize in Central Iowa. *Agronomy, 8(6)*, 88.

Jin, E., He, L., Zhang, Y., Richard, A. R., & Fan, M. (2014). A nanostructured CeO 2 promoted Pd/α-alumina diethyl oxalate catalyst with high activity and stability. *RSC Adv., 4(90)*, 48901–48904.

Johnson, J. E., & Berry, J. A. (2021). The role of Cytochrome b6f in the control of steady-state photosynthesis: A conceptual and quantitative model. *Photosynthesis Research, 148(3)*, 101–136.

Karthikeyan, D., Muthukumaran, M., & Balakumar, B. S. (2016). Mass Cultivation of Microalgae in Open Raceway Pond for Biomass and Biochemicals Production. *Int. J. Adv. Res. Biol. Sci. 3*(2): 247-260.

Kholssi, R., Lougraimzi, H., & Moreno-Garrido, I. (2023). Effects of global environmental change on microalgal photosynthesis, growth and their distribution. *Marine Environmental Research, 184*, 105877.

Kishi, M., Yamada, Y., Katayama, T., Matsuyama, T., & Toda, T. (2019). Carbon Mass Balance in Arthrospira platensis Culture with Medium Recycle and High CO2 Supply. *Applied Sciences, 10(1)*, 228.

Koo, K. M., Jung, S., Kim, J.-B., Kim, S. H., Kwon, S. J., Jeong, W.-J., Chung, G. H., Kang, S.-Y., Choi, Y.-E., & Ahn, J.-W. (2017). Effect of ionizing radiation on the DNA damage response in Chlamydomonas reinhardtii. *Genes & Genomics, 39(1)*, 63–75.

Krisnawati, A., & Adie, M. M. (2015). Variability of Biomass and Harvest Index from Several Soybean Genotypes as Renewable Energy Source. *Energy Procedia, 65*, 14–21.

Krzemińska, I., Nawrocka, A., Piasecka, A., Jagielski, P., & Tys, J. (2015). Cultivation of Chlorella protothecoides in photobioreactors: The combined impact of photoperiod and CO2 concentration. *Engineering in Life Sciences, 15*(5), 533–541.

Kumar, K., Mishra, S. K., Shrivastav, A., Park, M. S., & Yang, J.-W. (2015). Recent trends in the mass cultivation of algae in raceway ponds. *Renewable and Sustainable Energy Reviews, 51*, 875–885.

Kumawat, S., Rana, N., Bansal, R., Vishwakarma, G., Mehetre, S. T., Das, B. K., Kumar, M., Yadav, S. K., Sonah, H., Sharma, T. R., & Deshmukh, R. (2019). Expanding Avenue of Fast Neutron Mediated Mutagenesis for Crop Improvement. *Plants, 8*(6), 164.

Kurokawa, M., King, P. M., Wu, X., Joyce, E. M., Mason, T. J., & Yamamoto, K. (2016). Effect of sonication frequency on the disruption of algae. *Ultrasonics Sonochemistry, 31*, 157–162.

Lam, T. P., Lee, T.-M., Chen, C.-Y., & Chang, J.-S. (2018). Strategies to control biological contaminants during microalgal cultivation in open ponds. *Bioresource Technology, 252*, 180–187.

LaPanse, A. J., Krishnan, A., Dennis, G., Karns, D. A. J., Dahlin, L. R., Van Wychen, S., Burch, T. A., Guarnieri, M. T., Weissman, J. C., & Posewitz, M. C. (2024). Proximate biomass characterization of the high productivity marine microalga Picochlorum celeri TG2. *Plant Physiology and Biochemistry, 207*, 108364.

Lee, K.-K., Lim, P.-E., Poong, S.-W., Wong, C.-Y., Phang, S.-M., & Beardall, J. (2018). Growth and photosynthesis of Chlorella strains from polar, temperate and tropical freshwater environments under temperature stress. *Journal of Oceanology and Limnology, 36*(4), 1266–1279.

Lee, T., & Hsu, B. (2009). DISINTEGRATION OF THE CELLS OF SIPHONOUS GREEN ALGA CODIUM EDULE (BRYOPSIDALES, CHLOROPHYTA) UNDER MILD HEAT STRESS 1. *Journal of Phycology, 45(2)*, 348–356.

Levin, G., Yasmin, M., Liran, O., Hanna, R., Kleifeld, O., Horev, G., Wollman, F.-A., Schuster, G., & Nawrocki, W. J. (2024). Processes independent of nonphotochemical quenching protect a high-light-tolerant desert alga from oxidative stress. *Plant Physiology, 197*(1), kiae608.

Li, F.-F., Yang, Z.-H., Zeng, R., Yang, G., Chang, X., Yan, J.-B., & Hou, Y.-L. (2011). Microalgae Capture of CO 2 from Actual Flue Gas Discharged from a Combustion Chamber. *Industrial & Engineering Chemistry Research, 50*(10), 6496–6502.

Li, T., Wang, W., Yuan, C., Zhang, Y., Xu, J., Zheng, H., Xiang, W., & Li, A. (2020). Linking lipid accumulation and photosynthetic efficiency in Nannochloropsis sp. Under nutrient limitation and replenishment. *Journal of Applied Phycology, 32*(3), 1619–1630.

Li, Tianrui, Hu, J., & Zhu, L. (2021). Self-Flocculation as an Efficient Method to Harvest Microalgae: A Mini-Review. *Water*, *13*(18), 2585.

Li, X., Song, Y., Century, K., Straight, S., Ronald, P., Dong, X., Lassner, M., & Zhang, Y. (2001). A fast neutron deletion mutagenesis-based reverse genetics system for plants: Fast neutron deletion mutagenesis-based reverse genetics. *The Plant Journal, 27(3)*, Article 3.

Liu, B., Ma, C., Xiao, R., Xing, D., Ren, H., & Ren, N. (2015). The screening of microalgae mutant strain Scenedesmus sp. Z-4 with a rich lipid content obtained by 60 Co γ-ray mutation. *RSC Advances, 5*(64), 52057–52061.

Liu, K. (2019). Effects of sample size, dry ashing temperature and duration on determination of ash content in algae and other biomass. *Algal Research, 40*, 101486.

Liu, X., Sun, J., Wei, Y., & Liu, Y. (2023). Relationship between cell volume and particulate organic matter for different size phytoplankton. *Marine Pollution Bulletin, 194*, 115298.

Loftus, S. E., & Johnson, Z. I. (2019). Reused Cultivation Water Accumulates Dissolved Organic Carbon and Uniquely Influences Different Marine Microalgae. *Frontiers in Bioengineering and Biotechnology*, *7*, 101.

Ma, X.-N., Chen, T.-P., Yang, B., Liu, J., & Chen, F. (2016). Lipid Production from Nannochloropsis. *Marine Drugs, 14*(4), Article 4.

Ma, Y., Wang, Z., Zhu, M., Yu, C., Cao, Y., Zhang, D., & Zhou, G. (2013). Increased lipid productivity and TAG content in Nannochloropsis by heavy-ion irradiation mutagenesis. Bioresource Technology, 136, 360–367.

Malone, L. A., Proctor, M. S., Hitchcock, A., Hunter, C. N., & Johnson, M. P. (2021). Cytochrome b6f – Orchestrator of photosynthetic electron transfer. Biochimica et Biophysica Acta (BBA) - *Bioenergetics, 1862(5)*, 148380.

Mann, J. E., & Myers, J. (1968). ON PIGMENTS, GROWTH, AND PHOTOSYNTHESIS OF PHAEODACTYLUM TRICORNUTUM 1 2. *Journal of Phycology, 4(4)*, 349–355.

Marañón, E. (2015). Cell Size as a Key Determinant of Phytoplankton Metabolism and Community Structure. *Annual Review of Marine Science*, *7*(1), 241–264.

Marc Veillette, Anne Giroir-Fendler, Nathalie Faucheux & Michèle Heitz (2018) Biodiesel from microalgae lipids: from inorganic carbon to energy production, *Biofuels, 9:2*, 175-202,

Masojidek, J. (2001). Photosystem II Electron Transport Rates and Oxygen Production in Natural Waterblooms of Freshwater Cyanobacteria During a Diel Cycle. *Journal of Plankton Research, 23(1)*, 57–66.

Matter, I. A., Bui, V. K. H., Jung, M., Seo, J. Y., Kim, Y.-E., Lee, Y.-C., & Oh, Y.-K. (2019). Flocculation Harvesting Techniques for Microalgae: A Review. *Applied Sciences, 9*(15), 3069.

Maxwell, K., & Johnson, G. N. (2000). Chlorophyll fluorescence---A practical guide. *Journal of Experimental Botany, 51*(345), 659–668.

Melis, A. (2009). Solar energy conversion efficiencies in photosynthesis: Minimizing the chlorophyll antennae to maximize efficiency. *Plant Science, 177*(4), 272–280.

Meurer, J., Meierhoff, K., & Westhoff, P. (1996). Isolation of high-chlorophyll-fluorescence mutants of Arabidopsis thaliana and their characterization by spectroscopy, immunoblotting and Northern hybridization. *Planta, 198(3)*, 385–396.

Molitor, H. R., & Schnoor, J. L. (2020). Using Simulated Flue Gas to Rapidly Grow Nutritious Microalgae with Enhanced Settleability. *ACS Omega, 5(42)*, 27269–27277.

Motulsky, H., & Christopoulos, A. (2004). Fitting Models to Biological Data Using Linear and Nonlinear Regression: A practical guide to curve fitting. Oxford University Press.

Myers, J. A., Curtis, B. S., & Curtis, W. R. (2013). Improving accuracy of cell and chromophore concentration measurements using optical density. *BMC Biophysics, 6(1)*, 4.

Narala, R. R., Garg, S., Sharma, K. K., Thomas-Hall, S. R., Deme, M., Li, Y., & Schenk, P. M. (2016). Comparison of Microalgae Cultivation in Photobioreactor, Open Raceway Pond, and a Two-Stage Hybrid System. *Frontiers in Energy Research, 4*.

National Weather Service. *Wyoming Annual Climate Summary*. US Department of Commerce, *National Oceanic and Atmospheric Administration*.

Negoro, M., Shioji, N., Miyamoto, K., & Micira, Y. (1991). Growth of Microalgae in High CO2 Gas and Effects of SOX and NOX. *Applied Biochemistry and Biotechnology, 28–29(1)*, 877–886.

Nelson, D. W., & Sommers, L. E. (2015). Total Carbon, Organic Carbon, and Organic Matter. In A. L. Page (Ed.), *Agronomy Monographs (pp. 539–579)*. American Society of Agronomy, Soil Science Society of America.

Niu, Y., Lazár, D., Holzwarth, A. R., Kramer, D. M., Matsubara, S., Fiorani, F., Poorter, H., Schrey, S. D., & Nedbal, L. (2023). Plants cope with fluctuating light by frequency-dependent nonphotochemical quenching and cyclic electron transport. *New Phytologist, 239(5)*, 1869–1886.

Niyogi, K. K., Björkman, O., & Grossman, A. R. (1997). The roles of specific xanthophylls in photoprotection. *Proceedings of the National Academy of Sciences, 94(25)*, 14162–14167.

Novoveská, L., Nielsen, S. L., Eroldoğan, O. T., Haznedaroglu, B. Z., Rinkevich, B., Fazi, S., Robbens, J., Vasquez, M., & Einarsson, H. (2023). Overview and Challenges of Large-Scale Cultivation of Photosynthetic Microalgae and Cyanobacteria. *Marine Drugs, 21*(8), 445.

Ogden, K., Anderson, D., Simpson, S., Van Voorheis, W., Brown, J., Huesemann, M., ... & Waller, P. (2019). *Regional Algal Feedstock Testebed (RAFT) Final Report (No. DOE-UAZ-0006269)*. Univ. of Arizona, Tucson, AZ (United States).

Ögren, E., & Evans, J. R. (1993). Photosynthetic light-response curves: I. The influence of CO2 partial pressure and leaf inversion. *Planta, 189*(2).

Ong, S.-C., Kao, C.-Y., Chiu, S.-Y., Tsai, M.-T., & Lin, C.-S. (2010). Characterization of the thermal-tolerant mutants of Chlorella sp. With high growth rate and application in outdoor photobioreactor cultivation. *Bioresource Technology, 101*(8), 2880–2883.

Oslan, S. N. H., Tan, J. S., Oslan, S. N., Matanjun, P., Mokhtar, R. A. M., Shapawi, R., & Huda, N. (2021). Haematococcus pluvialis as a Potential Source of Astaxanthin with Diverse Applications in Industrial Sectors: Current Research and Future Directions. *Molecules, 26*(21), 6470.

Ova Ozcan, D., & Ovez, B. (2020). Evaluation of the interaction of temperature and light intensity on the growth of Phaeodactylum tricornutum: Kinetic modeling and optimization. *Biochemical Engineering Journal, 154*, 107456.

Patidar, S. K., Mitra, M., George, B., Soundarya, R., & Mishra, S. (2014). Potential of Monoraphidium minutum for carbon sequestration and lipid production in response to varying growth mode. *Bioresource Technology, 172*, 32–40.

Patwal, T., & Baranwal, M. (2021). Scenedesmus acutus extracellular polysaccharides produced under increased concentration of sulphur and phosphorus exhibited enhanced proliferation of peripheral blood mononuclear cells. *3 Biotech, 11*(4), 171.

Peers, G., Truong, T. B., Ostendorf, E., Busch, A., Elrad, D., Grossman, A. R., Hippler, M., & Niyogi, K. K. (2009). An ancient light-harvesting protein is critical for the regulation of algal photosynthesis. *Nature, 462(7272)*, 518–521.

Peers, G. (2014). Increasing algal photosynthetic productivity by integrating ecophysiology with systems biology. *Trends in Biotechnology, 32*(11), 551–555.

Pereira, E. G., Martins, M. A., Mendes, M. D. S. A., Mendes, L. B. B., & Nesi, A. N. (2017). OUTDOOR CULTIVATION OF Scenedesmus obliquus BR003 IN STIRRED TANKS BY AIRLIFT. *Engenharia Agrícola, 37*(5), 1041–1055.

Pereira, H., Sá, M., Maia, I., Rodrigues, A., Teles, I., Wijffels, R. H., Navalho, J., & Barbosa, M. (2021). Fucoxanthin production from Tisochrysis lutea and Phaeodactylum tricornutum at industrial scale. *Algal Research, 56*, 102322.

Perez-Gil, J., Behrendorff, J., Douw, A., & Vickers, C. E. (2024). The methylerythritol phosphate pathway as an oxidative stress sense and response system. *Nature Communications, 15(1)*, 5303.

Perri, K. A., Manning, S. R., Watson, S. B., Fowler, N. L., & Boyer, G. L. (2021). Dark adaptation and ability of pulse-amplitude modulated (PAM) fluorometry to identify nutrient limitation in the bloom-forming cyanobacterium, Microcystis aeruginosa (Kützing). *Journal of Photochemistry and Photobiology B: Biology, 219*, 112186.

Posten, C., & Walter, C. (Eds.). (2012). Microalgal Biotechnology: Potential and Production. *DE GRUYTER*.

Ren, H.-Y., Liu, B.-F., Ma, C., Zhao, L., & Ren, N.-Q. (2013). A new lipid-rich microalga Scenedesmus sp. strain R-16 isolated using Nile red staining: Effects of carbon and nitrogen sources and initial pH on the biomass and lipid production. *Biotechnology for Biofuels, 6*(1), 143.

Renaud, S. M., Thinh, L.-V., Lambrinidis, G., & Parry, D. L. (2002). Effect of temperature on growth, chemical composition and fatty acid composition of tropical Australian microalgae grown in batch cultures*. Aquaculture, 211*(1–4), 195–214.

Richmond, A. (Ed.). (2004). Handbook of microalgal culture: Biotechnology and applied Phycology (Nachdr.). *Blackwell Science*.

Rippka, R., Herdman, M., Waterbury, J. B., Stanier, R. Y., & Deruelles, J. (1979). Generic Assignments, Strain Histories and Properties of Pure Cultures of Cyanobacteria. *Microbiology, 111*(1), 1–61.

Ruban, A. V. (2016). Nonphotochemical Chlorophyll Fluorescence Quenching: Mechanism and Effectiveness in Protecting Plants from Photodamage. *Plant Physiology, 170*(4), 1903–1916.

Saxena, N., Chudasama, Y., Chawada, H., Kodgire, S., Dasgupta, S., & Sanyal, D. (2021). Evaluating Total Organic Carbon Derived Algae Biomass Productivity Compared with Ash Free Dry Weight Measurement. *Proceedings of the National Academy of Sciences, India Section B: Biological Sciences, 91*(1), 89–94.

Schreiber, U., Müller, J.F., Haugg, A. et al. New type of dual-channel PAM chlorophyll fluorometer for highly sensitive water toxicity biotests. *Photosynthesis Research 74*, 317–330 (2002). https://doi.org/10.1023/A:1021276003145

Schreiber, U. (2004). Pulse-Amplitude-Modulation (PAM) Fluorometry and Saturation Pulse Method: An Overview. In G. C. Papageorgiou & Govindjee (Eds.), *Chlorophyll a Fluorescence* (Vol. 19, pp. 279–319). Springer Netherlands.

Schult, K., Meierhoff, K., Paradies, S., Töller, T., Wolff, P., & Westhoff, P. (2007). The Nuclear-Encoded Factor HCF173 Is Involved in the Initiation of Translation of the psbA mRNA in Arabidopsis thaliana. *The Plant Cell, 19(4)*, 1329–1346.

Schuurmans, R. M., Van Alphen, P., Schuurmans, J. M., Matthijs, H. C. P., & Hellingwerf, K. J. (2015). Comparison of the Photosynthetic Yield of Cyanobacteria and Green Algae: Different Methods Give Different Answers. PLOS ONE, 10(9), e0139061.

Serôdio, J., Vieira, S., Cruz, S., & Coelho, H. (2007). Rapid light-response curves of chlorophyll fluorescence in microalgae: Relationship to steady-state light curves and non-photochemical quenching in benthic diatom-dominated assemblages. *Photosynthesis Research, 90(1)*, Article 1.

Shao, Y., Gu, W., Qiu, Y. A., Wang, S., Peng, Y., Zhu, Y., & Zhuang, S. (2020). Lipids monitoring in Scenedesmus obliquus based on terahertz technology. Biotechnology for Biofuels, 13(1), 161.

Shen, X.-F., Liu, J.-J., Chu, F.-F., Lam, P. K. S., & Zeng, R. J. (2015). Enhancement of FAME productivity of Scenedesmus obliquus by combining nitrogen deficiency with sufficient phosphorus supply in heterotrophic cultivation. *Applied Energy, 158*, 348–354.

Shin, W.-S., Lee, B., Jeong, B., Chang, Y. K., & Kwon, J.-H. (2016). Truncated light-harvesting chlorophyll antenna size in Chlorella vulgaris improves biomass productivity. *Journal of Applied Phycology, 28(6)*, 3193–3202.

Sikora, P., Chawade, A., Larsson, M., Olsson, J., & Olsson, O. (2011). Mutagenesis as a Tool in Plant Genetics, Functional Genomics, and Breeding. *International Journal of Plant Genomics, 2011*, 1–13.

Singh, A., Nigam, P. S., & Murphy, J. D. (2011). Mechanism and challenges in commercialisation of algal biofuels. Bioresource Technology, 102(1), 26–34.

Singh, R., Upadhyay, A. K., Singh, D. V., Singh, J. S., & Singh, D. P. (2019). Photosynthetic performance, nutrient status and lipid yield of microalgae Chlorella vulgaris and Chlorococcum humicola under UV-B exposure. Current Research in Biotechnology, 1, 65–77.

Steinbrenner, J., & Linden, H. (2001). Regulation of Two Carotenoid Biosynthesis Genes Coding for Phytoene Synthase and Carotenoid Hydroxylase during Stress-Induced Astaxanthin Formation in the Green Alga *Haematococcus pluvialis*. *Plant Physiology, 125*(2), 810–817.

Takagi, H., Kimoto, K., & Fujiki, T. (2022). Photosynthetic Carbon Assimilation and Electron Transport Rates in Two Symbiont-Bearing Planktonic Foraminifera. *Frontiers in Marine Science, 9,* 803354.

Tan, L., Xu, W., He, X., & Wang, J. (2019). The feasibility of Fv/Fm on judging nutrient limitation of marine algae through indoor simulation and in situ experiment. Estuarine, Coastal and Shelf Science, 229, 106411.

Teng, Z., Zheng, L., Yang, Z., Li, L., Zhang, Q., Li, L., Chen, W., Wang, G., & Song, L. (2023). Biomass production and astaxanthin accumulation of Haematococcus pluvialis in large-scale outdoor culture based on year-round survey: Influencing factors and physiological response. *Algal Research, 71*, 103070.

Tikkanen, M., & Aro, E.-M. (2014). Integrative regulatory network of plant thylakoid energy transduction. *Trends in Plant Science, 19*(1), 10–17.

Tsarenko, P. M., Borysova, O. V., Korkhovyi, V. I., & Blume, Y. B. (2020). High-Efficiency Ukrainian Strains of Microalgae for Biodiesel Fuel Production (Overview). *The Open Agriculture Journal, 14*(1), 209–218.

Trovão, M., Schüler, L. M., Machado, A., Bombo, G., Navalho, S., Barros, A., Pereira, H., Silva, J., Freitas, F., & Varela, J. (2022). Random Mutagenesis as a Promising Tool for Microalgal Strain Improvement towards Industrial Production. *Marine Drugs, 20(7)*, 440.

United States Department of Agriculture. (2022, June 3). USDA has provided $700 million to restore sustainable fuel markets hit by pandemic. USDA. Release No. 0120.22

Vorisek, F. E., Ji, Y., Hillis, M. H., Parker, J., Thompson, J., Liu, K., & Crocker, M. (2023). Towards an Integrated Process for CO2 Capture and Utilization: Cultivation of Scenedesmus acutus Using Gaseous CO2 and NH3. *BioEnergy Research*.

Walz GmbH. (n.d.). Applications for the PAM-2500: Light Saturation Curves of the Apparent Electron Transport Rate. WALZ.

Walz, H. (2019). IMAGING-PAM M-Series: Chlorophyll fluorometer instrument description and information for users (9th corrected ed.). Heinz Walz GmbH.

Wang, B., & Jia, J. (2020). Photoprotection mechanisms of Nannochloropsis oceanica in response to light stress. *Algal Research, 46*, 101784.

Wang, T.; He, X.; Gong, W.; Kou, Z.; Yao, Y.; Fulbright, S.; Reardon, K. F.; Fan, M., (2022). Threedimensional, heteroatom-enriched, porous carbon nanofiber flexible paper for freestanding supercapacitor electrode materials derived from microalgae oil. *Fuel Processing Technology 2022*, 225, 107055.

Wang, W., Wei, T., Fan, J., Yi, J., Li, Y., Wan, M., Wang, J., & Bai, W. (2018). Repeated mutagenic effects of 60Co-γ irradiation coupled with high-throughput screening improves lipid accumulation in mutant strains of the microalgae Chlorella pyrenoidosa as a feedstock for bioenergy. *Algal Research, 33*, 71–77.

Wang, X.-W., Liang, J.-R., Luo, C.-S., Chen, C.-P., & Gao, Y.-H. (2014). Biomass, total lipid production, and fatty acid composition of the marine diatom Chaetoceros muelleri in response to different CO2 levels. *Bioresource Technology, 161*, 124–130.

Ward, J. F. (1988). DNA Damage Produced by Ionizing Radiation in Mammalian Cells: Identities, Mechanisms of Formation, and Reparability. In *Progress in Nucleic Acid Research and Molecular Biology (Vol. 35, pp. 95–125)*. Elsevier.

Ware, M. A., Kendrick, J. M., Hantzis, L. J., & Peers, G. (2020). A fluorescence-based approach to screen for productive chemically mutagenized strains of Desmodesmus armatus. *Algal Research, 51*, 102028.

Wei, L., & Huang, X. (2017). Long-duration effect of multi-factor stresses on the cellular biochemistry, oil-yielding performance and morphology of Nannochloropsis oculata. *PLOS ONE, 12*(3), e0174646.

Weissman, J. C., Likhogrud, M., Thomas, D. C., Fang, W., Karns, D. A. J., Chung, J. W., Nielsen, R., & Posewitz, M. C. (2018). High-light selection produces a fast-growing Picochlorum celeri. *Algal Research, 36*, 17–28.

Woodyard, D. (2009). Fuels and Lubes: Chemistry and Treatment. *In Pounder's Marine Diesel Engines and Gas Turbines (pp. 87–142)*. Elsevier.

Xi, Y., Wang, J., Chu, Y., Chi, Z., & Xue, S. (2020). Effects of different light regimes on Dunaliella salina growth and β-carotene accumulation. *Algal Research, 52*, 102111.

Xia, Q., Tang, H., Fu, L., Tan, J., Govindjee, G., & Guo, Y. (2023). Determination of F_v / F_m from Chlorophyll a Fluorescence without Dark Adaptation by an LSSVM Model. *Plant Phenomics, 5*, 0034.

Young, E. B., & Beardall, J. (2003). Photosynthetic function in Dunaliella tertiolecta (Chlorophyta) during a nitrogen starvation and recovery cycle. *Journal of Phycology, 39*(5), 897–905.

Zepeda, J. B. F., & Custodio, C. G. (2018). The Costs of Regulatory Delays for Genetically Modified Crops. *International Service for the Acquisition of Agri-Biotech Applications*, *1*(1).

Zhao, L., Zhang, Y., Geng, X., Hu, X., Zhang, X., Xu, H., Yang, G., Pan, K., & Jiang, Y. (2021). Potential to resist biological contamination in marine microalgae culture: Effect of extracellular substances of Nannochloropsis oceanica on population growth of Euplotes vannus and other protozoa. *Marine Pollution Bulletin, 172*, 112868.

Zhao, L.-S., Li, K., Wang, Q.-M., Song, X.-Y., Su, H.-N., Xie, B.-B., Zhang, X.-Y., Huang, F., Chen, X.-L., Zhou, B.-C., & Zhang, Y.-Z. (2017). Nitrogen Starvation Impacts the Photosynthetic Performance of Porphyridium cruentum as Revealed by Chlorophyll a Fluorescence. *Scientific Reports, 7(1)*, 8542.

Zhu, C., Ji, Y., Du, X., Kong, F., Chi, Z., & Zhao, Y. (2022). A smart and precise mixing strategy for efficient and cost-effective microalgae production in open ponds. *Science of The Total Environment, 852*, 158515.

Xia, Q., Tang, H., Fu, L., Tan, J., Govindjee, G., & Guo, Y. (2023). Determination of F_v / F_m from Chlorophyll a Fluorescence without Dark Adaptation by an LSSVM Model. *Plant Phenomics, 5,* 0034.

Zhu, X.-G., Long, S. P., & Ort, D. R. (2010). Improving Photosynthetic Efficiency for Greater Yield. *Annual Review of Plant Biology, 61(1)*, 235–261.

Zhu, Y., Jones, S. B., & Anderson, D. B. (2018). Algae Farm Cost Model: Considerations for Photobioreactors (PNNL–28201, 1485133; p. PNNL–28201, 1485133).

Zijffers, J.-W. F., Schippers, K. J., Zheng, K., Janssen, M., Tramper, J., & Wijffels, R. H. (2010). Maximum Photosynthetic Yield of Green Microalgae in Photobioreactors. *Marine Biotechnology, 12(6)*, 708–718.

Zimny, T. (2023). Regulation of GMO field trials in the EU and new genomic techniques: Will the planned reform facilitate experimenting with gene-edited plants? *BioTechnologia, 104*(1), 75–83.

Zuo, G., Aiken, R. M., Feng, N., Zheng, D., Zhao, H., Avenson, T. J., & Lin, X. (2022). Fresh perspectives on an established technique: Pulsed amplitude modulation chlorophyll a fluorescence. *Plant-Environment Interactions, 3(2)*, 41–59.

APPENDICIES

1. Supplemental Results

Table S1: Comparison of OD_{680} and cell density derived specific growth rates. Six strains described in Table 2.1 were measured for both optical density and cell density (n=1). Maximum specific growth rates were calculated for each set of data and were determined to be consistent across multiple strains. Following this experiment, future specific growth rates were calculated using optical density of cultures.

Strain	**OD_{680} Derived Specific Growth Rate (day^{-1})**	**Cell Density Derived Specific Growth Rate (day^{-1})**
Monoraphidium minutum	0.9	1.0
Nannochloropsis oceanica	1.0	1.1
Picochlorum celeri	1.6	1.9
Picochlorum renovo	1.2	1.2
SAmud7	1.4	1.5
SRTC14	1.4	1.2

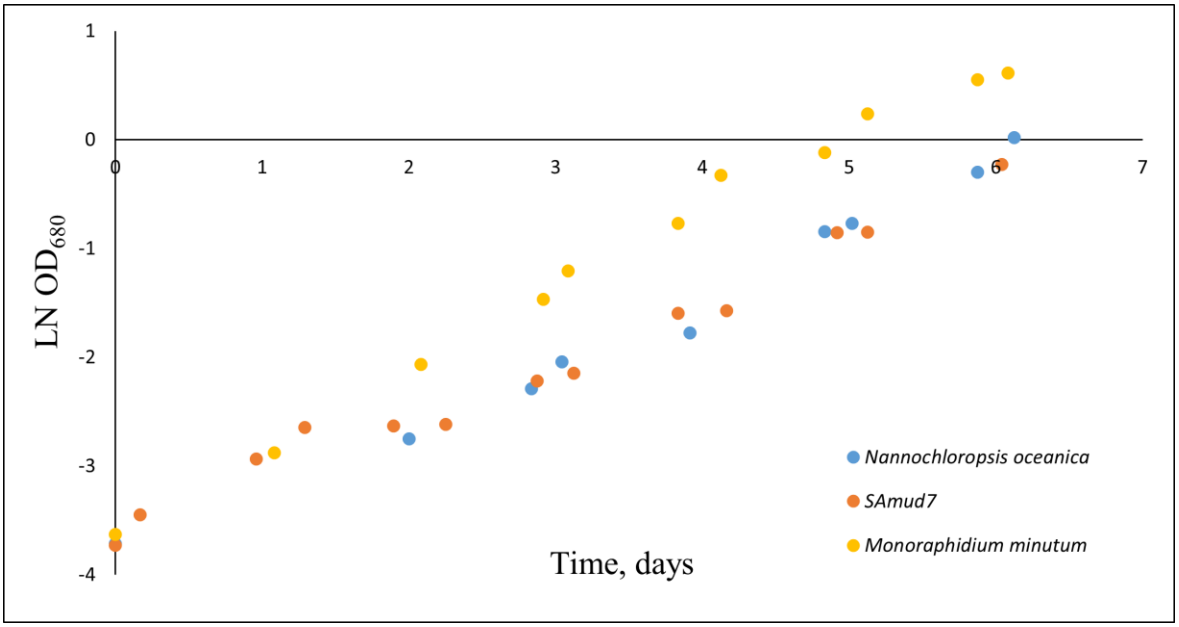

Figure S1: Comparison of average natural log of OD_{680} measurements of *Nannochloropsis oceanica,* SAmud7, and *Monoraphidium minutum.* Cultures were grown under the conditions specified in Table 1.3. Values shown are from single roux flask cultures (n=1).

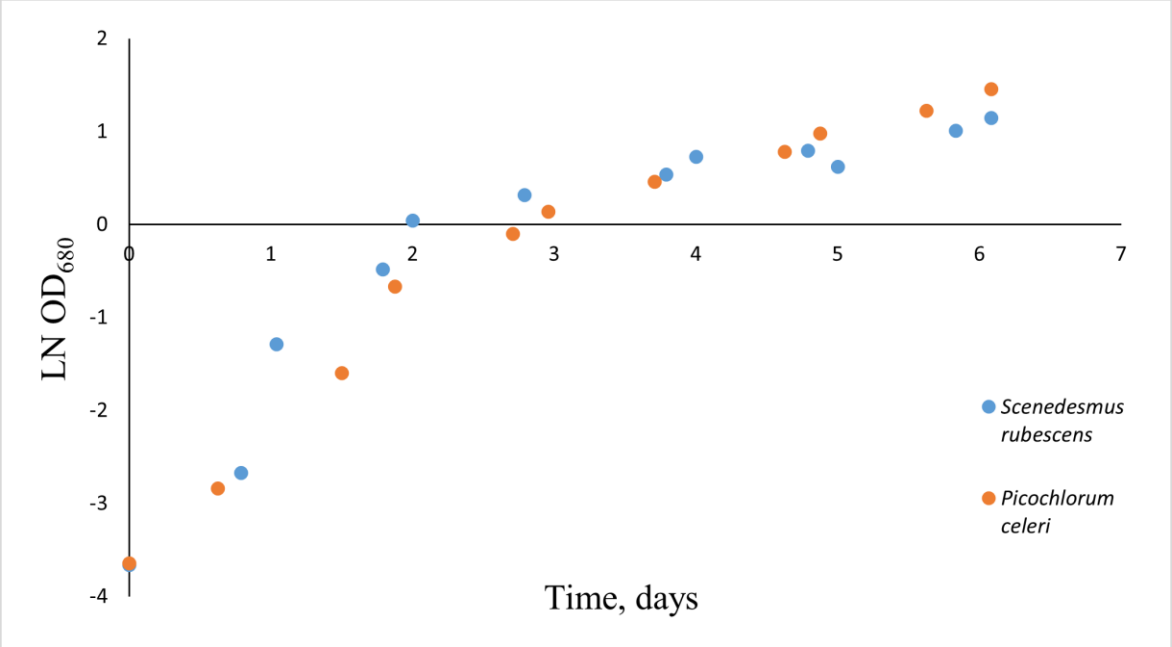

Figure S2: Comparison of the average natural log of OD_{680} measurements of *Scenedesmus rubescens* and *Picochlorum celeri.* Cultures were grown under the conditions specified in Table 1.4. Values shown are from single roux flask cultures (n=1).

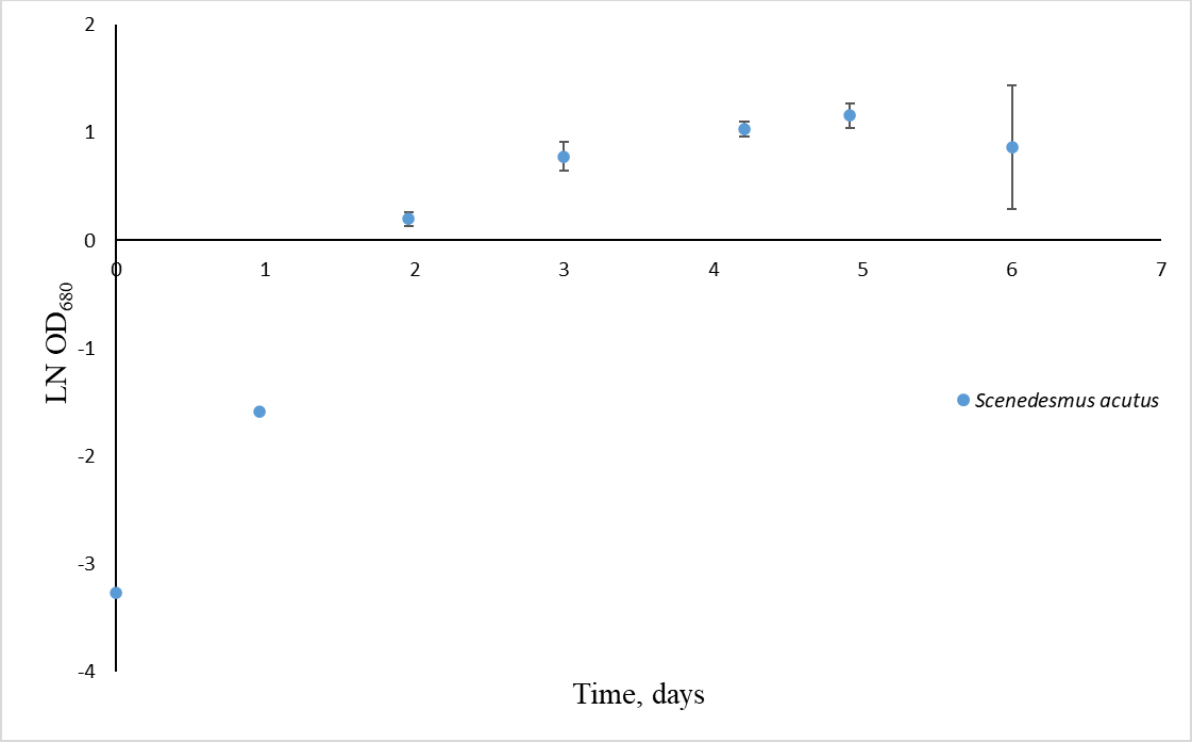

Figure S3: Average natural log of OD_{680} measurements of *Scenedesmus acutus.* Cultures were grown under the conditions specified in Table 1.5. Values shown are averages ± 1 standard deviation (n=3).

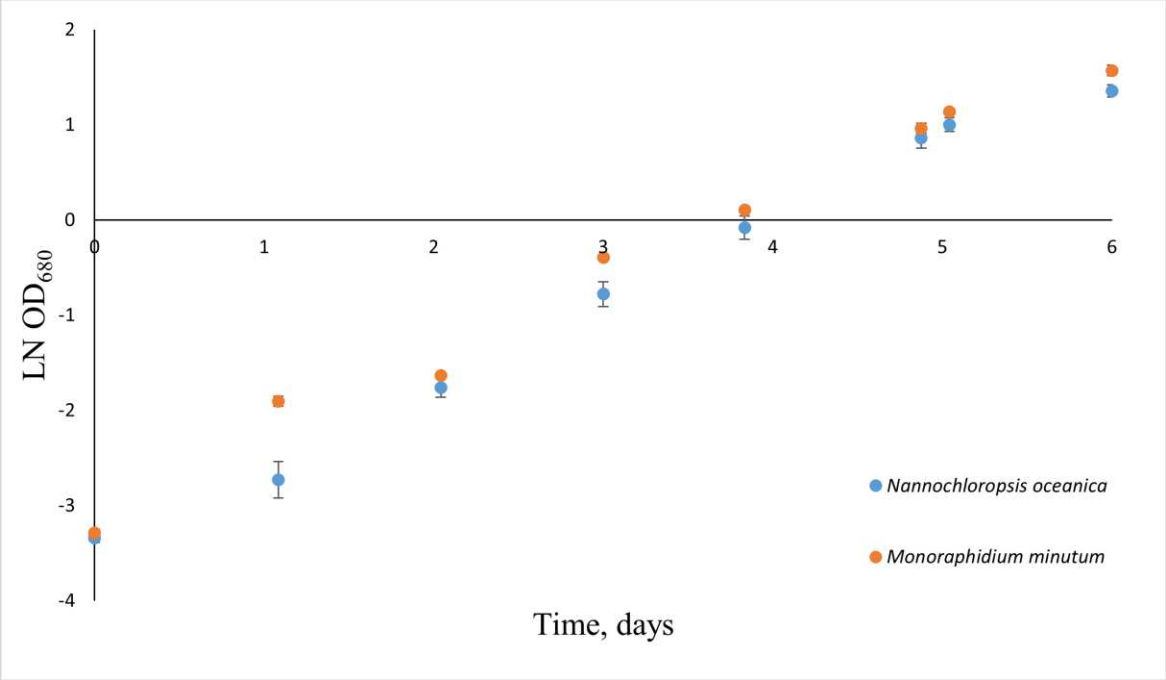

Figure S4: Comparison of the average natural log of OD_{680} measurements of *Nannochloropsis oceanica* and *Monoraphidium minutum.* Cultures were grown under the conditions specified in Table 1.5. Values shown are averages ± 1 standard deviation (n=3).

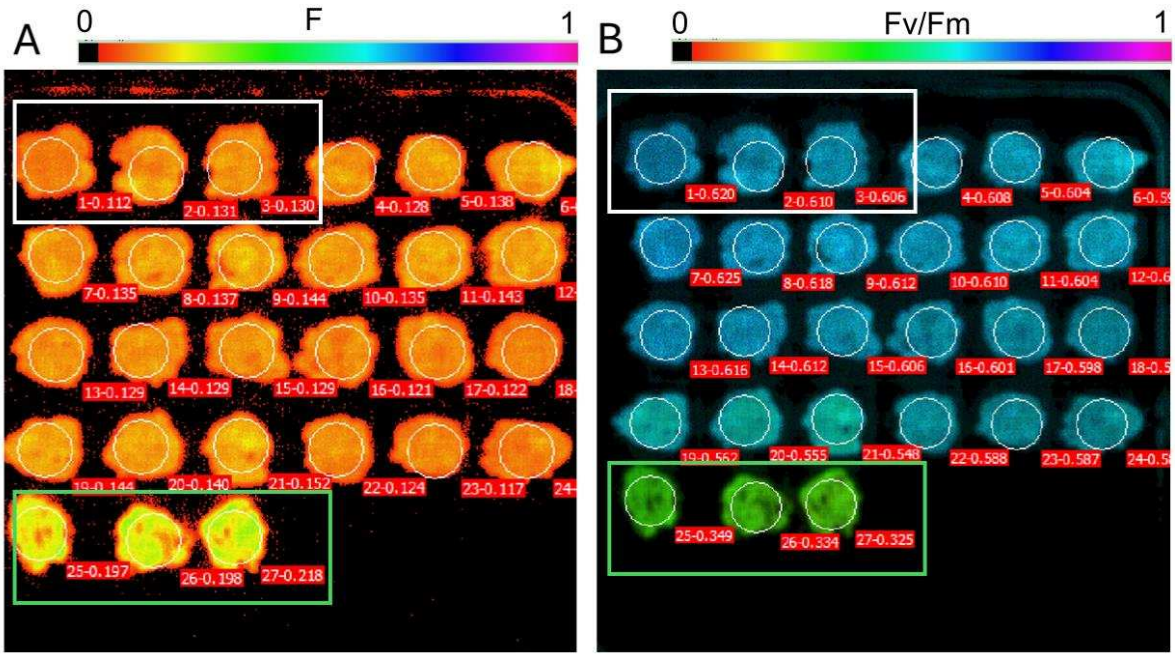

Figure S5: Observation of chlorophyll fluorescence and Fv/Fm of WT and high chlorophyll fluorescence (HCF) mutant *MRM K-227* measured via IMAGING-PAM. A) Relative fluorescence of triplicate WT (white box) and *MRM K-227* (green box). The average relative WT fluorescence was 0.124 while *MRM K-227* had an average of 0.204, an increase of around 65% over WT. Fluorescence values for each colony are shown in red boxes. B) Fv/Fm of triplicate WT (white box) and *MRM K-227* (green box). The average WT Fv/Fm was 0.612 while *MRM K-227* had an average of 0.336, a decrease of 45% compared to WT.

Measured plates containing irradiated strains using IMAGING-PAM fluorometry.

Identified any strains with altered fluorescence kinetics by comparing them to the WT control on the plate.

Compared Fv/Fm, NPQ, and qL values of putative mutants with WT.

Grew any mutants with promising photophysiological alterations in triplicates for re-screening.

Down-selected putative mutants that demonstrate repeated alterations.

22 putative *S. rubescens* mutants and 14 putative *M. minutum mutants* identified for growth comparison.

Figure S6: Summary of fluorescence-based screening strategy.